Improving the Biopharmaceutical Properties of Cyclic Opioid Peptide Prodrugs

By

Rebecca A. Nofsinger

B.S., The University of Toledo, 1998

M.S., The University of California, Los Angles, 2002

M.S., The University of Kansas, 2005

Submitted to the Department of Pharmaceutical Chemistry and the Faculty of the Graduate School of The University of Kansas in partial fulfillment of the requirements for the degree of Doctor of Philosophy.

Dissertation Committee:

_____
Chair, Dr. Ronald T. Borchardt

_____
Dr. Teruna J. Siahaan

_____
Dr. John F. Stoubaugh

_____
Dr. Jeffrey P. Krise

_____
Dr. David R. Benson

Dissertation defended: April 23, 2008

The Dissertation Committee for Rebecca Nofsinger certifies that this is the approved version of the following dissertation:

Improving the Biopharmaceutical Properties of Cyclic Opioid Peptide Prodrugs

Dissertation Committee:

_____
Chair, Dr. Ronald T. Borchardt

_____
Dr. Teruna J. Siahaan

_____
Dr. John F. Stoubaugh

_____
Dr. Jeffrey P Krise

_____
Dr. David R. Benson

Date approved: April 23, 2008

Improving the Biopharmaceutical Properties of Cyclic Opioid Peptide Prodrugs

Rebecca A. Nofsinger

The University of Kansas, 2008

The development of opioid peptides into orally viable therapeutics has been limited by their unfavorable drug-like properties. Poor intestinal permeation and enzymatic instability are some of the undesirable qualities exhibited by opioid peptides. To improve the "drugability" of these peptides, we have developed cyclic prodrugs of the opioid peptide DADLE (H-Tyr-D-Ala-Gly-Phe-D-Leu-OH). The parent cyclic prodrug CA-DADLE was formed by joining the N- and C-termini of the peptide via a coumarinic acid linker (CA). In the presence of liver microsomes and human recombinant cytochrome P450-3A4 (hCYP3A4), CA-DADLE was found to be metabolically unstable. Studies indicated that the instability was a result of cytochrome P450 metabolism. Under oxidative conditions, two main metabolites of CA-DADLE were discovered (hydroxylation on Tyr^1 and Phe^4 residues). CA-DADLE was found to be a substrate for efflux transports [i.e., P-glycoprotein (P-gp)], which lead to very low cell membrane permeation. Using this knowledge, analogs of CA-DADLE were designed to enhance metabolic stability and possibly improve membrane permeation.

Cyclic prodrug analogs CA-[Cha^4,D-Leu^5]-Enk and CA-[Cha^4,D-Ala^5]-Enk were successfully synthesized, investigated for metabolic stability, and evaluated for desirable physicochemical properties. The compounds were found to be metabolically unstable in the presence of liver microsomes and showed oxidative metabolite formation under these conditions (hydroxylation on Tyr^1 and Cha^4 residues). Surprisingly, the analogs did show stability in the presence of hCYP3A4, which is a major metabolic barrier to intestinal absorption. Molecular surface area, cLogP, and solution conformation studies indicated favorable physicochemical properties that could potentially lead to increased membrane permeability.

Finally, cell permeation was examined. Cyclic prodrug analogs were investigated using an *in vitro* cell culture model as well as an *in situ* rat intestinal perfusion model. The *in situ* perfusion model provided the opportunity to simultaneously test *in vivo* cell permeation as well as identify oxidative metabolites *in vivo*. No oxidative metabolites were detected in the *in situ* perfusion studies. In i*n vitro* and *in vivo* models, the analogs were found to be substrates for P-gp, which severely limited their membrane permeation. In conclusion, these molecules would need to have increased metabolic stability in the liver and enhanced membrane permeation to be orally bioavailable.

This dissertation is dedicated to my maternal grandmother,

Katherine W.S. Herrmann.

ACKNOWLEDGMENTS

I would like to thank my advisor Dr. Ronald T. Borchardt for his support and guidance during my graduate education. Dr. Borchardt, I sincerely appreciate all the time and effort you have put into training me to be a better scientist. It is not often that one is truly great at many things, but I think your teaching and mentoring over the years speaks for itself. I am honored to be counted among those. I would like to acknowledge my dissertation committee: Dr. Teruna J. Siahaan, Dr. John F. Stoubaugh, Dr. Jeffrey P. Krise, and Dr. David R. Benson. A special thanks to Dr. Siahaan and Dr. Krise for taking the time to read through my dissertation and offering helpful comments and advise. I would like to express my appreciation to Nancy Harmony for her editorial assistance and greatly improving my writing style in the process. Nancy, you have helped me learn how to put what is in my head down on paper in a coherent manor others will also understand, not a small task!

I would like to thank all the members of the Borchardt laboratory with whom I have had the pleasure to work. Your guidance and friendships have made my time at Kansas truly memorable. I would like to thank Dr. Vander Velde for his assistance in the NMR studies and Dr. Lushington for his help with the molecular modeling. A very special thank you to Dr. Tarra Fuchs-Knotts for her assistance in the synthesis of the cyclic prodrugs, helpful scientific discussions, and friendship. I want to also thank Dr. Daniel Mudra for his friendship and expertise with the rats. I am also

grateful to Dr. Aditya Wakankar for his friendship and making working in lab enjoyable.

A special thank you to the office staff in the Pharmaceutical Chemistry Department: Nancy Helm, Nicole Brooks, Anne Heptig, Karen Hall, and Trica Masenthin. Thank you ladies for helping with all those things that didn't seem to work out the first time and needed a little additional attention, I appreciate the extra effort you put forth on my behalf.

I would like to acknowledge those fellow graduate students whose friendship, encouragement, and kindness have helped me during my time here at Kansas. Maulik Trivedi, Nagarajan "Raja" Thyagarajapuram, Vikram Sadineni, Kelly Desino, Dan Mudra, Aditya Wakankar, Kevin Head, Maya Salnikova, Pallabi Mitra, Alana Toro-Ramos, and Courtney Kuhnline. Your positive influence has truly kept me sane.

Last but not least, I would like to thank my family. Mom and Dad, thank you so much for your love, support, and encouragement. Thank you for instilling in me a love of science and learning. You raised me to follow my dreams, and I am forever grateful. I also want to thank my husband and soul-mate David Nofsinger. Your unwavering love and support mean the world to me. I would like to also thank my daughter who has had to put up with Mommy constantly writing and having to go back to lab. Ester you are truly a blessing. You inspire me to make this world a better place.

Finally this research was made possible by the financial support of NIGMS Predoctoral Biotechnology Training Grant and NIH/NIDA (DA-03315).

Improving the Biopharmaceutical Properties of Cyclic Opioid Peptide Prodrugs

TABLE OF CONTANTS

Figure Index

List of Tables

Chapter 1

Cyclic Peptide Prodrugs of DADLE: A History

1.1 OPIOID PEPTIDES

Opioid peptides, which were among the first discovered neuropeptides discovered,[1] have been studied extensively for their possible therapeutic value in relieving pain. The advantage of opioid peptides is that they mimic the effect of opiates in the brain (i.e., possessing high affinity for opioid receptors). Opioid receptors are heterogeneous and exist in three main types, classified as μ, δ, and κ.[2] The highest abundance of opioid receptors is in the central nervous system (CNS),[3] but they have also been found in many peripheral tissues.[4] By targeting specific opioid receptors, opioid peptides can potentially provide therapeutic results with reduced side effects. There are two types of endogenous opioid peptides; they differ in the pharmacophoric amino acid sequence of the message domain (at the N-terminus).[5,6] The first class of opioid peptides (enkephalins, endorophins, and dynorphins) has a N-terminal sequence of -Tyr-Gly-Gly-Phe-, while the second class (endomorphins) has the sequence -Tyr-Pro-Phe/Trp-. Therapeutic opioid peptides and peptiodomimetics are typically modeled after these endogenous systems.

One of the early leading peptidomimetics to generate interest was a synthetic derivative of leucine enkephalin ([Leu^5]-Enk) called DADLE.[7-9] DADLE is a pentapeptide with a modified amino acid sequence of H-Tyr-D-Ala-Gly-Phe-D-Leu-OH. In the late 1970s, [Leu^5]-Enk's analgesic effect and specificity toward explicit opioid receptors were investiagated.[8-12] Wüster *et al*. and Robson *et al*. found that [Leu^5]-Enk and many enkephalin analogs, specifically DADLE, were selective for the δ-opioid receptor.[9,11] As new analogs were studied, identification of the functional

groups and residues important for biological activity was pursued.[13,14] Investigations for better and more potent analogs continued, and cyclic-enkephalin peptides were introduced. The first cyclic enkephalin peptides [D-Pen^2,D/L-Cyc^5]-Enk were developed by Mosberg.[15] They had δ-opioid receptor specificity and biological activity and were efficacious *in vivo*.[15] Also from the arena of new cyclic opioid peptides, penicillamines ([D-Pen^2,D-Pen^5]) or DPDPE emerged. These cyclic analogs were highly selective to the δ-opioid receptor and showed a significant reduction in side effects.[16] Later, the Borchardt and Siahaan laboratories introduced cyclic peptide prodrugs of DADLE.[17,18]

1.2 DEVELOPMENT OF CYCLIC PRODRUG STRATEGY

The development of cyclic opioid peptides with high affinity and selectivity toward specific opioid receptors has been ongoing.[19-23] Unfortunately, the development of these peptides into viable clinical candidates has been limited by their lack of enzymatic stability and undesirable physicochemical properties. These issues lead to limited intestinal mucosa permeation and, ultimately, low oral bioavailability. The cyclic prodrug strategy was employed to create cyclic peptide prodrugs that would overcome these problems while maintaining biological activity. The strategy has three main objectives: (i) to enhance membrane permeation, (ii) to increase metabolic stability toward exo- and endopeptidases, and (iii) to promote rapid prodrug bioconversion.

Many hydrophilic peptides, opioid peptides included, are restricted to cellular permeation via the paracellular pathway. During this route of permeation, the hydrophilic molecules travel through aqueous pores in between the cells. These pores are regulated by tight junctions that range in size from 7-9 Å.[24] Quite naturally, these pores restrict permeation based on the size and charge of the peptides.[24,25] The linear opioid peptide DADLE does have desirable paracellular characteristics (hydrophilic and charged at physiological pH). However, DADLE is significantly larger in size (MW = 570 DA) than is typical for paracellular penetration (< 300 DA) and, therefore, has very low intestinal permeation.[25,26]

Peptides that are hydrophobic, exhibit no charge, and have a low hydrogen-bonding potential can cross biological barriers via the transcellular pathway.[27] During this route of permeation, molecules travel through the cell membrane, and higher molecular weight molecules can be tolerated via the transcellular pathway. Based on DADLE's charged and hydrophilic nature as well as the multiple hydrogen bond donors and acceptors present, the transcellular permeation of DADLE would be predicted to be low. For DADLE to become a viable drug, the cellular permeation must be improved.

A successful cyclic peptide prodrug should be able to cross biological membranes with little to no metabolic degradation. The metabolic stability issue of peptide drugs has largely been resolved through structural modifications by medicinal chemists.[19,28] The development of DADLE is an example of this. Modifications to the amino acid sequence and stereochemistry of [Leu^5]-Enk (H-Tyr-Gly-Gly-Phe-

Leu-OH) affords DADLE (H-Tyr-D-Ala-Gly-Phe-D-Leu-OH). The replacement of glycine with alanine at the second residue of the peptide and modification of stereochemistry (L-amino acids to D-amino acids) at the second and fifth residues were shown to greatly increase stability towards amino- and carboxypeptidases.[7] Cyclic peptide prodrugs were designed to further increase the metabolic stability of DADLE by enhancing stability toward exo- and endopeptidases. This was accomplished with the cyclic structure itself, since the N- and C-termini are "masked" in the cyclic prodrugs. The cyclic design did provide DADLE prodrugs with greater stability against exo- and endopeptidases.[29,30]

Having a stabilized peptide is only one aspect to consider with a peptide prodrug; the promoiety and bioconversion of the prodrug must also be taken into account. Once across the membrane barrier, the prodrug should undergo a spontaneous or rapid enzyme-mediated biotransformation to release the active peptide. Much of the bioconversion depends on the choice of promoiety. However, the choice of promoiety also affects the physicochemical properties of the molecule (i.e., charge, conformation, lipophilcity, and hydrogen-bonding potential), which in turn affect the cellular permeation. In an attempt to improve the physicochemical properties and, ultimately, the cellular permeation of opioid peptides, the Borchardt and Siahaan laboratories have developed cyclic peptide prodrugs of the opioid peptide DADLE. In the cyclic prodrugs, the N- and C-termini of the peptide are joined via promoiety linkers.[17,18,31] Four new promoieties have been developed for

this task: phenylpropionic acid (PPA),[18] (acyloxy)alkox (AOA),[17] coumarinic acid (CA),[18] and oxymethyl-modified coumarinic acid (OMCA)[31] linkers (Figure 1.1).

1.3 PHYSICOCHEMICAL PROPERTIES OF CYCLIC PRODRUGS OF OPIOID PEPTIDES

Prodrugs can be used to enhance the pharmaceutical qualities and overall "drugability" of a moleule.[32] In making prodrugs of DADLE, the peptide was incorporated into a cyclic structure containing a promoiety. Model peptides, [Leu^5]-Enk, and DADLE were used to evaluate the physicochemical properties of these new prodrugs. Changes in physicochemical properties of the molecules were seen upon cyclization and can be related to lipophilicity and solution conformation. Ultimately, the goal of creating cyclic DADLE prodrugs was to enhance the physicochemical properties of the prodrugs resulting in increased membrane permeation compared to DADLE.

1.3.1 Liophilicity

The lipophilicity of DADLE is significantly increased by intramolecular cyclization and addition of a lipophilic promoiety. The cyclic prodrugs are uncharged as a result of linking the N- and C- termini of the peptide. Addition of lipophilic linkers (PPA, CA, and OMCA) contributes to the increased lipophilicity of the cyclic prodrugs, which is important to their transcellular permeation. During transcellular

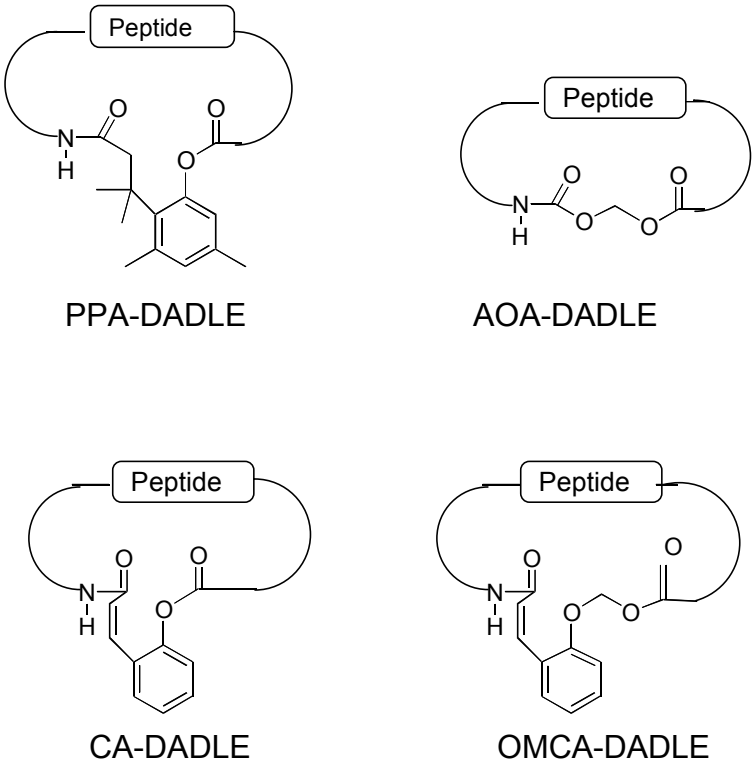

Figure 1.1. Structure of cyclic prodrugs of DADLE

permeation, hydrophobic molecules travel through the cell membrane and interact with the lipid biolayer. The membrane interaction potentials of the cyclic prodrugs and linear peptides were measured using immobilized artificial membranes (IAM) or estimated using cLogP values.

In measuring membrane interaction potentials, the interaction of the molecule with an IAM column gives an estimation of the combined effects of charge, polarity, and hydrogen-bonding potential. If a molecule is too hydrophilic, it will not interact with the lipophilic cell membrane (low interaction potentials). This signals that the molecule will not be able to cross the cell membrane in a transcellular fashion. Linear peptides, [Leu^5]-Enk, and DADLE were found to have low membrane interaction potentials.[17,18] Cyclic prodrugs of [Leu^5]-Enk and DADLE were found to have enhanced membrane interaction potentials compared to their linear counterparts. The PPA- and CA-cyclic prodrugs exhibited sevenfold to 20-fold increased interaction potentials over the linear peptides,[18] and AOA-cyclic prodrugs showed four to eightfold increased interaction potentials over the linear peptides.[17]

More recently, membrane interaction potentials have been replaced with cLogP values. cLogP values are computer-generated estimates of lipophilicity. The calculations are based on structure, polar surface area, molecular size, and charge of the molecule. The more lipophilic a molecule, the higher the cLogP value. The lipophilicity of a molecule can be used to relate directly to cell permeation. A low cLogP value would indicate that the molecule is not lipophilic enough to permeate the cell membrane via the transcellular route, but too high a cLogP value (typically

greater than 5) would indicate that the molecule is too lipophilic and is likely to get stuck in the lipid membrane. In the popular "rule of five" by Lipinski, having a cLogP value less than five is considered an important criterion in the drugability of a molecule.[33] DADLE was found to have a low cLogP value (-0.32), indicating a very low lipophilicity. The CA- and OMCA-DADLE cyclic prodrugs were found to have cLogP values of 4.96 and 4.95, respectively.[31] The higher cLogP values of the CA- and OMCA-cyclic prodrugs indicate a more favorable lipophilicity for transcellular permeation.

1.3.2 Solution Conformation

Solution conformation and molecular size are important physicochemical properties and can help to predict cell membrane permeation. Passive diffusion becomes increasingly difficult as the molecule becomes larger.[25,34-38] To gauge the molecular size of the cyclic prodrugs, NMR diffusion coefficients and molecular surface area calculations were determined. [Leu^5]-Enk and DADLE displayed diffusion coefficients similar to those of the cyclic prodrugs (PPA-, AOA-, and CA-).[17,18] Molecular surface area calculations showed DADLE , CA-DADLE, and OMCA-DADLE have areas similar in size.[31] These calculations show that, even with the addition of a linker to the cyclic prodrugs, the linear peptides and cyclic peptide prodrugs are comparable in size.

It is evident from the size measurements that the peptide prodrugs become more compact upon cyclization. This is a result of a distinct solution structure. For

example many of the cyclic prodrugs contain a β-turn structure.[31,39-41] This defined secondary structure has been shown to possess intramolecular hydrogen bonds. The result of this is twofold: (i) the intramolecular hydrogen bonding pulls the molecule into a tighter conformation, effectively reducing the molecular size, and (ii) increased intramolecular hydrogen bonding results in decreased opportunity for prodrug-solvent hydrogen bonding and a lower hydrogen-bonding potential overall. This illustrates that the unique solution structure of cyclic prodrugs helps to increase the lipophilicity of the molecule. Compared to linear peptides, the cyclic prodrugs are uncharged, more lipophilic, and have a decreased hydrogen-bonding potential. These physicochemical properties determine, in part, the pathway and extent of passive permeation across biological barriers.

1.4 BIOPHARMACEUTICAL PROPERTIES OF CYCLIC PRODRUGS OF OPIOID PEPTIDES

The goal in the development of cyclic DADLE prodrugs was to design prodrugs that are orally absorbed and localize in the brain. Physicochemical characteristics important to permeation across biological barriers [i.e., intestinal and blood brain barrier (BBB)] are size, charge, lipophilicity, and hydrogen-bonding potential. Cyclization of the peptides has produced cyclic prodrugs with favorable physicochemical properties that could potentially lead to enhanced membrane permeation. Investigations into cell permeability (*in vitro* and *in vivo*), metabolic

stability, and pharmacokinetics further detail the drug-like characteristics of the cyclic prodrugs and overall oral bioavailability.

1.4.1 *In Vitro* Cellular Permeation

A major barrier for orally delivered drugs is the intestinal mucosa. Looking at the physicochemical properties and structural features of cyclic prodrugs, one would expect them to have better transcellular permeation than linear peptides. However, DADLE was found to be from 36- to 52-times more permeable than AOA-DADLE in Caco-2 cell monolayers.[42] The intrinsic permeation [apical (AP) to basolateral (BL)] of DADLE demonstrated an apparent permeability coefficient (P_{app}) of 7.80×10^{8} cm/s, but the cyclic prodrug AOA-DADLE had a much lower value of 1.86×10^{8} cm/s.[42] This suggests that cyclic prodrugs are substrates for apically polarized efflux transporters[42-45], which can limit transcellular permeation.[46,47] Additional evidence that cyclic prodrugs are substrates for efflux transporters was seen by using Madin-Darby canine kidney cells (MDCK) transfected with human P-gp (MDR1) or multidrug resistance protein-2 (MRP2).[43-45] These studies showed that the intrinsic permeation of the cyclic prodrugs was recovered with the use of P-gp and/or MRP inhibitors.

There is extensive literature available on transporters and their role in drug disposition.[37,48-57] Currently however, there is limited information on substrate activity of cyclic prodrugs for specific efflux transporters. The Borchardt lab has determined cyclic prodrug substrate specificity for MDR1 and MRP2. AOA-DADLE

is primarily a substrate for MDR1[45], while CA- and OMCA-DADLE are substrates for both MDR1 and MRP2.[43,44] Cells used in these studies were found to have high levels of MDR1 expression, very low levels of MRP2 present, and no detectable amount of BCRP.[44,45] This suggests that differentiation of co-substrates for various efflux transporter systems (i.e., MDR1/BCRP, MPR2/BCRP or MDR1/MPR2/BCRP) would be unlikely. Using our knowledge of efflux transports in biological barriers, Caco-2 and MDCK cell permeation experiments can help predict oral bioavailability of DADLE *in vivo*. Poor *in vitro* permeation suggests that cyclic prodrugs would most likely possess characteristics that could lead to difficulties *in vivo*.

1.4.2 *In Situ* Intestinal Mucosal Perfusion

Low transcellular permeation of cyclic prodrugs in Caco-2 cells suggests that cyclic prodrugs would display low oral absorption. To determine the intestinal permeation of DADLE and cyclic prodrugs *in vivo*, *in situ* rat intestinal perfusion experiments were conducted.[58-60] In these experiments, a section of intestine was isolated and test compound was directly infused into the intestine. The mesenteric vein was cannulated to collect blood samples from the isolated intestinal region. Blood and perfusate samples were collected continuously and analyzed for the presence of cyclic prodrug and DADLE. The *in situ* intestinal perfusion experiments showed that DADLE is four times more able to permeate than AOA-, CA- or OMCA-DADLE.[60] These results parallel the *in vitro* Caco-2 intestinal cell permeation data, which confirm that DADLE permeates better than the cyclic prodrugs.[42,43,61]

The role of efflux transporters in restricting intestinal mucosal permeation of the cyclic prodrugs was determined using known P-gp inhibitors [PSC-833, cyclosporine (CyA), GF-120918]. An *in situ* rat ileum perfusion model and an *in vitro* cell culture model (Caco-2 cells) were used in these studies. The apparent permeability coefficients of the cyclic prodrugs were low in both models. However in the presence of inhibitors, the intestinal permeation of cyclic prodrugs was significantly increased.[59] Interestingly, the potency of the inhibitors differed in the two intestinal permeation models. The Caco-2 cell culture studies showed the inhibitors to be equipotent, but the *in situ* rat intestinal perfusion model showed PSC-833 to be significantly more potent than the other inhibitors.[59] This suggests that in the intestinal mucosa cyclic prodrugs are substrates for multiple efflux transporters, which are inhibited differently by P-gp inhibitors. The difference between the two models is not surprising seeing as the stock Caco-2 cells used were shown to lack some of the efflux transporters found *in vivo*.[59] Overall, these data clearly demonstrate the influence that efflux transporters have on restricting the permeation of cyclic prodrugs across the rat intestinal mucosa.

1.4.3 *In Situ* Brain Perfusion

Based on low transcellular permeation across MDCK-MDR1 cell monolayers,[43-45] one would expect very limited BBB permeation of cyclic prodrugs. BBB permeability studies of DADLE and cyclic prodrugs were conducted *in vivo*

using an *in situ* rat brain perfusion model.[62,63] In these experiments, test compound was infused directly into the brain via the carotid artery. Brain tissue samples were collected and analyzed for the presence of cyclic prodrug and DADLE. These experiments show that, in the absence of a P-gp inhibitor (GF-120918), DADLE and cyclic prodrugs have very similar BBB permeation, despite their different physicochemical characteristics. DADLE has a BBB apparent permeability coefficient (P_B) of 0.5×10^7 cm/s and cyclic prodrugs have P_B values ranging from $0.4 - 1.2 \times 10^7$ cm/s. [62] The data suggest that both DADLE and cyclic prodrugs have limited BBB permeation due to efflux transporters. To ascertain the role of efflux transporters *in vivo*, the permeation of DADLE and cyclic prodrugs was determined in the presence of GF-120918.[62] The P_B values of the cyclic prodrugs were consistently higher, from 50 to 450- times, in the presence of GF-120918. However, DADLE did not show increased BBB permeation in the presence of inhibitor. This suggests that the poor BBB permeation of DADLE is not due to efflux transporters but is most likely the result of poor physicochemical properties. Interestingly, cyclic prodrugs possess more favorable physicochemical properties than DADLE but are substrates for P-gp. Overall, cyclic prodrugs have limited BBB permeation *in vivo*. These data imply that changing the structure of the peptides to form cyclic prodrugs transforms the molecules into P-gp substrates.

The role of P-gp in restricting BBB permeation of the cyclic prodrugs was investigated using known P-gp inhibitors (PSC-833, CyA, GF-120918).[64] Two models were used in the studies: the *in situ* perfused rat brain model and an *in vitro*

cell culture model (MDCK-MDR1 cells). Cyclic prodrugs exhibited low permeation in both models but, in the presence of inhibitors, the BBB permeation was significantly increased. The *in vitro* BBB model showed the inhibitors to be approximately equipotent, while the *in vivo* BBB model showed GF-120918 to be slightly more potent than CyA and PSC-833.[64] This suggests that cyclic prodrugs are substrates for multiple efflux transporters, which are inhibited differently by P-gp inhibitors. Overall, it was established that (i) P-gp is a major factor in restricting BBB permeation both *in vitro* and *in vivo*, (ii) *in vitro* BBB model successfully predicts the *in vivo* BBB permeation in rat, and (iii) MDR1 and the equivalent rat P-gp have similar substrate specificities.[64] It is clear that efflux transporters play a role in restricting the permeation of cyclic prodrugs across the rat BBB.

1.4.4 Metabolic Stability

Metabolic stability is an important biopharmaceutical property. The success of cyclic prodrugs depends not only on their permeation, but also on the molecule reaching the site of action intact. Cyclic prodrugs show low cell permeation characteristics *in vitro* and *in vivo* related to their interaction with P-gp. It has been proposed that there is a strong correlation between the substrate specificity of P-gp and cytochrome P450-3A4 (CY3A4).[48,65-68] Thus, it is reasonable to suspect that cyclic prodrugs would also be substrates for phase I metabolizing enzymes. Liver microsomes were used to ascertain the importance of phase I metabolizing enzymes in the stability of the cyclic prodrugs.[60] DADLE was found to be stable in the

presence of rat liver microsomes, but AOA-, CA-, and OMCA-DADLE were highly unstable. Less than 18% of cyclic parent remained after a 30-min incubation.[60] Inhibitors were used to probe the stability of the cyclic prodrugs under these conditions. Cyclic prodrug disappearance was found to be largely dominated by cytochrome P450 oxidation. In the presence of ketoconazole, a known CYP3A4 inhibitor, greater than 50% of the parent remained.[60] The data clearly indicate the importance of P450 metabolizing enzymes to the stability of the cyclic prodrugs and suggests that oral bioavailability of the cyclic prodrugs would be limited *in vivo* by first-pass metabolism in the liver.

1.4.5 *In Vivo* Pharmacokinetics

Modifying DADLE through cyclization and addition of a linker could lead to potential changes in drug-like properties (i.e., solubility, bioconversion, metabolism, clearance). Important biopharmaceutical properties of cyclic prodrugs were characterized after i.v. administration. The stability, bioconversion, brain-uptake, and clearance of the cyclic prodrugs were considered.

1.4.5.1 In Rat

Disappearance of cyclic prodrugs and DADLE from systemic circulation was found to be rapid in rat. Improved plasma half-lives were observed for cyclic prodrugs compared to DADLE. DADLE showed a $t_{1/2plamsa}$ of 5 min, while CA-,

OMCA-, and AOA-DADLE had plasma half-lives of 24 min, 18 min, and 14 min, respectively.[69]

Bioconversion *in vivo* paralleled *in vitro* bioconversion data (Figure 1.2).[69] For AOA-DADLE, the labile ester bond was cleaved via an esterase-catalyzed reaction to form intermediate I, which underwent further chemical degradation to release DADLE. In the case of AOA-DADLE, intermediate I was not detected; this implies rapid degradation to DADLE, CO_2, and formaldehyde. The bioconversion of CA-DADLE proceeded through intermediate II, and the OMCA-DADLE bioconversion profile proceeded through two intermediates (II and III). For OMCA-DADLE, only intermediate II was detected. This suggests that the rate-limiting step for CA- and OMCA-DADLE is the release of DADLE, while hydrolysis of the ester bond is the rate-limiting step for the bioconversion of AOA-DADLE.

Cyclic prodrugs and DADLE show very low uptake into rat brain after i.v. administration.[69] Contrary to their permeation-favorable design, cyclic prodrugs did not show better permeation than DADLE. However, DADLE was detected in rat brain after the i.v. administration of cyclic prodrugs. This is evidence of prodrug-to-DADLE bioconversion in rat brain.

The pathways of elimination for cyclic prodrugs and DADLE were found to differ. Cyclic prodrugs were quickly eliminated from systemic circulation with a significant amount removed through biliary clearance and a minor percentage via renal clearance.[69] Experiments using bile duct-cannulated rats showed 46% of AOA-DADLE, 26% of CA-DADLE, and 38% of OMCA-DADLE was recovered in the bile

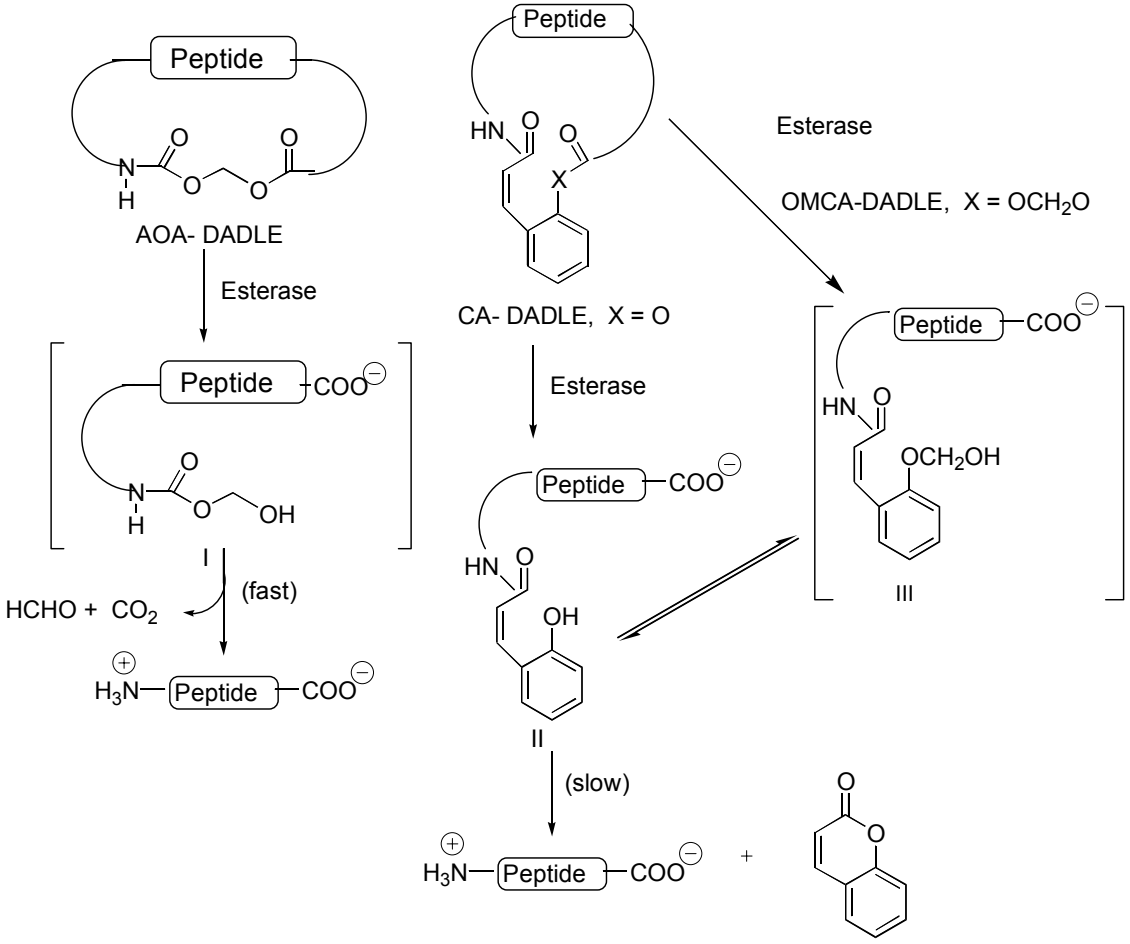

Figure 1.2. Bioconversion of AOA-, CA-, and OMCA-DADLE

after a 2-hr sample period.[69] In contrast, DADLE showed only a small recovery in bile and urine. This implies that metabolism by exo- and endopeptidases is a major elimination route for DADLE, while cyclic prodrugs are eliminated by the liver.

1.4.5.2 In Guinea Pig

The bioconversion of OMCA-DADLE was found to be much faster in rat plasma than in rat brain; however, in guinea pig, bioconversion was faster in brain than plasma.[69,70] Since the cyclic prodrugs of DADLE were designed to target the brain, an attempt to optimize the bioconversion of OMCA-DADLE was undertaken with the synthesis of amino acid-modified prodrugs of OMCA-DADLE.[41] Investigations into the bioconversion of these cyclic prodrugs led to two conclusions[70]: (i) the prodrug bioconversion profile in human biological media correlated better with the stability profile observed in guinea pig than in rat and (ii) the prodrugs containing diastereomers of DADLE had more favorable brain-to-plasma conversion profiles than DADLE itself.

Pharmacokinetic studies were undertaken with OMCA-DADLE (OMCA-[D-Ala^2,D-Leu^5]) and OMCA-[D-Ala^2,Leu^5]-Enk. In guinea pig, OMCA-cyclic prodrugs were found to disappear rapidly after i.v. administration. OMCA-DADLE showed very similar pharmacokinetic parameters in guinea pig and rat, but there was a significant species difference observed for OMCA-[D-Ala^2,Leu^5]-Enk.[71] OMCA-[D-Ala^2,Leu^5]-Enk was found to be more stable in guinea pig than in rat. A plasma half-life of 2.7 min was seen in guinea pig, but OMCA-[D-Ala^2,Leu^5]-Enk was not

detected in rat plasma.[71] The prodrug bioconversion profile for both OMCA-cyclic prodrugs in guinea pig plasma was found to be the same as the bioconversion profile in rat plasma. Intermediate II (Figure 1.2) was detected, but in levels too low to quantify.

There was a significant species difference in brain permeation of OMCA-prodrugs after i.v. administration. OMCA-DADLE showed an 80-fold increase in permeation across the BBB of guinea pig compared to the permeation across the BBB of rat.[71] The dramatically increased ability of OMCA-DADLE to penetrate the BBB in guinea pig can most likely be attributed to different substrate specificities of the efflux transporters that are expressed in guinea pig and rat BBB. This is a reasonable assumption since other studies have documented species differences in efflux transporter disposition.[72-74] Linear peptide was detected in guinea pig brain after the i.v. administration of OMCA-cyclic prodrugs. The prodrug-to-linear peptide bioconversion was 8.5 times higher in guinea pig brain than in rat brain.[71]

OMCA-cyclic prodrugs were found to be quickly eliminated in guinea pig. Biliary clearance, however, was not the major elimination route. Only 4% of the OMCA-cyclic prodrugs were recovered from bile in guinea pig compared to 40% recovery in rat.[71] This 10-fold decrease in biliary clearance is attributed to species differences in substrate specificity of the efflux transporters expressed in the liver. To investigate cyclic prodrug elimination in guinea pig, *in vitro* liver microsomal studies were performed. It was found that OMCA-DADLE cyclic prodrugs showed a greater increase in phase I metabolism in guinea pig liver microsomes than in rat liver

microsomes.[71] This suggests that the reduced bile clearance in guinea pig is, in part, due to increased phase I metabolism.

1.5 CONCLUSIONS

In the past 10 years, the development and characterization of cyclic DADLE prodrugs has been intriguing. Compared to DADLE, the cyclic prodrugs are uncharged and hydrophobic and have a unique solution structure with a lower hydrogen-bonding potential. These physicochemical properties are advantageous for increased membrane permeation. Permeation by the cyclic prodrugs, however, is limited by their substrate specificity for efflux transporters. This translates into low intestinal mucosal and BBB permeability *in vitro* and *in vivo*. While low membrane permeation contributes to the overall low bioavailability of these compounds, the pharmacokinetic profile is also responsible. The cyclic prodrugs rapidly disappear from systemic circulation in rat and guinea pig. There is very little brain uptake in rat, but a significant amount of cyclic prodrug is seen in guinea pig brain after i.v. administration. Cyclic prodrugs are eliminated by the liver, but the extent of biliary clearance is highly variable and dependent on animal species. Cyclization of the molecules transforms the peptides into substrates for cytochrome P450 enzymes. Oral bioavailability of cyclic prodrugs is most significantly limited by poor membrane permeation (i.e., intestinal and BBB), but first-pass effects in the liver and phase I oxidative metabolism are also restrictive factors.

1.6 OBJECTIVES AND SPECIFIC AIMS

Poor pharmaceutical properties have slowed the development of opioid peptides into drug products.[29,75,76] Especially troubling is low permeation through biological barriers. Our laboratory has designed cyclic prodrugs to significantly alter the physicochemical properties of the peptides. The opioid peptide prodrugs were designed to be uncharged, stable to exo- and endopeptidases, and more lipophilic, thereby potentially increasing membrane permeation. This has been accomplished using a cyclic structural design in which the N- and C-termini are joined. Cyclization of the peptides was found to bring about more favorable physicochemical properties,[17,18,31] but did not enhance membrane permeation.[44,45,59] Cyclic prodrugs were found to be substrates for efflux transporters and phase I oxidative metabolizing enzymes.[44,45,59,60] Considering that oral bioavailability is largely affected by these two factors, the objective of my dissertation research was to design metabolically stable cyclic prodrugs (Figure 1.3) and investigate their biopharmaceutical properties. This objective was accomplished through the following specific aims:

Specific Aim 1: To determine the metabolically labile sites of a parent cyclic prodrug containing a coumarinic acid linker (CA).

Specific Aim 2: To design and synthesis more metabolically stable CA-cyclic prodrugs.

Specific Aim 3: To evaluate the physicochemical properties and solution conformation of the new cyclic prodrug analogs.

Specific Aim 4: To evaluate the *in vitro* and *in vivo* permeation of the new cyclic prodrug analogs.

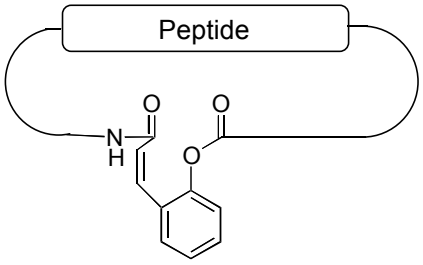

Tyr-D-Ala-Gly-Phe-D-Leu (DADLE)
Tyr-D-Ala-Gly-Cha-D-Leu ([Cha^4,D-Leu^5]-Enk)
Tyr-D-Ala-Gly-Cha-D-Ala ([Cha^4,D-Ala^5]-Enk)

Figure 1.3. Structure of CA-DADLE and cyclic prodrug analogs

1.7 REFERENCES

1. Hughes J, Smith TW, Kosterlitz HW, Fothergill LA, Morgan BA, Morris HR 1975. Identification of two related pentapeptides from the brain with potent opiate agonist activity. Nature 258:577-580.

2. Reisine T, Bell GI 1993. Molecular biology of opioid receptors. Trends Neurosci 16:506-510.

3. Mansour A, Watson SJ. 1993. Anatomical distribution of opioid receptors in mammalians: An overview. In Herz A. AH, Simon E.J., editor Handbook of Experiemental Pharmacology ed., Berlin: Springer. p 79-105.

4. Wittert G, Hope P, Pyle D 1996. Tissue distribution of opioid receptor gene expression in the rat. Biochem Biophys Res Commun 218:877-881.

5. Janecka A, Fichna J, Janecki T 2004. Opioid receptors and their ligands. Curr Top Med Chem 4:1-17.

6. Przewlocki R, Prezewlocka B 2001. Opioids in chronic pain. Eur J Pharmacol 429:79-91.

7. Beddell CR, Clark RB, Lowe LA, Wilkinson S, Chang KJ, Cuatrecasas P, Miller R 1977. A conformational analysis for leucine-enkephaline using activity and binding data of synthetic analogues. Br J Pharmacol 61:351-356.

8. Belluzzi JD, Stein L, Dvonch W, Dheer S, Gluckman MI, McGregor WH 1978. Enhanced analgesic activity of [D-Ala^2]-enkephalinamides following D-isomer substitutions at position five. Life Sciences(23):99-104.

9. Wuester M, Schulz R, Herz A 1978. Specificity of opioids towards the mu-, delta- and e-opiate receptors. Neurosci Lett 15:193-198.

10. Chang KJ, Cuatrecasas P 1979. Multiple opiate receptors. Enkephalins and morphine bind to receptors of different specifictiy. J Biol Chem 254:2610-2618.

11. Robson LE, Kosterlitz HW 1979. Specific protection of the binding sites of [D-Ala^2-D-Leu^5]-enkephalin (delta-receptors) and dihydromorphine (mu-receptors). Proc R Soc Lond B Biol Sci 205:425-432.

12. Vaught JL, Takemori AE 1979. A further characterization of the differential effects of leucine enkephalin, methionine enkephalin and their analogs on morphine-induced analgesia. J Pharmacol Exp Ther 211:280-283.

13. Deschamps JR, George C, Flippen-Anderson JL 1998. The relationship between structure and activity among opioid peptides. Lett Pept Sci 5:337-340.

14. Gorin FA, Balasubramanian TM, Cicero TJ, Schwietzer J, Marshall GR 1980. Novel analogs of enkephalin: Identification of functional groups required for biological activity. J Med Chem 23:1113-1122.

15. Mosberg HI, Hurst R, Hruby VJ, Galligan J, J., Burks TF, Gee K, Yamamura HI 1982. [D-Pen^2, L-Cys^5]Enkephalinamide and [D-Pen^2, D-Cys^5]Enkephalinamide, conformationally constrained cyclic enkephalinamide analogs with delta receptor specificity. Biochem Biophys Res Commun 106:506-512.

16. Tortella FC, Robles L, Mosberg HI, Holaday JW 1984. Electroncephalographic assessemnt of the role of delta-receptors in opioid peptide-induced seizures. Neuropeptides 5:213-216.

17. Bak A, Gudmundsson OS, Gangwar S, Friis GJ, Siahaan TJ, Borchardt RT 1999. Synthesis and evaluation of the physicochemical properties of esterase sensitive cyclic prodrugs of opioid peptides using an (acyloxy)alkoxy linker. J Pept Res 53:393-402.

18. Wang B, Nimkar K, Wang W, Zhang H, Shan D, Gudmundsson O, Gangwar S, Siahaan T, Borchardt RT 1999. Synthesis and evaluation of the physicochemical properties of esterase sensitive cyclic prodrugs of opioid peptides using coumarinic acid and phenylpropionic acid linkers. J Pept Res 53:370-382.

19. Bartosz-Bechowski H, Davis P, Slaninova J, Malatynska E, Stropova D, Porreca F, Yamamura HI, Hruby VJ 1999. Cyclic enkephalin analogs that are hybrids of DPDPE-related peptides and Met-enkephalin-Arg-Gly-Leu: Prohormone analogs that retain good potency and selectivity for delta-opioid receptors. J Pept Res 53:329-336.

20. Fowler CB, Pogozheva ID, Lomize AL, LeVine III H, Mosberg HI 2004. Complex of an active mu-opioid receptor with a cyclic peptide agonist modeled from experimental constraints. Biochemistry 43:15796-15810.

21. Hruby VJ, Bartosz-Bechowski H, Davis P, Slaninova J, Zalewska T, Stropova D, Porreca F, Yamamura HI 1997. Cyclic enkephalin analogs with exceptional potency and selectivity for delta-opioid receptors. J Med Chem 40:3957-3962.

22. Przydzial MJ, Pogozheva ID, Ho JC, Bosse KE, Sawyer E, Traynor JR, Mosberg HI 2005. Design of high affinity cyclic pentapeptide ligands for kappa-opioid receptors. J Pept Res 66:255-262.

23. Pswlak D, Oleszczuk M, Wojcik J, Pachulska M, Chung NN, Schiller PW, Izdebski J 2001. Highly potent side-chan to side-chain cycliczed enkephalin analogues containing a carbonyl bridge: synthesis, biolog and conformation. J Pept Sci 7:128-140.

24. Pauletti GM, Gangwar S, Siahaan TJ, Aube J, Borchardt RT 1997. Improvement of oral peptide bioavailability: peptide mimetics and prodrug strategies. Adv Drug Delivery Rev 27:235-256.

25. Pauletti GM, Okumu FW, Borchardt RT 1997. Effect of size and charge on the passive diffusion of peptides across Caco-2 cell monolayers via the paracellular pathway. Pharm Res (2):164-168.

26. Knipp GT, Vander Velde DG, Siahaan TJ, Borchardt RT 1997. The effect of β-turn structure on the passive diffusion of peptides across Caco-2 cell monolayers. Pharm Res 14:1332-1340.

27. Burton PS, Conradi RA, Ho NFH, Hilgers A, R., Borchardt RT 1996. How structural features influence the biomembrane permeability of peptides. J Pharm Sci 85:1336-1340.

28. Adessi C, Soto C 2002. Converting a peptide into a drug: Strategies fo improve stability and bioavailability. Curr Med Chem 9:963-978.

29. Borchardt RT 1999. Optimizing oral absorption of peptides using prodrug strategies. J Control Release 62:231-238.

30. Pauletti GM, Gangwar S, Knipp GT, Nerurkar MM, Okumu FW, Tamura K, Siahaan T, Borchardt RT 1996. Structural requiremetns fo intestinal absorption of peptide drugs. J Control Release 41:3-17.

31. Ouyang H, Borchardt RT, Siahaan TJ, Vander Velde DG 2002. Synthesis and conformational analysis of a coumarinic acid-based cyclic prodrug of an opioid peptide with modified sensitivity to esterase-catalyzed bioconversion. J Pept Res 59:183-195.

32. Stella VJ. 2007. Prodrug approaches to enhancing delivery of poorly permable drugs. In Stella VJ, Borchardt RT, Hageman MJ, Oliyai R, Maag H, Tilley JW, editors. Prodrugs: Challenges and rewards: Part I, ed., Arlington, VA: AAPS Press. p 37-82.

33. Lipinski CA, Lombardo F, Dominy BW, Feeney PJ 1997. Experimental and computational approaches to estimate solubility and permeability in drug discovery and development settings. Adv Drug Delivery Rev 23:3-25.

34. Atkinson F, Cole S, Green C, Van de Waterbeemd H 2002. Lipophilicity and other parameters affecting brain penetration. Curr Med Chem: Cent Nerv Syst Agents 2:229-240.

35. Camenisch G, Alzenz J, van de Waterbeemd H, Folkers G 1998. Estimation of permeability by passive diffusion through Caco-2 cell monolayers using the drug's lipophilicity and molecular weight. Eur J Pharm Sci 6:313-319.

36. Habgood MD, Begley DJ, Abbott NJ 2000. Determinants of passive drug entry into the central nervous system. Cell Mol Neurobiol 20:231-253.

37. Raub TJ 2006. P-glycoprotein recognition of substrates and circumvention through rational drug design. Mol Pharm 3:3-25.

38. Seelig A 2007. The role of size and charge for blood-brain barrier permeation of drugs and fatty acids. J Mol Neurosci 33:32-41.

39. Gudmundsson OS, Jois SDS, Velde DGV, Siahaan TJ, Borchardt RT, Wang B 1999. The effect of conformation on the membrane permeation of coumarinic acid and phenylpropionic acid based cyclic prodrugs of opioid peptides. J Pept Res 53:383-392.

40. Gudmundsson OS, Vander Velde DG, Jois SDS, Bak A, Siahaan TJ, Borchardt RT 1999. The effect of conformation of the acyloxyalkoxy based cyclic prodrugs of opioid peptides on their membrane permeability. J Pept Res 53:403-413.

41. Liederer BM, Fuchs T, VanderVelde D, Siahaan TJ, Borchardt RT 2006. Effects of amino acid chirality and the chemical linker on the cell permeation characteristics of cyclic prodrugs of opioid peptides. J Med Chem 49:1261-1270.

42. Bak A, Gudmundsson OS, Friis GJ, Siahaan TJ, Borchardt RT 1999. Acyloxyalkoxy-based cyclic prodrugs of opioid peptides: Evaluation of the chemical and enzymatic stability as well as their transport properties across Caco-2 cell monolayers. Pharm Res 16:24-29.

43. Ouyang H, Tang F, Siahaan TJ, Borchardt RT 2002. A modified coumarinic acid-based cyclic prodrug of an opioid peptide: Its enzymatic and chemical stability and cell permeation characteristics. Pharm Res 19:794-801.

44. Tang F, Borchardt RT 2002. Characterization of the efflux transporter(s) responsible for restricting intestinal mucosa permeation of the coumarinic acid-based cyclic prodrug of the opioid peptide DADLE. Pharm Res 19:787-793.

45. Tang F, Borchardt RT 2002. Characterization of the efflux transporter(s) responsible for restricting intestinal mucosa permeation of an acyloxyalkoxy-based cyclic prodrug of the opioid peptide DADLE. Pharm Res 19:780-786.

46. Hidalgo IJ, Weinstein K, Kardos P, Stab R. 2004. Cultured epithelial cell assays used to estimate intestinal absorption potential. In Borchardt RT, Kerns EH, Lipinsik CA, Thakker DR, Wang B, editors. Pharmaceutical profiling in drug discovery for lead selection, ed., Arlington, VA: AAPS Press. p 217-234.

47. Thakker DR. 2006. Strategic use of preclinical pharmacokinetics and *in vitro* models in optimizing ADME properties of lead compounds. In Borchardt RT, Kerns EH, Hageman MJ, Thakker DR, Stevens JL, editors. Optimizing the "drug-Like" properties of leads in drug discovery, ed., Arlington, VA: AAPS Press. p 1-23.

48. Benet LZ, Cummins CL 2001. The drug efflux-metabolism alliance: Biochemical aspects. Adv Drug Delivery Rev 50:S3-S11.

49. Raub TJ, Lutzke BS, Andrus PK, Sawada GA, Staton BA. 2006. Early precliniarl evaluation of brain exposure in support of hit identification and lead optimization. In Borchardt RT, Kerns EH, Hageman MJ, Thakker DR, Stevens JL, editors. Optimizing the "drug-like" properties of leads in drug discovery, ed., Arlington, VA: AAPS Press. p 355-410.

50. Hunter J, Hirst BH 1997. Adv Drug Delivery Rev 25:129-157.

51. Benedetti MS, Whomsley R, Espie P, Baltes E 2004. The role of efflux transporter P-glycoprotein (P-gp) on the disposition of antiepileptic drugs: Implications for drug interactions. Focus on Epilepsy Research:199-200.

52. Couture L, Nash JA, Turgeon J 2006. The ATP-binding cassette transporters and their implication in drug disposition: A speical look at the heart. Pharmacol Rev 58:244-258.

53. Feng B, Mills JB, Davidson RE, Mireles RJ, Janiszewsik JS, Troutman MD, de Morais SM 2008. *In vitro* P-glycoprotein assays to predict the *in vivo* interactions of P-glycoprotein with drugs in the central nervous system. Drug Metab Dispos 36:268-275.

54. Lau YY, Okochi H, Huang Y, Benet LZ 2006. Multiple transporters affect the disposition of atorvastatin and its two active hydroxy metabolites: Application of *in vitro* and *ex situ* systems. Expert Opin Drug Deliv 3:23-35.

55. Lin JH 2007. Transporter-mediated drug interactions: Clinical implications and *in vitro* assessment. Expert Opin Drug Metab Toxicol 3:81-92.

56. Winiwarter S, Hilgendorf C 2008. Modeling of drug-transporter interactions using structural information. Curr Opin Drug Discovery Dev 11:95-103.

57. Xia CQ, Milton MN, Gan L-S 2007. Evaluation of drug-transporter interactions using *in vitro* and *in vivo* models. Curr Drug Metab 8:341-363.

58. Griffiths R, Lewis A, Jeffray P. 1996. Models of drug absoprtion *in situ* and in conscious animals. In Borchardt RT, Smith LP, Wilson G, editors. Models for assessing drug absorption, ed., New York, NY: Plenum Press. p 67-84.

59. Ouyang H, Chen W, Anderson TE, Steffansen B, Borchardt RT 2008. Factors that restrict the cell permation of cyclic prodrugs of an opioid peptide (DADLE): (I) The role of efflux transporters in the intestinal mucosa. J Pharm Sci: Submitted

60. Ouyang H, Weiqing C, Anderson TE, Steffansen B, Borchardt RT 2008. Factors that restrict the cell permeation of cyclic prodrugs of an opioid peptide (DADLE): (II) The role of metabolic enzymes in the intestinal mucosa. J Pharm Sci:Submitted.

61. Gudmundsson OS, Pauletti GM, Wang W, Shan D, Zhang H, Wang B, Borchardt RT 1999. Coumarinic acid-based cyclic prodrugs of opioid peptides that exhibit metabolic stability to peptidases and excellent cellular permeability. Pharm Res 16:7-15.

62. Chen W, Yang JZ, Andersen R, Nielsen LH, Borchardt RT 2002. Evaluation of the permeation characteristics of a model opioid peptide, H-Tyr-D-Ala-Gly-Phe-D-Leu-OH (DADLE), and its cyclic prodrugs across the blood-brain barrier using an *in situ* perfused rat brain model. J Pharmacol Exp Ther 303:849-857.

63. Smith QR. 1996. Brain perfusion systems for the studies of drug uptake and metabolism in the central nervous system. In Borchardt RT, Smith PL, Wilson G, editors. Models for assessing drug absorption, ed., New York, NY: Plenum Press. p 285-307.

64. Ouyang H, Anderson TE, Chen W, Nofsinger R, Steffansen B, Borchardt RT A comparison of the effects of P-glycoprotein inhibitors on th blood-brain barrier permeation of cyclic prodrugs of an opioid peptide (DADLE). in preparation

65. Patel J, Mitra AK 2001. Strategies to overcome simultaneous P-glycoprotein-mediated efflux and CYP3A4-mediated metabolism of drugs. Pharmacogenomics 2:401-415.

66. Wacher VJ, Silverman JA, Zhang Y, Benet LZ 1998. Role of P-glycoprotein and cytochrome P450-3A in limiting oral absorption of peptides and peptidomimetics. J Pharm Sci 87:1322-1330.

67. Wang E-j, Lew K, Barecki M, Casciano CN, Clement RP, Johnson WW 2001. Quantitative distrinctions of active molecular recognition by P-glycoprotein and cytochrome P450 3A4. Chem Res Toxicol 14:1596-1603.

68. Zhang Y, Guo Z, Lin ET, Benet LZ 1998. Overlapping substrate specificties of cytochrome P450-3A and P-glycoprotein for a novel cysteine protease inhibitior. Drug Metab Dispos 26:360-366.

69. Yang JZ, Chen W, Borchardt RT 2002. *In vitro* stability and *in vivo* pharmacokinetic studies of a model opioid peptide, H-Tyr-D-Ala-Gly-Phe-D-Leu-OH (DADLE), and its cyclic prodrugs. J Pharmacol Exp Ther 303:840-848.

70. Liederer BM, Borchardt RT 2005. Stability of oxymethyl-modified coumarinic acid cyclic prodrugs of diastereomeric opioid peptides in biological media from various animal species including human. J Pharm Sci 94:2198-2206.

71. Liederer BM, Phan KT, Ouyang H, Borchardt RT 2005. Significant differences in the disposition of cyclic prodrugs of opioid peptides in rats and guinea pigs following IV administration. J Pharm Sci 94:2676-2687.

72. Baltes S, Gastens AM, Fedrowitz M, Potschka H, Kaever V, Loescher W 2007. Differences in the transport of the antiepileptic drugs phenytoin, levetiracetam, and carbamazepine by human and mouse P-glycoprotein. Neuropharmacology 52:333-346.

73. Cisernino S, Bourasset F, Archimbaud Y, Semiond D, Sanderink G, Scherrmann J-M 2003. Nonlinear accumulation in the brain of the new taxoid TXD258 following saturation of P-glycoprotein at the blood-brain barrier in mice and rats. Br J Pharmacol 138:1367-1375.

74. Culter L, Howes C, Deeks NJ, Buck T, Jeffrey P 2006. Development of P-glycoprotein knockout model in rodents to define species differences in its functional effect at the blood-brain barrier. J Pharm Sci 95:1944-1953.

75. Han C, Liu S, Wang B 2002. Major factors influencing peptide drug absorption. Frontiers of Biotechnology & Pharmaceuticals 3:270-290.

76. Wang W, Camenisch G, Sane DC, Zhang H, Hugger E, Wheeler GL, Borchardt RT, Wang B 2000. A courmarin-based prodrug strategy to improve the oral absorption of RGD peptidomimetics. J Controlled Release 65:245-251.

Chapter 2

Metabolic Stability of CA-DADLE and Identification of Its Metabolites

2.1 INTRODUCTION

Peptide and peptidomimetics have long been evaluated for therapeutic use due to their intrinsic receptor specificity and promising pharmacological properties.[1-5] Unfortunately, the development of these peptides into viable oral dosage forms has been limited by their undesirable physicochemical properties, including poor intestinal mucosa permeation and enzymatic instability.[6-9] The challenge in making orally viable opioid peptides lies in improving the physicochemical properties of the peptides while maintaining their high affinity for opioid receptors.

In an attempt to improve membrane permeability of opioid peptides, we have developed cyclic peptide prodrugs of the opioid DADLE (H-Tyr-D-Ala-Gly-Phe-D-Leu-OH) in which the N- and C-termini of the peptide are joined via chemical linkers, specifically the coumarinic acid linker (CA) (Figure 2.1). The resultant cyclized prodrugs are uncharged at physiological pH and exhibit unique solution structures. The solution structure of CA-DADLE has been found to contain a conformationally restricting β-turn, which enhances intramolecular hydrogen-bonding within the molecule.[10] The resultant cyclized prodrugs are uncharged, lipophilic, and exhibit lower hydrogen-bonding potential than DADLE; thus, they should display a improved membrane permeability.[11] These cyclic DADLE prodrugs, however, did not show the expected increased cell permeation. Using cell culture models, it has been determined that the cyclic prodrugs are substrates for apically polarized efflux transporters [i.e., P-glycoprotein (P-gp)] in the intestinal mucosa.[10,12-16] Considering

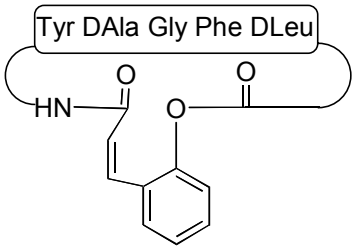

Figure 2.1. Structure of cyclic opioid peptide prodrug CA-DADLE

the fact that many P-gp substrates are also substrates for phase I enzymes,[17-20] the oxidative metabolism of these prodrugs has come into question.

CA-DADLE was used to investigate the metabolism of cyclic peptide prodrugs. Metabolic stability of CA-DADLE was evaluated in the presence of rat liver microsomes (RLM), guinea pig liver microsomes (GPLM), human liver microsomes (HLM), and human recombinant cytochrome P450 (hCYP3A4). Oxidative metabolites of CA-DADLE under these *in vitro* conditions have also been identified.

2.2 MATERIALS AND METHODS

2.2.1 Materials

The cyclic prodrug CA-DADLE was synthesized in our laboratory following described procedures.[8,21] Pooled male Sprague-Dawley rat liver microsomes (RLM), pooled male Hartely albino guinea pig liver microsomes (GPLM), pooled human liver microsomes, mixed gender microsomes(HLM), and human recombinant cytochrome P450 3A4 expressed in bactosomes (hCYP3A4) were purchased from Xenotech, LLC (Lenexa, KS). DADLE, diethyl *p*-nitrophenyl phosphate (paraoxon, approx. 90%), ketoconazole, β-nicotinamide adenine dinucleotide phosphate (β-NADPH; reduced form), sodium phosphate monobasic (NaH_2PO_4) and sodium phosphate dibasic (Na_2HPO_4,) were obtained from Sigma-Aldrich. All chemicals and solvents (HPLC grade) were used as received.

2.2.2 Metabolic Stability

Metabolic stability studies of the cyclic prodrug were preformed using RLM, GPLM, HLM and hCYP3A4. These biological media were chosen as a result of the "prodrug conversion profile" of the cyclic peptide prodrugs in the presence of various biological media and tissue homogenates previously reported by our laboratory.[22] The cyclic prodrug (2.5 μM) was incubated for 30 min at 37°C in the presence of NADPH (1 mM) in sodium phosphate buffer (100 mM, pH 7.4) with or without inhibitors (inhibitors: 100 μM paraoxon, an esterase inhibitor, and 5 μM ketoconazole, a CYP3A4 inhibitor). The assay was stopped with 100 μL of methanol and 750 μL of acetonitirile, vortexed, and the debris removed with centrifugation (13,000 × g for 15 min). The supernatant (500 μL) was evaporated to dryness (Centrivap concentrator, Labconco, Kansas City, MO) and the pellet was dissolved in 100 μL of 25% acetonitrile. Control samples were run with the addition of 100 μL of methanol to the 500 μL phosphate buffer solution (100 mM, pH 7.4) containing 1 mM NADPH and 2.5 μM cyclic prodrug. After the addition of the liver microsomes/recombinant 3A4, 750 μL of ACN was quickly added and the sample was processed as stated above. The amount of substrate remaining was calculated by dividing the average substrate peak area by the average substrate peak area in the control sample. Statistics were preformed with Sigma Stat 3.5 using a one-way ANOVA with a Hohn-Sidik multiple comparison.

2.2.3 Metabolite Identification

Phase I oxidative metabolites were identified using the same biological media as in the metabolic stability studies. The cyclic prodrug (2.5 μM) was incubated for 15 min at 37°C in the presence of NADPH (1 mM) in sodium phosphate buffer (100 mM, pH 7.4). The assay was stopped with 100 μL of methanol and 750 μL of acetonitrile, vortexed, and the debris removed by centrifugation (13,000 × g for 15 min). The supernatant (500 μL) was evaporated to dryness (Centrivap concentrator, Labconco, Kansas City, MO) and the pellet was dissolved in 100 μL of 25% acetonitrile.

2.2.4 Analytical Methods

High-performance liquid chromatography with tandem mass spectrometry detection (LC/MS/MS) was employed using a Quattro Micro triple quadrupole mass spectrometer. Liquid chromatography was conducted using a Waters 2690 HPLC system. The separation was preformed on a Vydac C18 column (50 × 1.0 mm i.d., 300 Å). The cyclic peptide prodrugs were isolated using a gradient from 5% to 95% of solvent B [solvent A: water with 0.1% formic acid (v/v) and solvent B: acetronitrile with 0.1% formic acid (v/v)]. The total run time was 20 min with a flow rate of 0.2 mL/min (3 min gradient from 5% to 40% B; 3 min gradient from 40% to 95% B; 2 min at 95%; 2 min return to 5% B; 10 min equilibration at 5% B). The eluate was analyzed by electrospray ionization (ESI) in positive mode. Precursor scans were used for detection of fragmentation with m/z = 86.6, 120.1, 136.2, 207.0.

Multiple reaction monitoring (MRM) scans were used to determine oxidative metabolites with the following *m/z* transitions: parent > 102.6, 136.1, 152.2 and 223.0 with parent *m/z* set at: 714.4 (CA-DADLE + OH). MRM scans were also used to determine the metabolic stability. Detection of the tyrosine common product ion (un-oxidized) was used to qualitatively determine the amount of cyclic parent remaining. The *m/z* transition of parent > 136.1 with the parent *m/z* set at 698.0 (CA-DADLE) was used.

2.3 RESULTS

2.3.1 Metabolic Stability

DADLE and cyclic CA-DADLE show significantly different metabolic stability profiles under the conditions studied. The metabolic stability of both DADLE and CA-DADLE has been investigated in the presence of RLM, GPLM, HLM, and hCYP3A4 with and without inhibitors. In the case of the liver microsomes, paraoxon, an esterase B inhibitor, as well as ketoconazole, a cytochrome P450 inhibitor, have been used. The metabolic stability assay conducted with hCYP3A4 contains only active P450 enzymes with no esterases present. For this reason only ketoconazole is used as an inhibitor in these assays. The studies indicate that, in the presence of RLM, DADLE has 100% parent compound remaining when no inhibitors are present (Figure 2.2). CA-DADLE, however, shows only 9% of the cyclic parent remaining with no inhibitors present (Figure 2.2). The presence of an

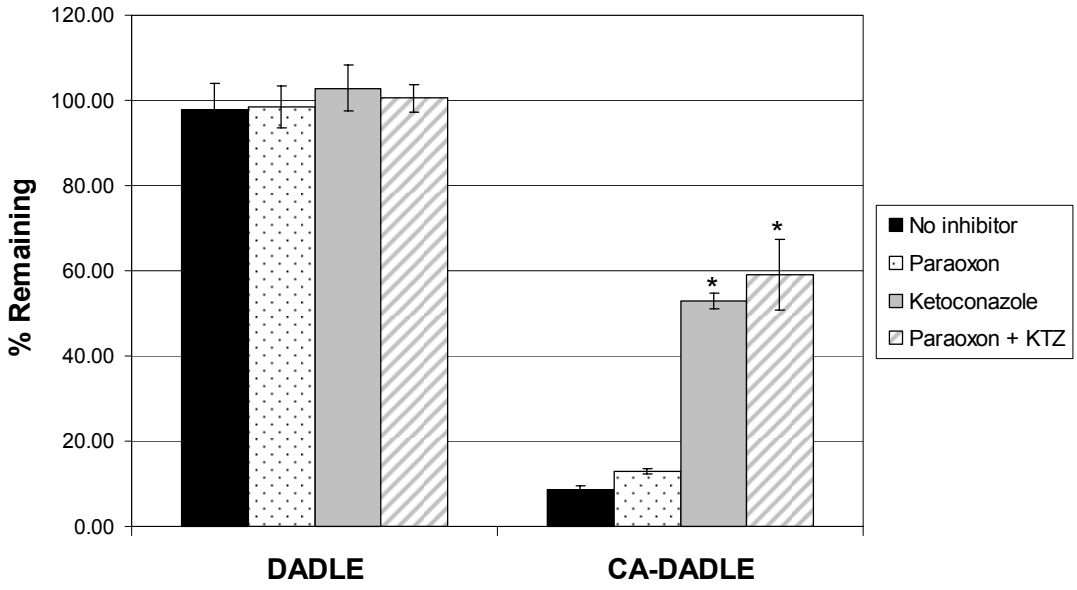

Figure 2.2. Metabolic stability of CA-DADLE in the presence of rat liver microsomes. (*$P < 0.001$)

esterase inhibitor, paraoxon, did little to enhance the metabolic stability of the cyclic prodrug, with only 13% of the cyclic parent remaining. The addition of ketoconazole, a cytochrome P450 inhibitor, produces a significant increase (53 %) in cyclic parent. A combination of both inhibitors results in 59% of the CA-DADLE being detected.

In the GPLM assays, DADLE again shows a significant amount (90%) of parent drug remaining under all conditions (Figure 2.3). With no inhibitors present, only 6% of CA-DADLE remains (Figure 2.3). Addition of paraoxon did little to enhance the amount of cyclic prodrug, with only 10% cyclic remaining after a 30-min incubation. Significant increases in the amount of CA-DADLE remaining are seen with the addition of ketoconazole (43%) and the ketoconazole/paraoxon inhibitor combination (63%).

The metabolic stability assays with HLM mirror the results of the other liver microsomal assays. DADLE is stable under all conditions, showing greater then 89% of parent drug remaining without inhibitors and above 95% parent drug remaining with inhibitors (Figure 2.4). Contrary to DADLE , CA-DADLE did not show high stability in the presence of HLM without inhibitors, showing only 15% of the parent drug remaining. The metabolic stability of CA-DADLE dramatically increases with the addition of ketoconazole and the ketoconazole/paraoxon cocktail to 85% and 90% respectively, but remains low at 12% of parent drug remaining with the addition of paraoxon alone.

Similar metabolic stability is seen in the presence of recombinant human hCYP3A4. DADLE in the presence of hCYP3A4 shows 98% of the parent remaining

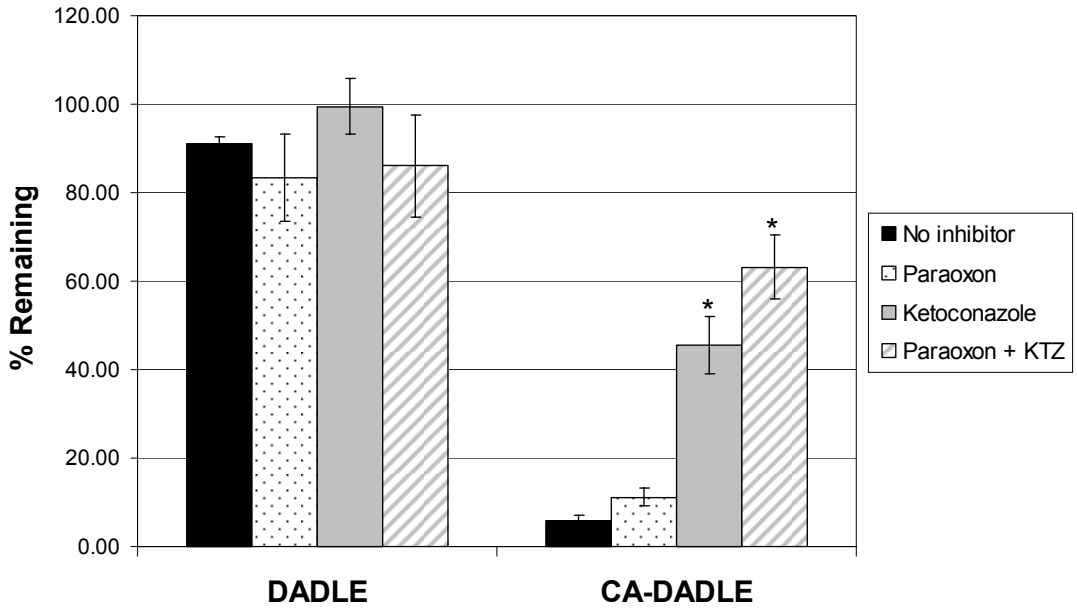

Figure 2.3. Metabolic stability of CA-DADLE in the presence of guinea pig liver microsomes. (*$P < 0.001$)

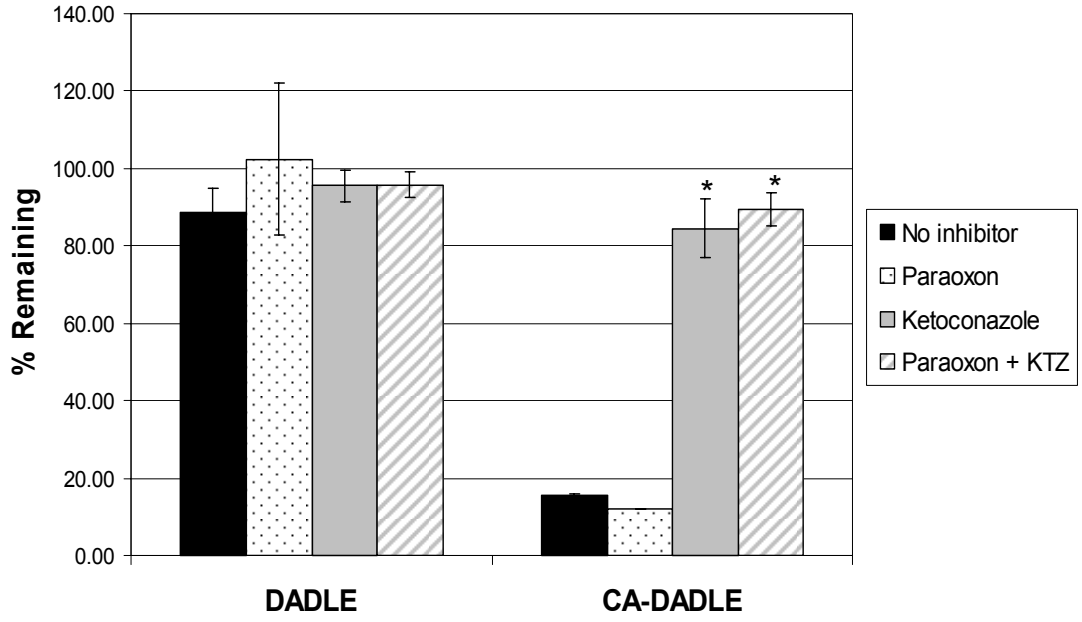

Figure 2.4. Metabolic Stability of CA-DADLE in the presence of human liver microsomes. (*P < 0.001)

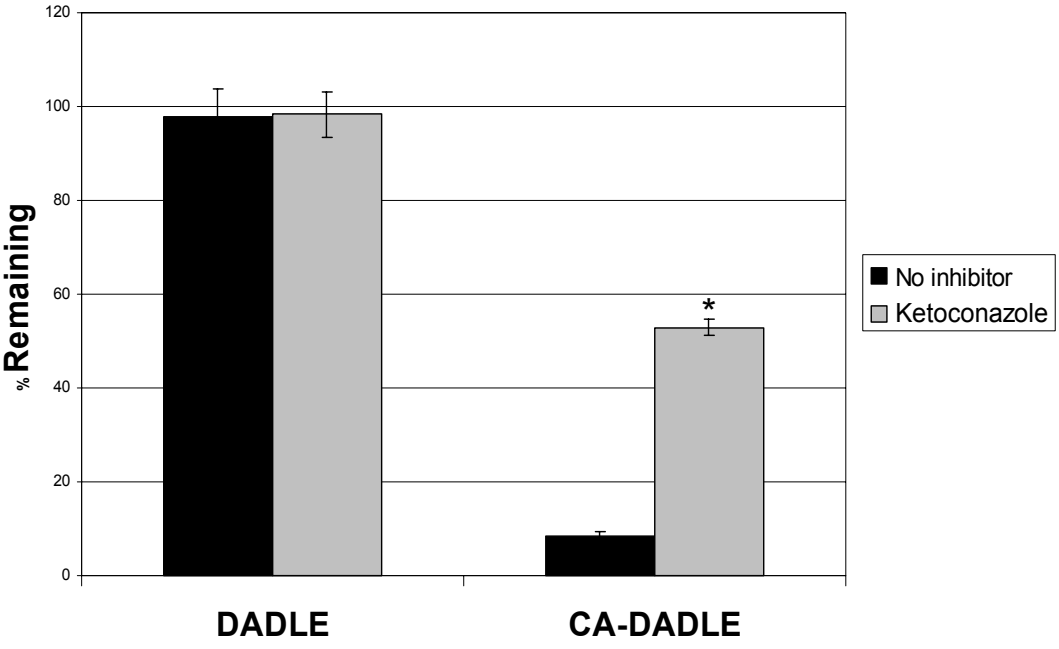

Figure 2.5. Metabolic stability of CA-DADLE in the presence of hCYP3A4. (*P < 0.001)

with and without inhibitors (Figure 2.5). Without inhibitors, only 9% of CA-DADLE remains in the presence of hCYP3A4, but with the addition of ketoconazole, 78% of the cyclic parent remains (Figure 2.5).

2.3.2 Metabolite Identification

DADLE and the cyclic peptide prodrug CA-DADLE have been analyzed by LC/MS/MS, and for both compounds similar common immonium product ions resulted (Figure 2.6). The *m/z* of these common product ions correlate with portions of the peptide that contain various amino acid fragments. The fragmentation shows peaks at *m/z* of 86.6, 120.1, 136.2, and 207.0 (Figure 2.7). These fragments are related to the amino acids of the peptide and have been identified as Leu, Phe, Tyr, and a di-peptide fragment, Tyr-Ala, respectively. In the CA-DADLE spectra there is an additional product ion peak being identified at *m/z* 147 (Figure 2.6). This fragment corresponds to the coumarin linker of the cyclic peptide prodrug compound. With the common product ions being identified for both the linear and cyclic peptide molecules, the oxidative metabolites of the CA-DADLE could be determined.

CA-DADLE was subjected to oxidative conditions, and the oxidative product ions were identified with multiple reaction monitoring (MRM). The basic schematic for an MRM scan is presented pictorially in Figure 2.8. Ions passing through Quadrupole 1 (Q1) are limited to the cyclic oxidized parent molecule containing one hydroxyl (*m/z* 714). Using the optimized collision energy from the MS/MS scans, the cyclic compound is then fragmented and the oxidized product ions are investigated in

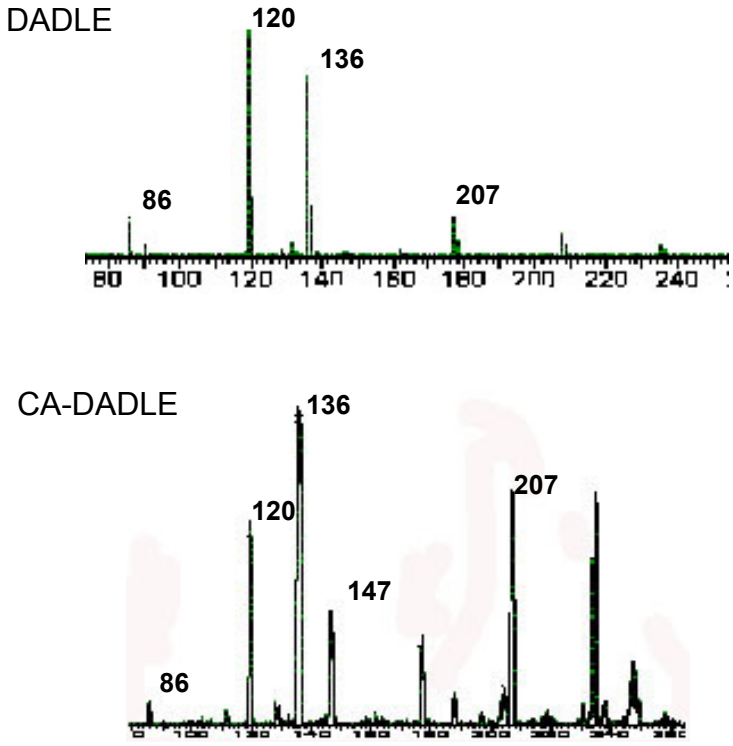

Figure 2.6. Detection of the common product ions of linear DADLE and the cyclic peptide prodrug, CA-DADLE.

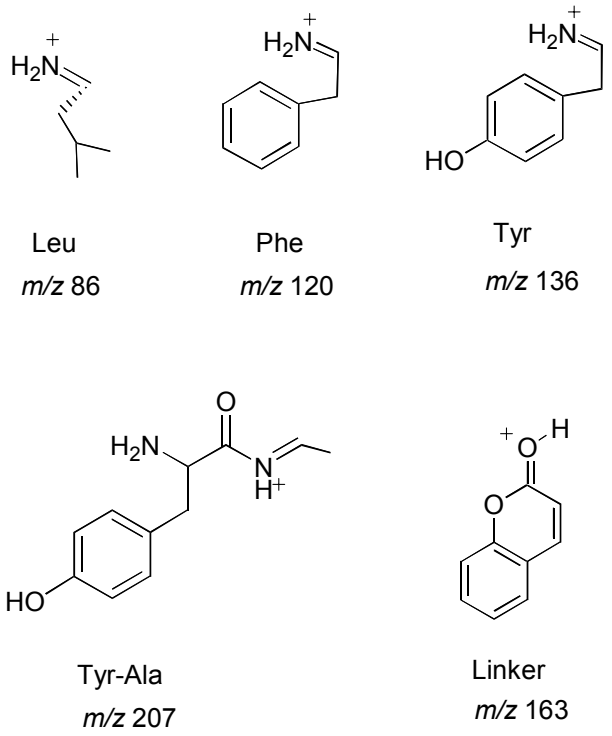

Figure 2.7. Structures of the common ion products of DADLE and CA-DADLE.

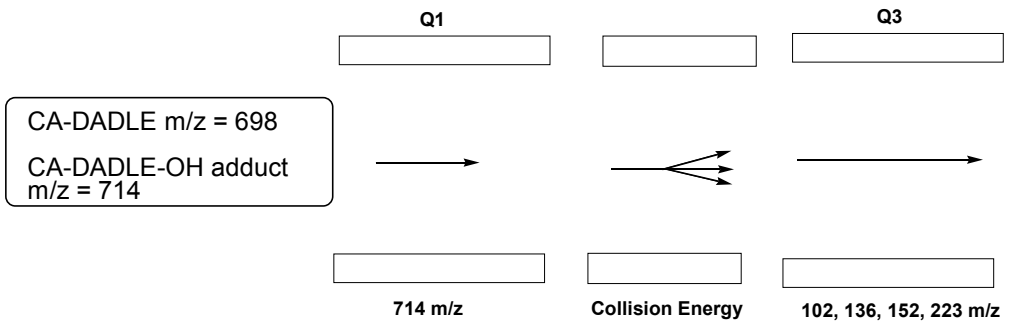

Figure 2.8. MRM scan design to detect oxidative metabolites of CA-DADLE.

quadrupole 3 (Q3). The oxidized product ions being investigated have *m/z* of 102.6, 136.1, 152.2, and 223.0. The *m/z* of these ions correlate to the previous determined product ions with the addition of a hydroxyl (Figure 2.9). Detection channels relating to each product ion *m/z* fragment are monitored and, if a peak is seen in a hydroxylated fragment channel, this is evidence that the product ion and, therefore, the corresponding amino acid, has been oxidatively metabolized. It should be noted that with this method only the amino acid undergoing oxidation can be identified. The exact location of the hydroxyl on the amino acid has not been determined. Also, when no oxidative metabolites are detected, an un-oxidized compound is identified, confirming the metabolic stability of either DADLE or CA-DADLE.

The metabolite identification studies correlate well with the metabolic stability studies. DADLE is metabolically stable under the four oxidative conditions studied; RLM, GPLM, HLM, and hCYP3A4 show no oxidative metabolites under these conditions (Figure 2.10). Confirmation of the metabolically stable DADLE is established in the sample by evidence of the presence of un-oxidized product ions. The metabolism of CA-DADLE has been studied under the same oxidative conditions but yields very different results. In the presence of rat liver microsomes and guinea pig liver microsomes, two oxidative products are observed, with the parent compound being hydroxylated on either the Tyr^1 or Phe^4 amino acid (Figure 2.11,2.12). In contrast, human liver microsomes give evidence of hydroxylation only at one amino acid position, the Phe^4 amino acid (Figure 2.13). Metabolism of CA-DADLE in the presence of hCYP3A4 reveals significant oxidation only at the Phe^4 amino acid

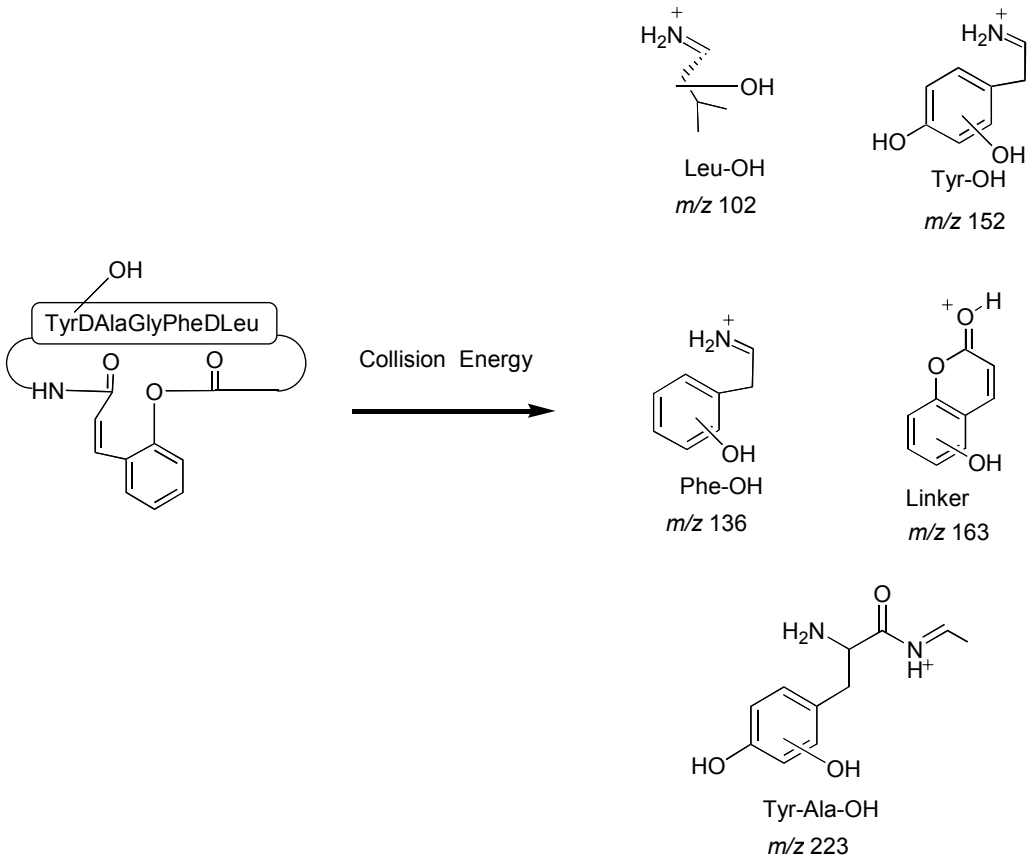

Figure 2.9. Possible oxidative product ions of CA-DADLE.

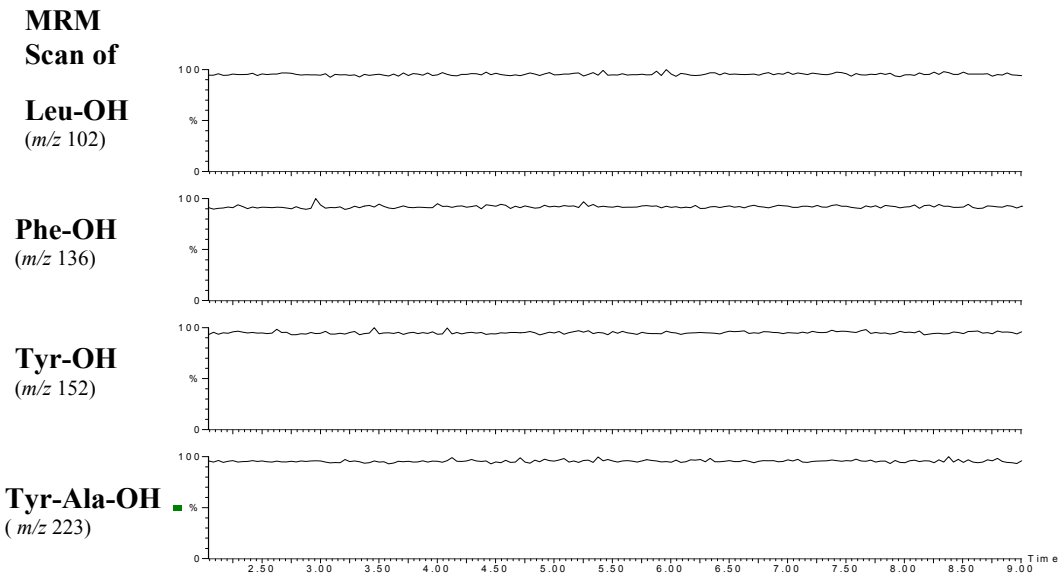

Figure 2.10. MRM Scan of DADLE metabolism in the presence of liver microsomes and hCYP3A4.

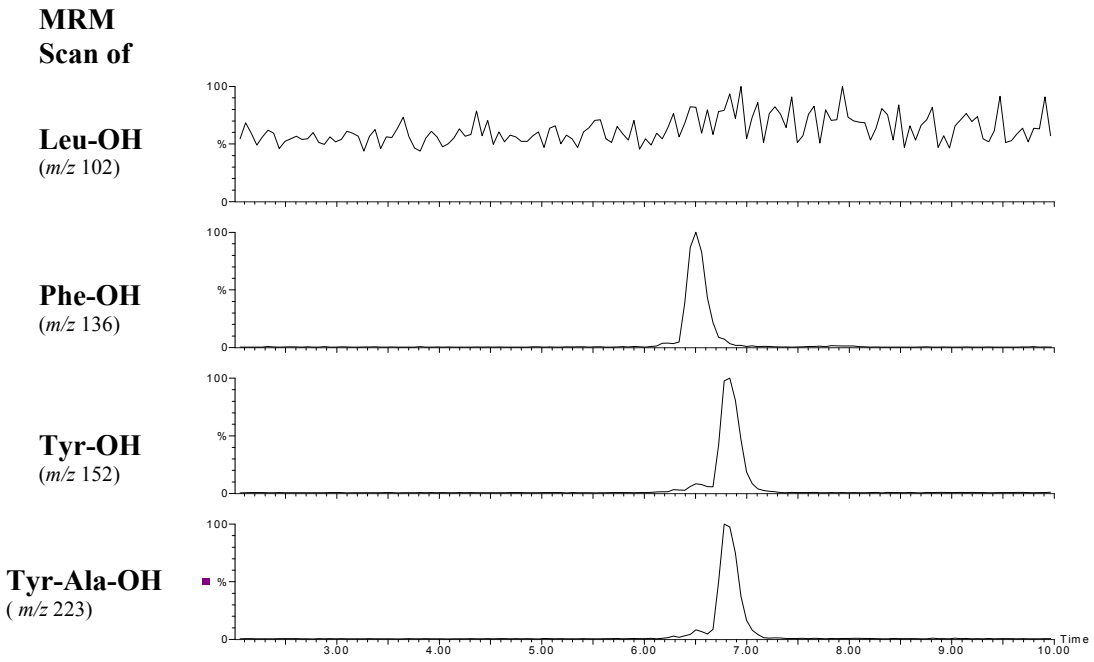

Figure 2.11. MRM scan of CA-DADLE metabolism in the presence of rat liver microsomes.

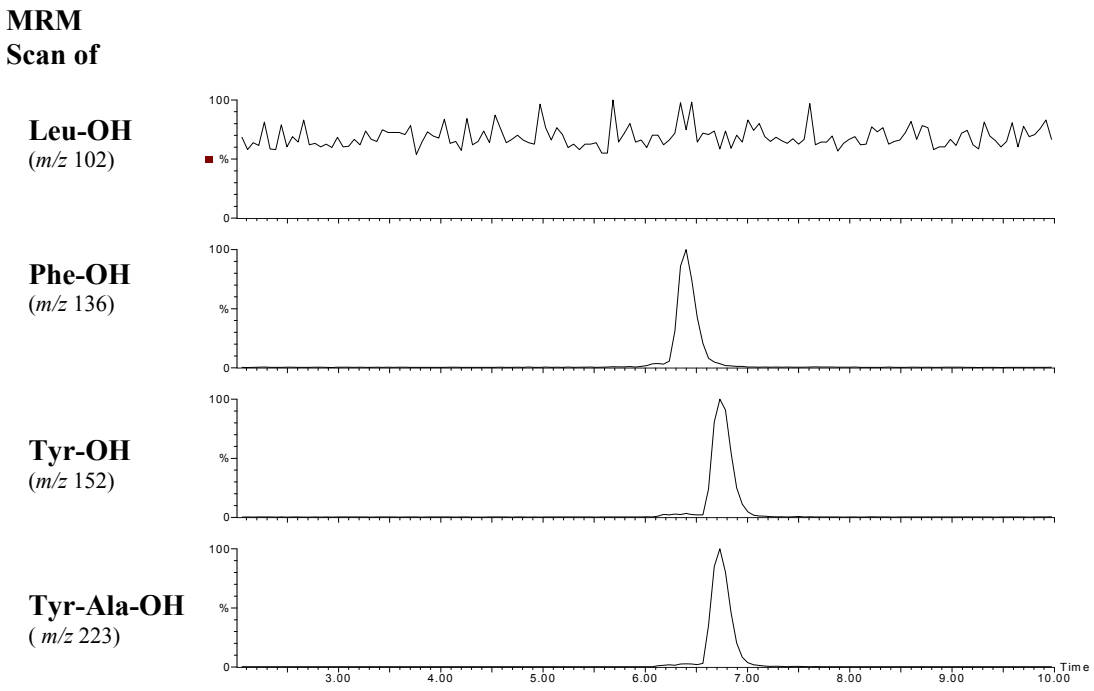

Figure 2.12. MRM scan of CA-DADLE metabolism in the presence of guinea pig liver microsomes.

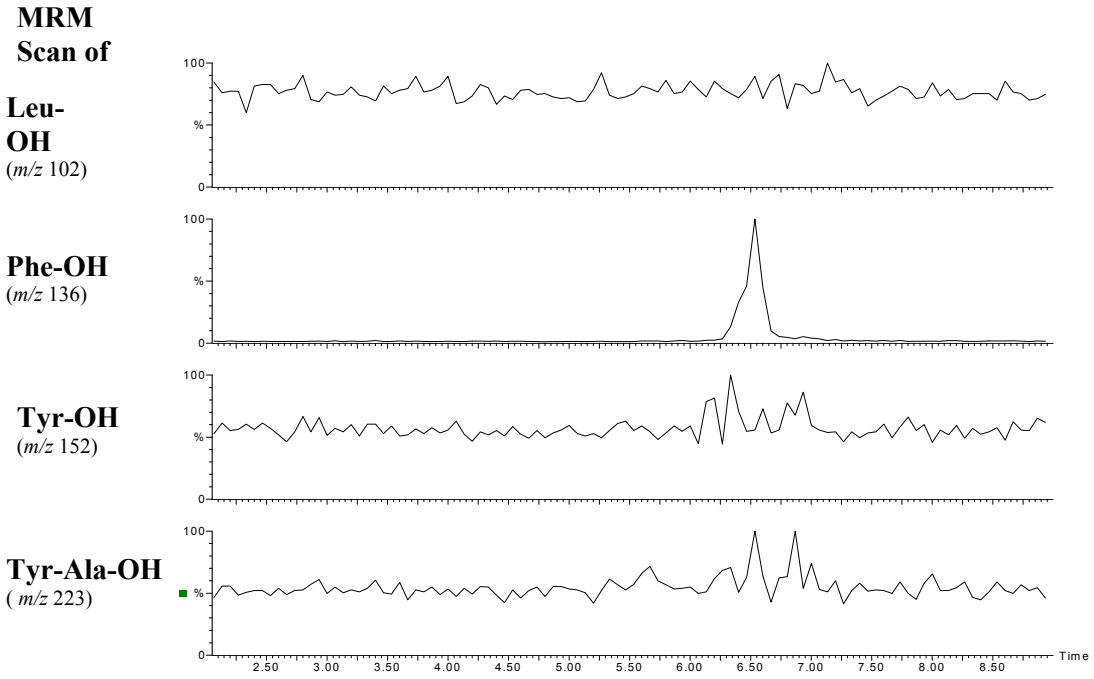

Figure 2.13. MRM scan of CA-DADLE metabolism in the presence of human liver microsomes.

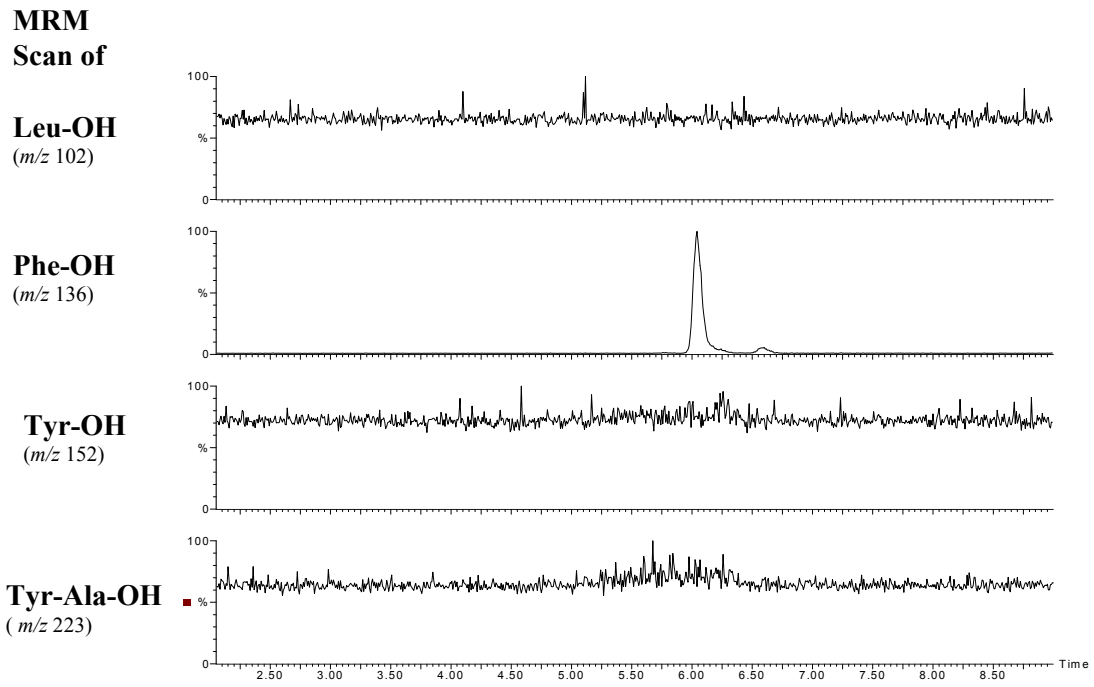

Figure 2.14. MRM scan of CA-DADLE metabolism in the presence of hCYP3A4.

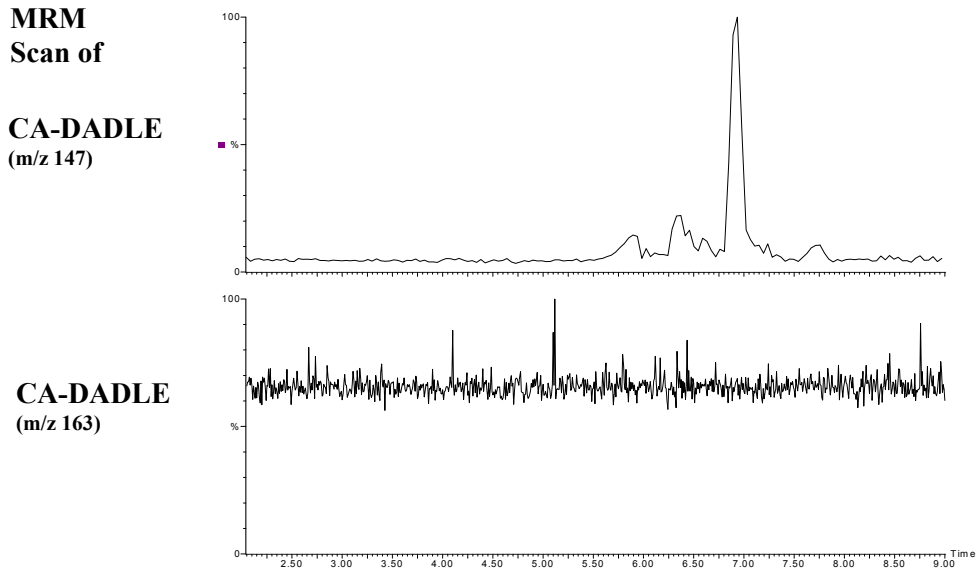

Figure 2.15. MRM Scan of the CA-DADLE reveals no significant metabolism at the coumarinic acid linker.

position, similar to what has been seen in the presence of human liver microsomes (Figure 2.14). Oxidative stability of the coumarinic acid linker has been confirmed, given that hydroxylated coumarin has not been identified under the conditions studied and only coumarin has been detected (Figure 2.15). Oxidative addition of two or three hydroxyls is not seen under any of the conditions studied.

2.4 DISCUSSION

It has been previously reported by our laboratory that the cyclic peptide prodrugs of DADLE do not have the expected increased cell membrane permeability[12-14] and that they are potentially subject to phase I oxidative metabolism. *In vitro* metabolic stability studies reveal DADLE to be metabolically stable in the presence of liver microsomes and recombinant human CYP3A4 bactosomes (Figures 2.2-2.5), while CA-DADLE shows metabolic instability under the same conditions. In assays without the presence of inhibitors, less then 10% of the cyclic CA-DADLE remains (Figures 2.2-2.5). This clearly indicates metabolic instability of CA-DADLE in the presence of these biological media. In the presence of liver microsomes, addition of an esterase B inhibitor, paraoxon, did not result in a significant increase in the amount of cyclic parent recovered (Figures 2.2-2.4). Seeing only a slight increase in the recovery of parent compound with the addition of paraoxon indicates that the metabolic instability of CA-DADLE is not likely due to a premature bioconversion of the ester prodrug. The addition of ketoconazole, a cytochrome P450 inhibitor,

significantly increased the amount of cyclic parent recovered with recovery results between 50%-60% for each assay (Figure 2.2-2.5). This strongly suggests that CA-DADLE is metabolized by P450 enzymes. There does not seem to be a large additive effect with respect to the two inhibitors, as the results from including both inhibitors mimic the results of ketoconazole alone.

Metabolite identification studies have been performed to identify the susceptibility of the linker moiety and/or amino acid(s) to oxidative metabolism. The metabolically stable DADLE shows no oxidative metabolites under all the conditions studied (Figure 2.10). This demonstrates good agreement between the metabolic stability studies and the metabolite identification studies in relation to DADLE. The more metabolically labile CA-DADLE, however, shows oxidative metabolites at either the Tyr^1 or Phe^4 amino acids in the presence of RLM or GPLM (Figures 2.11,2.12) and Phe^4 amino acid (Figure 2.13) in the presence of HLM. Since CA-DADLE is seen to be metabolically labile in the presence of liver microsomes, it is not unexpected to find oxidative metabolites being formed under these conditions. Interestingly, the HLM yielded only one oxidative metabolite (at amino acid Phe^4) while the rodent liver microsomes yielded two oxidative metabolites. Since metabolic stability and, ultimately, oral bioavailability in humans is the goal in developing these cyclic peptide prodrugs, the diminished number of oxidative metabolites in the presence of HLM is encouraging. In the presence of human recombinant cytochrome P450 containing only the 3A4 isozyme (hCYP3A4), oxidation only at Phe^4 is detected (Figure 2.14). This is consistent with the oxidative

metabolite of Phe[4] resulting from the use of human liver microsomes. Oxidation at solely the Phe[4] amino acid position is therefore continuous for the two conditions containing human biological media. This is compelling evidence that Phe[4] is a labile site for human P450 oxidative metabolism. Identification of oxidative metabolites of CA-DADLE complements the low percentage of cyclic compound recovered in the metabolic stability studies. This confirms the fact that the degradation of CA-DADLE results in part from the oxidative metabolism of the compound.

The oxidative metabolism of the coumarinic acid linker has also been investigated. Oxidation at the site of the coumarinic acid linker is considered a high probability due the known metabolic susceptibility of coumarin.[23-25] Metabolite identification studies of CA-DADLE, however, show no detection of hydroxy-coumarin (Figure 2.15), and the detection of unhydroxylated coumarin confirms the metabolic stability of the CA-linker moiety. This indicates the oxidative metabolic stability of the CA-linker when it is incorporated as part of the cyclic peptide prodrug.

The metabolic stability profile of CA-DADLE is quite unique. The fact that, in all assays and under all conditions, DADLE shows metabolic stability reveals that it is not the peptide arm itself that is subject to metabolic instability. The metabolic stability of the CA-linker moiety when incorporated within the cyclic peptide prodrug reveals that the addition of the linker itself is not the exclusive cause for the metabolic instability. Since the CA-linker moiety within the cyclic peptide prodrug is stable and the peptide arm is stable as well, this leads to the conclusion that the overall solution conformation or rigidity of the molecule leads to the metabolic instability. The

addition of the conformational restriction and decrease in rigidity appears to favor the molecule taking on a conformation that produces P450 substrate specificity. This concept of increased/decreased rigidity leading to a change in substrate specificity is not unknown. Opioid peptides themselves have been shown to have a diminished binding affinity to the opioid receptor upon cyclization, this is hypothesized as mainly due to the decrease in flexibility of the cyclic compound[26-28]. It is most likely that the decreased flexibility introduced by the conformationally restricting β-turn is causing the increased substrate specificity in the cyclized CA-DADLE. Overall, DADLE, being a linear peptide, is stable to liver microsomes and hCYP3A4, but the cyclic peptide prodrug CA-DADLE is metabolized under these conditions.

It should be noted that an in-depth investigation into the oxidative metabolite formation has not been performed. The focus of this study is to determine the amino acids that are sites of oxidative metabolism on CA-DADLE. The goal is to modify these sites in order to design cyclic peptide prodrugs that are metabolically stable to cytochrome P450.

2.5 CONCLUSION

Cyclization of the peptide DADLE with a coumarinic acid linker has the promise of increasing cell permeation characteristics but as these studies reveal, at the cost of metabolic stability. The new confined solution structure of cyclized DADLE makes the metabolically stable linear peptide vulnerable to oxidative metabolism at

Tyr^1 and Phe^4 on the peptide arm. It is also evident from these studies that cyclization leads to cytochrome P450 metabolic instability in CA-DADLE. Attempts will be made to redesign cyclic CA-DADLE via amino acid modification to increase its metabolic stability.

2.6 REFERENCES

1. Schiller PW 2005. Opioid peptide-derived analgesics. The AAPS Journal 7:Article 56.

2. Gentilucci L 2004. New trends in the development of opioid peptide analoguges as advanced remedies for pain relief. Curr Top Med Chem 4:19-38.

3. Knipp GT, Vander Velde DG, Siahaan TJ, Borchardt RT 1997. The effect of β-turn structure on the passive diffusion of peptides across Caco-2 cell monolayers. Pharm Res 14:1332-1340.

4. Schiller PW. 1993. Development of receptor-selective opioid peptide analogs as pharmacological tools and as potential drugs. Handb Exp Pharmacol, ed. p 681-710.

5. Witt KA, Davis TP 2006. CNS drug delivery; opioid peptides and the blood-brain barrier. The AAPS Journal 8:Article 9.

6. Borchardt RT 1999. Optimizing oral absorption of peptides using prodrug strategies. J Control Release 62:231-238.

7. Han C, Liu S, Wang B 2002. Major factors influencing peptide drug absorption. Frontiers of Biotechnology & Pharmaceuticals 3:270-290.

8. Wang W, Camenisch G, Sane DC, Zhang H, Hugger E, Wheeler GL, Borchardt RT, Wang B 2000. A courmarin-based prodrug strategy to improve the oral absorption of RGD peptidomimetics. J Controlled Release 65:245-251.

9. Yang JZ, Chen W, Borchardt RT 2002. *In vitro* stability and *in vivo* pharmacokinetic studies of a model opioid peptide, H-Tyr-D-Ala-Gly-Phe-D-Leu-OH (DADLE), and its cyclic prodrugs. J Pharmacol Exp Ther 303:840-848.

10. Ouyang H, Borchardt RT, Siahaan TJ, Vander Velde DG 2002. Synthesis and conformational analysis of a coumarinic acid-based cyclic prodrug of an opioid peptide with modified sensitivity to esterase-catalyzed bioconversion. J Pept Res 59:183-195.

11. Pauletti GM, Gangwar S, Wang B, Borchardt RT 1997. Esterase-sensitive cyclic prodrugs of peptides: Evaluation of a phenylpropionic acid promoiety in a model hexapeptide. Pharm Res 14:11-17.

12. Bak A, Gudmundsson OS, Friis GJ, Siahaan TJ, Borchardt RT 1999. Acyloxyalkoxy-based cyclic prodrugs of opioid peptides: Evaluation of the chemical and enzymatic stability as well as their transport properties across Caco-2 cell monolayers. Pharm Res 16:24-29.

13. Gudmundsson OS, Nimkar K, Gangwar S, Siahaan T, Borchardt RT 1999. Phenylpropionic acid-based cyclic prodrugs of opioid peptides that exhibit metabolic stability to peptidases and excellent cellular permeation. Pharm Res 16:16-23.

14. Gudmundsson OS, Pauletti GM, Wang W, Shan D, Zhang H, Wang B, Borchardt RT 1999. Coumarinic acid-based cyclic prodrugs of opioid peptides that exhibit metabolic stability to peptidases and excellent cellular permeability. Pharm Res 16:7-15.

15. Tang F, Borchardt RT 2002. Characterization of the efflux transporter(s) responsible for restricting intestinal mucosa permeation of the coumarinic acid-based cyclic prodrug of the opioid peptide DADLE. Pharm Res 19:787-793.

16. Tang F, Borchardt RT 2002. Characterization of the efflux transporter(s) responsible for restricting intestinal mucosa permeation of an acyloxyalkoxy-based cyclic prodrug of the opioid peptide DADLE. Pharm Res 19:780-786.

17. Patel J, Mitra AK 2001. Strategies to overcome simultaneous P-glycoprotein-mediated efflux and CYP3A4-mediated metabolism of drugs. Pharmacogenomics 2:401-415.

18. Wacher VJ, Silverman JA, Zhang Y, Benet LZ 1998. Role of P-glycoprotein and cytochrome P450-3A in limiting oral absorption of peptides and peptidomimetics. J Pharm Sci 87:1322-1330.

19. Wang E-j, Lew K, Barecki M, Casciano CN, Clement RP, Johnson WW 2001. Quantitative distrinctions of active molecular recognition by P-glycoprotein and cytochrome P450 3A4. Chem Res Toxicol 14:1596-1603.

20. Zhang Y, Guo Z, Lin ET, Benet LZ 1998. Overlapping substrate specificties of cytochrome P450-3A and P-glycoprotein for a novel cysteine protease inhibitior. Drug Metab Dispos 26:360-366.

21. Ouyang H, Tang F, Siahaan TJ, Borchardt RT 2002. A modified coumarinic acid-based cyclic prodrug of an opioid peptide: Its enzymatic and chemical stability and cell permeation characteristics. Pharm Res 19:794-801.

22. Liederer BM, Borchardt RT 2006. Enzymes involved in the bioconversion of ester-based prodrugs. J Pharm Sci 95:1177-1195.

23. Lewis DFV, Ito Y, Lake BG 2006. Metabolism of coumarin by human P450's: A molecular modeling study. Toxicol In Vitro 20:256-264.

24. Mead JA, Smith JN, Williams RT 1958. Stuides in detoxication.72. The metabolism of coumarin and of *o*-coumarinc acid. The Biochemical journal 68:67-74.

25. Mead JA, Smith JN, Williams RT 1958. Studies in detoxication.71. The metabolism of hydroxycoumains. The Biochemical journal 68:61-67.

Chapter 3

Synthesis of CA-DADLE Analogs and Characterization of Their Physicochemical and Conformational Properties

3.1 INTRODUCTION

Our laboratory has previously investigated the pharmacokinetic properties of the opioid peptide DADLE (H-Tyr-D-Ala-Gly-Phe-D-Leu-OH) and the cyclic prodrugs of DADLE.[1-12] These cyclic prodrugs displayed promising physicochemical properties that were expected to enhance cellular permeation.[1-4] The cyclic prodrugs, however, did not exhibit improved *in vitro* cell permeation as expected,[3,5] and recent studies also confirmed the poor permeation of the prodrugs *in vivo*.[6] It was discovered that the poor permeability of the cyclic prodrugs is attributable to their substrate specificity for efflux transporters [e.g., P-glycoprotein (P-gp)].[3,5,7,8] Since it has been established that many P-gp substrates are also substrates for phase I enzymes,[9-12] the potential oxidative metabolism of these prodrugs became of interest.

Based on the connection between substrate specificity of phase I enzymes and P-gp , the oxidative stability of the cyclic prodrugs was investigated. As reported in the previous chapter, the cyclic peptide prodrug CA-DADLE undergoes rapid oxidative metabolism in the presence of liver microsomes and human recombinant cytochrome P450-3A4 (hCYP3A4). The two main sites of oxidative metabolism on CA-DADLE were discovered to be located on the Tyr^1 and Phe^4 residues of the peptide. Using this knowledge and our general understanding of opioid peptides, two new CA-DADLE analogs were designed (Figure 3.1). This was accomplished through chemical modification of the amino acid sequence, creating the new cyclic prodrugs CA-[Cha^4,D-Leu^5]-Enk **(1)** and CA-[Cha^4,D-Ala^5]-Enk **(2)**. Ultimately, these prodrugs were designed in an attempt to improve metabolic stability and to

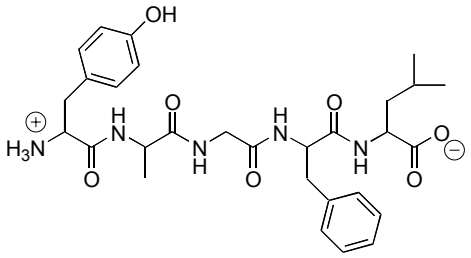

DADLE

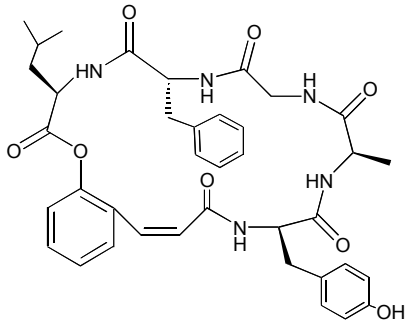

CA-DADLE

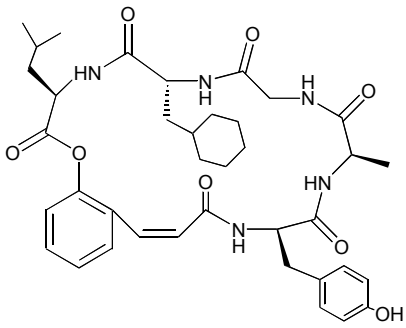

CA-[Cha^4,D-Leu^5]-Enk

(1)

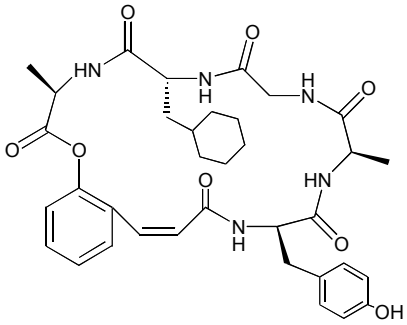

CA-[Cha^4,D-Ala^5]-Enk

(2)

Figure 3.1. Structures of DADLE, CA-DADLE, and CA-DADLE analogs.

potentially enhance oral bioavailability. In this chapter, the design, synthesis, physicochemical characterization, and solution conformation of the two CA-DADLE analogs will be discussed.

3.2 MATERIALS AND METHODS

3.2.1 Materials

Lindlar's catalysis was purchased from Fluka Chemical Corporation (Milwaukee, WI). The amino acids were purchased from Novabiochem (La Jolla, CA), and the final coupling reagent, *N*-*N*-Bis(2-oxo-3-oxozolidinyl)-phosphinic chloride was purchased from TCI-America (Portland, OR). Silica gel (Selecto Scientific) and solvents (HPLC grade) were purchased from Fisher Scientific (Pittsburgh, PA). All other chemicals were purchased from Sigma-Aldrich (St. Louis, MO). Tetrahydrofuran was distilled from sodium metal in the presence of benzophenone. Dichloromethane was distilled over calcium hydride. All other chemicals and solvents were used as received.

3.2.2 Synthesis

Abbreviations: ACN, acetonitrile; Boc, *t*-butoxy carbonyl; Bop-Cl, bis(2-oxo-3-oxazolidinyl) phosphinic chloride; $CDCl_3$, chloroform-D; CH_2Cl_2, dichloromethane; DMAP, 4-dimethylamino pyridine; DMSO, dimethylsulfoxide; EDC-HCl, 1-(3-dimethylaminoproply)-3-ethylcarbodiimide; HOBt, 1-hydroxybenzotriazole; LDA,

lithium diisopropylamide; MeOD, methanol-D4; $MgSO_4$, magnesium sulfate; $NHCO_3$, sodium biocarbonate; OAll, allyl protecting group; Pac, phenacyl protecting group; P-gp, P-glycoprotein; ROESY, rotating frame Overhauser effect spectroscopy; TEA, triethyl amine; TFA, trifluoracetic acid; THF, terahydrofuran; TOCSY, total correlation spectroscopy

Standard solution-phase peptide synthesis using Boc-amino acid chemistry

Coupling: The Boc-protected amino acid (26 mmol) was dissolved in dry tetrahydrofuran (300 mL) and put on ice. To this solution was added EDC-HCl (7 g, 37 mmol) and HOBt (5.7 g, 42 mmol). The solution was stirred for 5 min, and then to this solution was added TEA (5.6 g, 55 mmol), DMAP (353 mg, 3 mmol), and the C-terminal-protected peptide (30 mmol). The reaction was stirred at room temperature for 5 hr. The tetrahydrofuran was removed *in vacuo*. The residue was dissolved in ethyl acetate (500 mL) and extracted with 10% citric acid (3 × 200 mL), 5% $NHCO_3$ solution (3 × 200 mL), and saturated brine (1 x 200 mL). The organic layer was dried over $MgSO_4$ and filtered. The solvent was removed to give the desired peptide. The product was used in the next step without purification.

Deprotection: To remove the N-terminal Boc group, the peptide (34.3 mmol) was dissolved in ethyl acetate (50 mL) and cooled to 0°C. HCl gas was bubbled through the solution for 15 min. The gas was removed, and the reaction was stirred an

additional 15 min at 0°C. The solvent was removed *in vacuo*. The product was used unpurified in the next reaction.

Peptide arm:

Boc-D-Ala-Gly-OAll (4). Yield: 100 %. R_f = 0.51 (chloroform/methanol, 3:1). ^{1}H NMR (400 MHz, $CDCl_3$) δ 1.28 (d, 3H, J=7.0), 1.34 (s, 9H), 3.96 (m, 2H), 4.21 (s, 1H), 4.53 (d, 2H, J=5.6), 5.13 (d, 1H, J=10.4), 5.21 (d, 1H, J=17.2), 5.54 (s, 1H), 5.79 (m, 1H). ^{13}C NMR (400 MHz, $CDCl_3$) δ 28.22, 41.08, 49.85, 79.67, 118.63, 124.85, 128.73, 131.48, 143.25, 155.49, 169.4, 173.6.

H-D-Ala-Gly-OAll (5). Yield: 100%. R_f = 0.12 (dichloromethane/methanol/acetic acid, 20:3:0.1). ^{1}H NMR (400 MHz, MeOD) δ 1.56 (d, 3H, J=5.8), 3.99 (m, 2H), 4.59 (d, 2H, J=4.8), 5.18 (d, 1H, J=10.3), 5.27 (d, 1H, j=17.1), 5.89 (m, 1H). ^{13}C NMR (400 MHz, $CDCl_3$) δ 40.74, 49.03, 65.55, 117.58, 131.9, 169.29, 170.39.

Boc-Tyr-D-Ala-Gly-OAll (6). Yield: 100%. R_f = 0.23 (chloroform/acetonitrile, 3:1). ^{1}H NMR (400 MHz, $CDCl_3$) δ 1.20 (d, 3H, J=6.5), 1.37 (s, 9H), 2.91 (m, 2H), 4.05 (dd, 2H, J_1=17.4, J_2=52.3), 4.16 (m, 1H), 4.33 (d, 1H, J=7.2), 4.61 (d, 2H, J=5.6), 5.21 (dd, 1H, J_1=1.2, J_2=10.5), 5.31 (dd, 1H, J_1=1.5, J_2=17.2), 5.93 (m, 1H), 6.72 (d, 2H, J=8.5), 7.04 (d, 2H, J=8.3). ^{13}C NMR (400 MHz, MeOD) δ 17.58, 28.28, 41.27, 48.62, 56.64, 66.05, 80.32, 115.63, 118.94, 127.39, 130.32, 131.43, 155.55, 155.85, 169.67, 172.06, 172.87.

Boc-Tyr-D-Ala-Gly-OH (7). Yield: 100%. R_f= 0.11 (chloroform/methanol, 3:1). ^{1}H NMR (400 MHz, MeOD) δ 1.21 (t, 3H J_1= 7.0, J_2=14.1) 1.10 (s, 9H), 2.92 (m, 2H), 3.69 (dd, 2H, J_1=17.1, J_2=76.0), 4.21 (s, 1H), 4.31 (m, 1H), 6.72 (d, 2H, J=7.7), 7.05 (d, 2H, J=7.7). ^{13}C NMR (400 MHz, MeOD) δ 17.01, 27.37,36.88,42.55,56.95, 79.46,114.86,127.44, 130.02, 155.99, 156.42, 173.21, 173.45.

Boc-Tyr-D-Ala-Gly-Cha-OAll (8). Yield: 100%. R_f= 0.78 (chloroform/methanol, 3:1). ^{1}H NMR (400 MHz, MeOD) 0.91 (m, 2H), 1.25 (m, 6H), 1.41 (s, 9H), 1.71 (m, 7H), 2.90 (m, 2H). 3.90 (m 2H), 4.14 (m, 1H), 4.52 (m, 1H0, 4.61(m, 2H), 5.31 (dd, 2H, J_1=1.4, J_2=17.2), 5.91 (m, 1H),6.72 (d, 2H J=8.3), 7.03 (d, 2H, J=8.2). ^{13}C NMR (400 MHz, MeOD) δ15.72, 25.72, 25.97, 26.17, 27.42, 31.86, 33.35, 33.79, 38.62, 42.02, 49.48, 50.20, 56.91, 65.28, 79.45, 114.83, 117.29, 127.37, 130.02, 131.96, 156.01, 156.54, 170.22, 172.27, 173.27, 173.94.

H-Tyr-D-Ala-Gly-Cha-OAll (9). Yield: 100%. R_f= 0.68 (chloroform/methanol, 3:1). ^{1}H NMR (400 MHz, MeOD) δ 0.95 (m, 2H), 1.25 (d, 3H, J=7.2), 1.40 (m, 1H), 1.70 (m, 7H), 3.07 (m, 2H), 3.91 (s, 2H), 4.10 (t, 1H, J_1=7.5, J_2=15.0), 4.25 (d, 1H, J=7.2), 4.55 (dd, 1H, J_1=6.5, J_2=8.4), 4.62 (s, 2H), 5.23 (d, 1H J=10.5), 5.31 (d, 1H, J=17.2), 5.92 (m, 1H), 6.80 (d, 2H J=8.3), 7.11 (d, 2H J=8.3). ^{13}C NMR (400 MHz, MeOD) δ16.04, 25.72, 25.93, 26.13, 31.89, 33.29, 33.88, 36.28, 38.74, 41.81, 49.58, 50.10, 54.80, 65.47, 115.38, 117.43, 124.69, 130.22, 131.86, 156.88, 168.73, 170.07, 170.15, 172.67, 173.56.

CA-Linker:

Phenacyl 3-(2-hydroxyphenyl)-propynoate (10). Compound **10** was synthesized using a method previously described.[2] ^{1}H NMR (400 MHz, $CDCl_3$) δ 5.52 (s,2H), 6.93 (t, 1H, J_1=7.5, J_2=16.1), 7.00 (d, 1H, J=8.4), 7.39 (t, 1H, J_1=8.3, J_2=17.4), 7.49 (m, 3H), 7.64 (t, 1H, J_1=7.4, J_2=13.7), 7.94 (d, 2H, J=9.5). ^{13}C NMR (400 MHz, $CDCl_3$) δ 67.18, 83.69, 83.33, 105.84, 115.96, 120.69, 127.87, 128.99, 133.38, 133.75, 133.83, 134.22, 153.14, 159.07, 191.02.

Phenacyl 3-(2'-Boc-alacylocyl hydroxyphenyl)-propynoate (11). Phenacyl 3-(2-hydroxylphenyl)-propynoate **(10)** (1g, 3.7 mmol) was dissolved in 40 mL of dry dichloromethane. In another flask containing 10 mL of dry dichloromethane was dissolved Boc-D-Ala-OH (840 mg, 4.4 mmol), EDC (707 mg**,** 3.7 mmol), and DMAP (452 mg, 3.7 mmol). The mixture was stirred at 0°C for 5 min. The solution with compound **10** was transferred to the flask containing the activated amino acid via cannula and stirred at 0°C for 5 hr. Dichloromethane was removed *in vacuo*. The residue was dissolved in ethyl acetate (200 mL) and extracted with 10% citric acid (3 × 100 mL), 5% $NaHCO_3$ solution (3 × 100 mL), and brine (1 × 100 mL). The organic layer was dried over $MgSO_4$, filtered, and evaporated to a foam (1.05 g, 66%). The foam was purified by silica gel column chromatography with chloroform/ethyl acetate (20:1) to give a yellowish oil (750 mg, 47%). R_f = 0.37 (chloroform/ ethyl acetate, 20:1). ^{1}H NMR (400 MHz, $CDCl_3$) δ 1.46 (s, 9H), 1.68 (d, 3H, J=7.28), 4.64 (m, 1H), 5.31 (m, 1H), 5.48 (s, 2H), ^{13}C NMR (400 MHz, $CDCl_3$) δ 17.99, 28.29, 49.56,

67.15, 79.82, 82.52, 84.48, 85.20, 113.51, 122.75, 126.32, 127.77, 128.92, 132.41, 133.77, 134.26, 152.78, 155.36, 171.29, 190.76.

Phenacyl 3-(2'-Boc-alacylocyl hydroxyphenyl)-propenoate (12). Phenacyl 3-(2'-Boc-alacylocyl hydroxyphenyl)-propynoate **(11)** (750 mg, 1.72 mmol) was dissolved in absolute ethanol (60 mL). To this was added Lindlar catalyst (5 wt % of palladium on calcium carbonate, poisoned with lead; 10% w/w, 75 mg) and quinoline (2% w/w, 15 mg). The reaction was stirred at 0°C. Hydrogen gas was bubbled through the solution for 30 min. The HCl gas was removed and the reaction, which was monitored by ^{1}H NMR, was stirred under a hydrogen atmosphere until complete. Upon completion, the catalyst was removed and the solvent evaporated *in vacuo* to give a yellowish foam (680 mg, 82%). The foam was purified by silica gel column chromatography with hexanes/ethyl acetate (4:1) to give a light yellow solid (670 mg, 80%). R_f =0.65 (ethyl acetate/hexanes/methanol, 2:4:1). ^{1}H NMR (400 MHz, $CDCl_3$) δ 1.46 (s, 9H), 1.56 (d, 3H, J=7.3), 4.53 (t, 1H, J_1=7.2, J_2=14.5), 5.37 (d, 2H, J=16.4), 6.22 (d, 1H, J=12.2), 7.08 (m, 2H), 7.21 (t, 1H, J_1=7.6, J_2=15.2), 7.32 (m, 1H), 7.46 (m, 2H), 7.59 (m, 2H), 7.87 (d, 2H, J=7.2). ^{13}C NMR (400 MHz, $CDCl_3$) δ 18.35, 28.34, 49.56, 66.09, 79.96, 121.21, 121.74, 125.73, 127.80, 128.83, 129.93, 130.30, 133.92, 134.09, 139.60, 147.86, 155.38, 164.52, 171.62, 192.09.

3-(2'-Boc-alacylocyl hydroxyphenyl)-propenoic (13). A mixture of phenacyl 3-(2'-Boc-alacylocyl hydroxyphenyl)-propenoate **(12)** (100 mg, 0.21 mmol**)** and zinc

powder (271 mg, 4.14 mmol) was cooled to 10°C. Acetic acid (22 mL) was slowly added to the reaction. The mixture was stirred at 10°C for 30 min. The supernant was filtered and concentrated *in vacuo*. The residual oil was purified by silica gel column chromatography with ethyl acetate/hexanes/methanol (2:4:1) to give a colorless oil (90 mg, 75%). R_f = 0.43 (ethyl acetate/hexanes/methanol (2:4:1). ^{1}H NMR (400 MHz, MeOD) δ 1.48 (s, 9H), 1.52 (d, 3H, J=7.3), 4.38 (m, 1H), 6.10 (d, 1H, J=12.4), 6.87 (d, 1H, J=12.4), 7.11 (d, 1H, J=8.0), 7.22 (t, 1H, J_1=7.4, J_2=14.6), 7.35 (t, 1H, J_1=7.6, J_2=15.2), 7.64 (d, 1H, J=7.3). ^{13}C NMR (400 MHz, $CDCl_3$) δ 18.07, 28.30, 49.43, 80.25, 121.72, 122.81, 125.78, 128.16, 129.80, 130.47, 137.88.

Compound (14). A mixture of compound **13** (112 mg, 0.31 mmol), EDC (82 mg, 0.43 mmol), and HOBt (66 mg, 0.49 mmol) was dissolved in dry tetrahydrofuran (6 mL) and stirred at 0°C for 5 min. To this solution was added DMAP (4 mg, 0.03 mmol) and TEA (66 mg, 0.64 mmol). In another flask, H-Tyr-D-Ala-Gly-Cha-OAll **(9)** (170mg, 0.33 mmol) was dissolved in 4 mL dry tetrahydrofuran and transferred via cannula to the reaction flask containing compound **13**. The mixture was stirred at room temperature for 6 hr. Tetrahydrofuran was removed *in vacuo*. The residue was dissolved in ethyl acetate (100 mL) and extracted with 10% citric acid (2 × 50mL), 5% $NaHCO_3$ solution (2 × 50 mL), and brine (1 × 500 mL). The organic layer was dried over $MgSO_4$, filtered, and evaporated to a yellowish white solid (200 mg, 80%). The solid was purified by silica gel column chromatography with chloroform/methanol (20:1) to give a white solid (110 mg, 44%). R_f = 0.26

(chloroform/methanol, 20:1). ^{1}H NMR (400 MHz, $CDCl_3$) δ 0.87 (m, 2H), 1.16 (m, 6H), 1.40 (s, 9H), 1.53 (d, 3H, J=7.2), 1.63 (m, 7H), 2.55 (m, 1H), 2.74 (m, 1H), 3.90 (m, 2H), 4.35 (m, 2H), 4.59 (m, 3H), 5.24 (d, 2H, J=10.4), 5.33 (d, 2H, J=17.3), 5.85 (m, 1H), 6.10 (d, 1H J=12.1), 6.67 (m, 3H), 6.84 (d, 2H, J=7.3), 7.00 (m, 2H), 7.20 (m, 1H), 7.32 (m, 1H). ^{13}C NMR (400 MHz, $CDCl_3$) δ 18.11, 25.91, 26.10, 26.36, 28.37, 32.32, 33.40,33.92, 39.40,49.33, 50.35, 65.85, 80.33, 115.65, 118.70, 121.88, 126.52, 127.15, 129.01, 130.28, 131.61, 147.80, 155.51, 166.84, 169.65, 172.59, 173.01.

Compound (15)

Removal of Allyl group: Compound **14** (110 mg, 0.13 mmol) was dissolved in 10 mL dry tetrahydrofuran. To this solution was added $Pd(PPh_3)_4$ (15.5 mg, 1.0 mmol) and morpholine (117 mg, 1.34 mmol). The reaction was then stirred at room temperature for 90 min. The tetrahydrofuran was evaporated *in vacuo* and the residual oil was purified by silica gel column chromatography with chloroform/methanol (3:1). R_f = 0.43 (chloroform/methanol, 3:1).

Removal of Boc-group: The -OAll deprotected product from above was dissolved in ethyl acetate (60 mL) and cooled to 0°C. HCl (gas) was bubbled through the solution for 10 min. The HCl gas was removed, and the solution stirred for another 10 min at 0°C. The ethyl acetate was evaporated to give a white solid in quantitative yield. The product was used in the next step without further purification. Total yield for these

two steps was 49%. R_f = 0.47 (chloroform/methanol, 20:1). ^{1}H NMR (400 MHz, MeOD) δ 0.94 (m, 2H), 1.17 (d, 3H, J=7.3), 1.43 (m, 1H), 1.57 (m, 1H), 1.72 (d, 3H, J= 7.1), 1.76 (m, 7H), 2.87 (d, 2H, J=7.5), 3.66 (dd, 2H, J_1=16.8, J_2=50.6), 3.86 (m, 1H), 4.30 (m, 1H), 4.40 (m, 2H), 6.25 (d, 1H, J=12.1), 6.72 (d, 2H, J=8.3), 6.83 (d, 1H, J=12.2), 7.01 (d, 2H, J=8.1), 7.17 (d, 1H, J=8.5), 7.23 (t, 1H, J_1=7.3, J_2= 14.7), 7.38 (d, 2H, J=7.4). ^{13}C NMR (400 MHz, MeOD) δ 19.38, 25.70, 25.97, 26.18, 31.83, 33.43, 33.81, 36.17, 38.92, 42.06, 48.66, 56.10, 60.15, 114.87, 121.33, 125.53, 126.13, 126.85, 129.05, 129.15, 129.91, 130.13, 133.25, 147.13, 156.12, 166.79, 168.31, 170.40, 172.70.

CA-[Cha^4,D-Ala^5]-Enk (2). Compound **15** was dissolved in 1 mL anhydrous N,N-dimethylformamide and then diluted with 50 mL of dichloromethane. To this solution was added TEA (30 mg, 0.3 mmol) and Bop-Cl (53 mg, 0.21 mmol). A cloudy mixture resulted, and the reaction was stirred at room temperature for 18 hr. The resultant clear yellow solution was evaporated *in vacuo* to give a yellow solid. The solid was dissolved in ethyl acetate (10 mL) and washed with another 10 mL of water. The ethyl acetate layer was collected and washed with 10% citric acid (1 × 10 mL), and 5% $NaHCO_3$ solution (1 × 10mL). The organic layer was collected, dried with $MgSO_4$, filtered, and evaporated to a clear oil. The oil was purified by semi-preparative HPLC with UV detection. The elulate was analyzed by ESI-MS. Fractions containing peptide prodrug were combined and lyophilized to give a white solid (6.7 mg, 34%). Semi-preparative HPLC was done using a C18 Dynamax

column (300 Å). The cyclic peptide prodrug was isolated using a gradient from 10% to 100% B (solvent A: 90% water with 0.01% formic acid; solvent B: 90% acetonitrile with 0.01% formic acid). The gradient was applied stepwise for a total run time of 121 min with a flow rate of 5 mL/min (16 min gradient from 10% to 30% B; 10 min gradient from 30% to 40% B; 40% B for 10 min; 15 min gradient from 40% to 45% B; 10 min gradient from 45% to 100% B; 15 min at 100% B; 15 min return to 10% B; 30 min equilibration at 10% B). The peptide prodrug had a retention time of about 45 min. R_f = 0.22 (chloroform/methanol, 20:1) ^{1}H NMR (400 MHz, MeOD) δ 0.99 (m, 4H), 1.20 (d, 3H, J=7.3), 1.25 (m, 9H), 1.56 (d, 3H, J=7.4), 1.74 (m, 7H), 2.85 (m, 2H), 3.88 (m, 2H), 4.03 (m, 1H), 4.28 (m, 1H), 4.46 (m, 1H), 4.65 (m, 1H), 6.20 (d, 1H, J=12.1), 6.70 (d, 2H, J=8.5), 6.78 (d, 1H, J=12.0), 6.97 (d, 2H, J=8.3), 7.07 (m, 1H), 7.23 (m, 1H), 7.36 (m, 2H). ESI-MS *m/z* 662.6 (M+1)

CA-[Cha^4,D-Leu^5]-Enk (1). ^{1}H-NMR (500 MHz, MeOD-d_4) δ 1.37 (dd, 6H, J_1=6.0, J_2=17.3), 1.57 (d, 3H, J=7.3), 1.65 (m, 3H), 1.82 (m, 2H), 2.11 (m, 9H), 3.10 (dd, 1H, J_1=7.3, J_2=13.7), 3.21 (m, 1H), 4.18 (d, 1H, J=17.1), 4.31 (dd, 1H, J_1=7.3, J_2=14.6) 4.68 (t, 1H, J_1=7.7, J_2=15.1), 4.86 (dd, 1H, J_1=5.5, J_2=10.0), 5.05 (m, 1H), 6.55 (d, 1H, J=12.1), 7.06 (d, 2H, 8.5), 7.14 (d, 1H, J=12.1), 7.28 (d, 2H, J=8.4), 7.42 (d, 1H, J=8.0), 7.60 (m, 2H), 7.73 (m, 1H). ESI-MS *m/z* 704.5 (M+1).

3.2.3 Physicochemical Properties

The molecular surface area and cLogP estimations were performed on a Silicon Graphics Computer using Sybyl Version 7.2.3 (Tripos Inc., St. Louis, MO). Calculations were performed on a final energy-minimized form of the cyclic prodrugs **1** and **2**. The cLogP values were obtained from the Molecular Spreadsheet. The molecular surface areas were calculated using Connolly molecular surfaces.

3.2.4 Conformation

The solution conformations of cyclic prodrugs **1** and **2** were determined by NMR and molecular dynamics (MD) simulations. The NMR data were collected using 2-3 mg of the cyclic prodrugs dissolved in DMSO-d_6 (0.6 mL). One- and two-dimensional NMR experiments were performed on a Varian Inova 800 at 293 K. Coupling constants were obtained from a DQF-COSY spectrum at 293 K. ROESY spectra were collected with a 300 ms spin-lock time. The through space inter-proton interactions were calculated using the volume integration of the ROE amide cross-peaks. The intensities of the interactions were classified as strong, medium, or weak using the upper and lower boundary distances of 1.8-2.8, 1.8-3.6, and 1.8-5 Å, respectively. The NMR data were processed using FELIX software (version 95, Biosym Technologies, San Diego, CA) with a final matrix of 1K x 1K data points.

The solution structures of cyclic prodrugs **1** and **2** were also evaluated using MD simulations. Because of the highly restricted nature of the cyclic prodrugs (i.e., the conformationally restricting *cis*-alkene and *trans* peptide bonds), the MD

simulations were determined starting from an energy minimized cyclic structure generated in Sybyl (Version 7.2.3; Tripos Inc., St. Louis, MO). From this energy minimized structure, a single peptide bond between the linker moiety and the fifth amino acid was broken to give a linear precursor. This linear precursor was energy minimized using the following constraints: (i) the *cis*-alkene moiety was held to a *cis* conformation and (ii) all the bonds in the peptide backbone were held in the *trans* conformation. MD simulations using the ROE constraints from the 2D NMR data (see above) were then performed to slowly bring the two ends of the linear precursor together. The MD simulations were performed stepwise in 5 simulations at 300 K for 5 ps each. The starting bond closure distance between the ends of the linear precursor was 5 Å. A starting penalty force of 25 kcal/mol $Å^2$ was used for both the closing of the terminal ends of the linear precursor, and the ROE constraint distances within the backbone. During each subsequent MD simulation step, the bond closure distance was decreased to 3, 2, and 1.7Å, and the penalty force constant was doubled. Once the ends of the linear precursor were within 1.7-2.0 Å, a covalent bond was made joining the two ends. A final MD simulation using only the ROE constraints with the maximum penalty force constant was performed. This gave the final cyclic prodrug structure. The dielectric constant was used to simulate solvent effects. Dielectric constants of 45 and 87.74 were used to represent DMSO and water, respectively. The final cyclic prodrug structures were analyzed in terms of dihedral angles and observed ROE distances.

3.3 RESULTS

3.3.1 Synthesis

The synthesis and characterization of the new CA-DADLE analogs (Figure 3.1) was undertaken using methodology described earlier by our labortary.[2] Generally, the cyclic prodrugs were synthesized by cyclization of a linear precursor, forming the peptide bond between the fourth and fifth amino acids in the peptide sequence (Figure 3.2). These linear precursors were built from a linker moiety and a tetrapeptide (Figure 3.2). The general synthesis of the linker moiety was reported elsewhere.[13] The tetrapeptides were synthesized utilizing standard solution phase Boc-amino acid chemistry with L-amino acids unless otherwise designated. The structural identities of the cyclic prodrugs were confirmed by ^{1}H-NMR and ESI-MS.

3.3.2 Physicochemical Properties

Cyclic peptide prodrugs **1** and **2** were designed to have permeation-favorable physicochemical properties and, thus, optimized cell membrane permeability. Lipophilicity and molecular size are two important physicochemical properties that directly affect cell membrane permeation.[14-16] cLogP values give a good estimate of a molecule's lipophilicity, and the calculated molecular surface area gives a good estimate of the overall size of the molecule. For these reasons, the molecular surface area and cLog P values were determined for CA-[Cha^{4},D-Leu^{5}]-Enk **(1)** and CA-[Cha^{4},D-Ala^{5}]-Enk **(2).** The cyclic prodrug analogs **1** and **2** exhibited cLogP values of 6.19 and 4.73, respectively (Table 3.1). These results illustrate that the cyclic

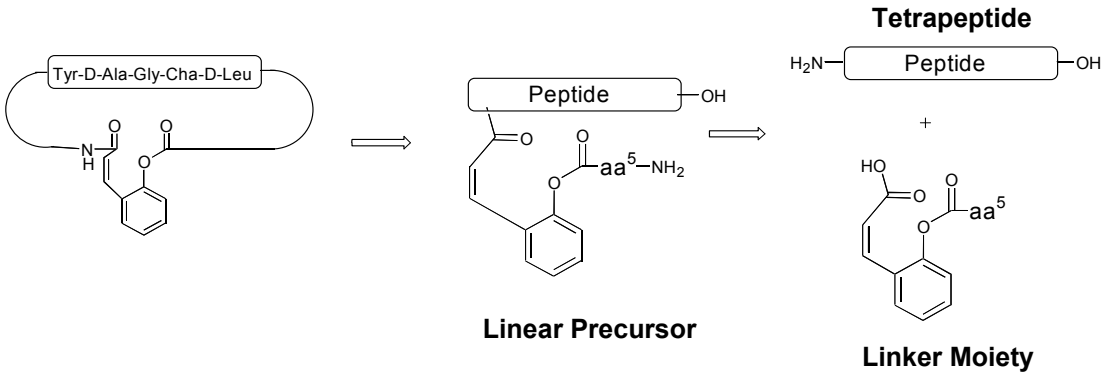

Figure 3.2. Retrosynthetic analysis leading to the peptide arm and coumarinic acid linker fragments.

Table 3.1. Physicochemical properties of DADLE and its cyclic peptide prodrugs.

	Molecular mass	cLogP	Molecular surface area (A^2)[a]
DADLE	571	-0.32	529.89
CA-DADLE	697	4.96	548.50
CA-[Cha^4,D-Leu^5]-Enk	703	6.19	536.99
CA-[Cha^4,D-Ala^5]-Enk	661	4.73	474.34

[a]MOLCAD of SYBL 7.2.3 was used to calculate the Connolly molecular surface.

peptide prodrugs **(1** and **2)** display higher cLogP values than does DADLE (cLogP = -0.32; Table 3.1). This verifies the increased lipophilic character of cyclic prodrugs **1** and **2** compared to DADLE.

Along with lipophilicity, molecular surface area is another important physicochemical property to consider when characterizing a molecule. With the addition of a linker moiety, the cyclic prodrugs have a higher molecular weight than DADLE (Table 3.1). Despite this fact, the cyclic prodrugs were found to have molecular surface areas similar to DADLE (Table 3.1). This confirms the idea that when linear, the peptides are conformationally mobile. Once cyclized, however, they adopt a more compact structure. Having a defined solution structure could play a role in the cellular membrane permeability of cyclic prodrugs **1** and **2**.

3.3.3 Conformation

2D NMR studies were conducted to elucidate the solution conformation of CA-[Cha^4,D-Leu^5]-Enk **(1)** and CA-[Cha^4,D-Ala^5]-Enk **(2)**. Proton chemical shifts were identified from total correlation spectroscopy (TOCSY) and rotating frame Overhauser effect spectroscopy (ROESY). Characterization of the peptide backbone conformation and intramolecular hydrogen bonding of the cyclic prodrug was determined using amide-amide peak correlations in the ROESY spectrum. CA-[Cha^4,D-Leu^5]-Enk **(1)** shows through-space interactions between the NH of Gly^3 and the NH of cychexalanine^4 (Cha) and also between the NH of Cha^4 and the NH of Leu^5 (Figure 3.3; Panel A). The same ROE cross-peaks are observed in CA-[Cha^4,D-

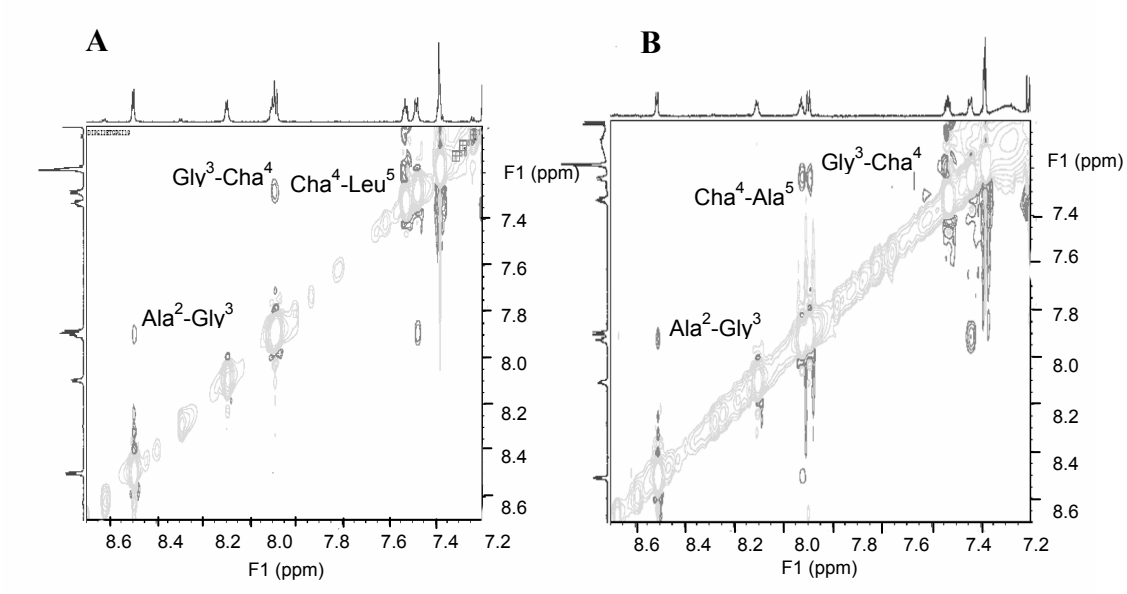

Figure 3.3. Amide region of the ROESY spectrum for cyclic CA-DADLE analogs; CA-[Cha^4,D-Leu^5]-Enk (Panel A) and CA-[Cha^4,D-Ala^5]-Enk (Panel B).

Ala^5]-Enk **(2)** (Figure 3.3; Panel B). In the spectrum of CA-[Cha^4,D-Ala^5]-Enk **(2)**, these two peaks are resolved, but they overlap in the CA-[Cha^4,D-Leu^5]-Enk **(1)** spectrum. This overlap in the cyclic prodrug **1** spectrum makes the strength of the connectivity and, thus, the through space inter-proton interactions difficult to determine exactly. Therefore, the NMR distance constraints determined for CA-[Cha^4,D-Leu^5]-Enk **(1)** are more variable than for CA-[Cha^4,D-Ala^5]-Enk **(2)**. The data clearly indicate, however, that the two cyclic analogs **1** and **2** both show ROE cross-peaks indicative of a β-turn structure.

The solution conformations of cyclic prodrugs **1** and **2** were additionally characterized by MD simulations. The simulations were performed using distance constraints obtained from the ROESY spectra (see above) with the energy-minimized average structures shown in Figure 3.4 (Panels A and B). The measured dihedral angles (φ,ψ) were all within 36° of the dihedral angles calculated from the NMR-derived coupling constant with two exceptions (Table 3.2). These deviations occurred with CA-[Cha^4,D-Leu^5]-Enk **(1),** where the phi angle (φ) related to Gly^3 solvated in water was measured to be slightly higher than the NMR calculated values. Also, the phi (φ) and psi (ψ) dihedral angles related to Gly^{3}and Cha^4 in cyclic prodrug **1** were found to be higher than expected. These derivations most likely resulted from applying the estimated NMR distance constraints related to Gly^3 and Cha^4 in the MD simulations. The simulations were further validated using through-space intramolecular ROE distance constraints. In the MD-derived models, the measured distances from the NH of the peptide backbone to the Hα of the amino acid side chain

were found to correlate well with the NMR-derived distance constraints. In these experiments, solvation was mimicked by changes in the dielectric constant. Varying the dielectric constant in the MD simulations was found to have very little effect on the measured dihedral angles (Table 3.2) and, ultimately, the final energy-minimized structure of cyclic prodrugs **1** and **2** (Figure 3.4, Panel C).

3.4 DISCUSSION

In an attempt to improve the biopharmaceutical properties of cyclic DADLE prodrugs, two new analogs of CA-DADLE, CA-[Cha^4,D-Leu^5]-Enk **(1)** and CA-[Cha^4,D-Ala^5]-Enk **(2)**, were synthesized and their physicochemical properties characterized (Figure 3.1). The main goal in designing these new CA-DADLE analogs was to add stability toward oxidative metabolism while still maintaining high affinity for the opioid receptor. Previous studies from our laboratory illustrated that CA-DADLE was oxidized on the Tyr^1 and Phe^4 residues (Chapter 1). Since it has been well established that modification to the Tyr^1 residue of an opioid peptide dramatically decreases opioid receptor affinity,[17-20] changes at this site were not attempted. We decided instead to modify the Phe^4 residue of CA-DADLE.

The cyclic prodrug analog **1** was designed to differ from CA-DADLE at a selected metabolically labile amino acid. A modification of the fourth amino acid residue from Phe to Cha created CA-[Cha^4,D-Leu^5]-Enk **(1)**. In the enkephalin class of opioid peptides, peptides with this structural change (Phe to Cha) have been shown

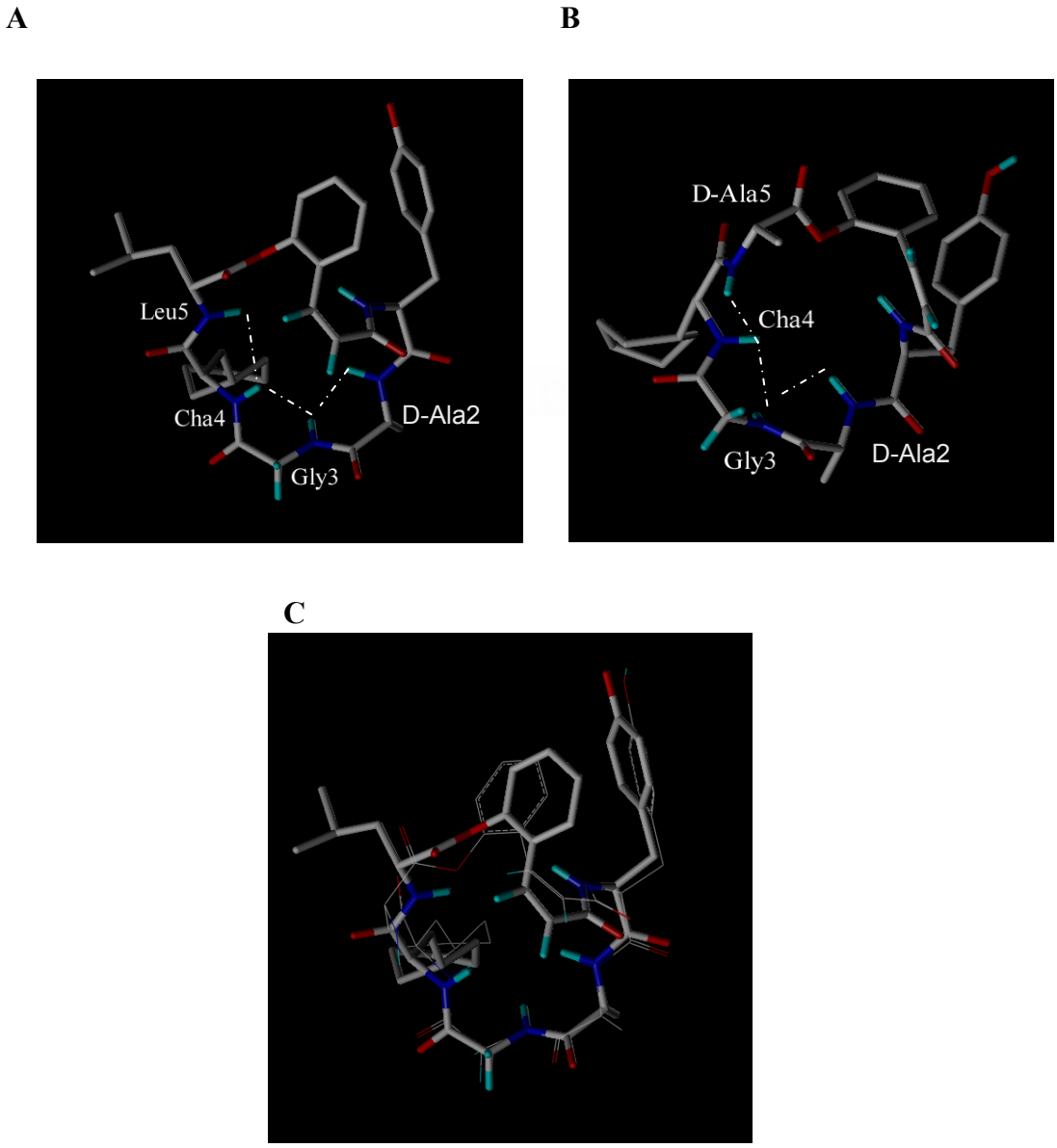

Figure 3.4. Energy-minimized average structures of CA-[Cha^4,D-Leu^5]-Enk **(1)** (Panel A) and CA-[Cha^4,D-Leu^5]-Enk **(2)** (Panel B) with intramolecular hydrogen bonds shown (- -- - -). CA-DADLE analogs overlaid, capped stick = CA-[Cha^4,D-Leu^5]-Enk (Panel C).

Table 3.2. Chemical shifts, coupling constants, and dihedral angles (calculated from coupling constants and measured from energy-minimized average structures) for CA-DADLE analogs.

	Chemical shift (ppm) NH	Coupling constant $^3J_{NH\alpha}$ (Hz)	calcd φ (deg)	Measured			
				φ (deg) DMSO	φ (deg) water	ψ (deg) DMSO	ψ (deg) water
			CA-[Cha^4,D-Leu^5]-Enk				
Tyr-1	8.10	3.9	-179, -65, 8, 104	-41	-40	-47	-48
D-Ala-2	8.50	4.6	-175, -70, 19, 102	-150	-156	-62	-59
Gly-3*	7.91	9.0	-149, -43, 43, 149	-164	-193	57	55
Cha-4	7.29	3.0	-172, -112, 12, 60	-136	-138	-65	-69
D-Leu-5	7.89	3.4	-175, -115, 15, 54	-149	-149	NA	NA
			CA-[Cha^4,D-Ala^5]-Enk				
Tyr-1	8.11	3.6	-178, -65, 7, 106	-48	-54	-48	-54
D-Ala-2	8.51	4.6	-175, -70, 19, 102	-170	-164	-50	-60
Gly-3*	7.93	9.1	-148, -43, 43, 148	-162	-150	57	47
Cha-4	7.25	3.0	-172, -112, 12, 60	-136	-136	32	41
D-Ala-5	7.90	3.6	-119, -12, 58, 180	56	48	NA	NA

* $\Sigma J_{NH\text{-}CH2.}$

to retain opioid-like activity *in vivo*[21] with only slight modification of the potency and binding affinity of the peptide.[22] Other opioid peptides have also been shown to maintain modest binding affinity to the opioid receptors with a Phe to Cha modification in the amino acid sequence.[23-25]

The second analog, CA-[Cha^4,D-Ala^5]-Enk **(2)**, contains the aforementioned Phe^4-to-Cha^4 structural change with an additional modification at the fifth amino acid residue. The rationale for changing this amino acid from D-Leu^5 to D-Ala^5 was to increase the bioconversion of the prodrugs. The bioconversion is catalyzed by esterases and is thought to proceed first through hydrolysis of the ester bond (Figure 3.5). Cleavage of this bond leaves a phenolic group on the aromatic linker moiety and releases the C-terminal end of the peptide, forming an intermediate. Finally, intramolecular lactonization results in the formation of coumarin and the linear peptide. Since hydrolysis of the ester bond is the rate-determining step in the bioconversion, a quick cleavage of this bond would be preferred. The new cyclic prodrug analog **2** reduces steric bulk around the ester bond, leaving it more exposed to esterases and potentially aiding in the bioconversion of the cyclic prodrug. In support of this idea, it has been shown that a decrease in steric bulk around the ester bond increases the lactonization rate in similar cyclic prodrugs.[26]

The strategy for the synthesis was taken from a retrosythetic analysis of the desired molecules. Retrosythethically, the bond between the fourth and fifth amino acid was broken, leading to a linear precursor (Figure 3.2). The molecule was than further broken down into two parts: (i) a tetrapeptide arm and (ii) a linker moiety

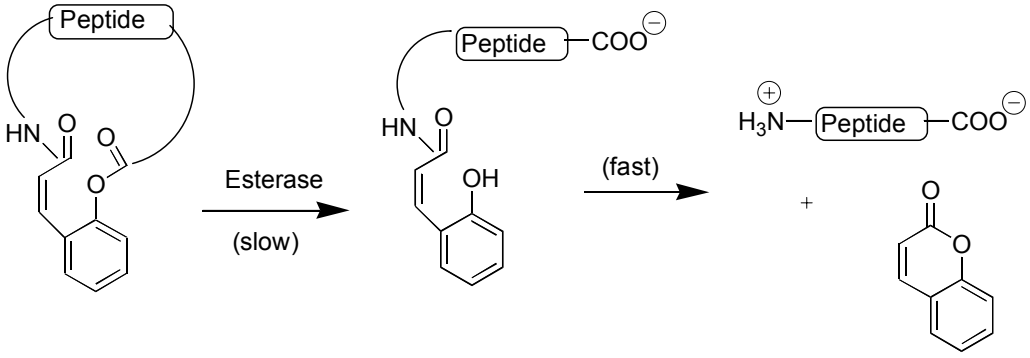

Figure 3.5. Scheme for the bioconversion of the ester-based cyclic prodrugs.

containing the fifth amino acid (Figure 3.2). These two parts were the building blocks for the convergent synthesis of the cyclic peptide prodrug analogs. The advantage to using this method is that all the cyclic prodrugs can be constructed from these two building blocks. Thus, this strategy provides a reduction in the amount of synthesis required to make the cyclic prodrugs.

Upon completion of the synthesis, the physicochemical properties of the new prodrugs CA-[Cha^4,D-Leu^5]-Enk **(1)** and CA-[Cha^4,D-Ala^5]-Enk **(2)** were determined. The addition of the lipophilic linker and removal of charge by cyclization generated molecules that were more lipophilic than DADLE (Table 3.1). It was found that the addition of the linker to the cyclic prodrugs increased the molecular surface area of CA-[Cha^4,D-Leu^5]-Enk **(1)** only slightly and actually slightly decreased the molecular surface area of CA-[Cha^4,D-Ala^5]-Enk **(2)** compared to DADLE (Table 3.1). Since an overall increase in the molecular surface area of a molecule typically leads to a decrease in cell membrane permeation,[12,27,28] having cyclic molecules with molecular surface area similar to that of linear DADLE is advantageous to increasing their cell membrane permeation. The results indicate that cyclic prodrug analogs **1** and **2** have no charge, are more lipophilic, and have a molecular surface area similar to that of DADLE, all of which will presumably lead to increased cell membrane permeation.

Solution conformation is another important key to understanding the physicochemical properties and permeation of the cyclic prodrugs. NMR and molecular modeling experiments were performed to probe the solution conformation

of cyclic prodrugs **1** and **2**. The cyclic structures were found to contain intramolecular hydrogen bonding not present in linear DADLE. These interactions lead to a solution structure that is more defined in the cyclic prodrug analogs **1** and **2**. Restricted conformations in cyclic DADLE prodrugs have been shown to alter the hydrogen-bonding potential and, therefore, change the physicochemical properties of the cyclic prodrugs.[29-31] For cyclic prodrugs **1** and **2,** the intramolecular hydrogen bonding is easily seen in the NMR spectra (Figure 3.3) and the MD models (Figure 3.4; Panels A and B). The ROE cross-peaks for both CA-[Cha^4,D-Leu^5]-Enk **(1)** and CA-[Cha^4,D-Ala^5]-Enk **(2)** (Figure 3.3) suggest a type I β-turn at D-Ala^2-Gly^3-Cha^4-Ala/Leu^5 (Figure 3.6; Panel A).[32] Evidence of the type I β-turn structure is seen between the same positions on the peptide regardless of the amino acid residues present. This suggests that modification of the amino acid in the fifth position of the peptide leads to minimal differences in the conformational structure between the analogs. An overlap of the MD models confirms the structural similarities between cyclic prodrugs **1** and **2** (Figure 3.4; Panel C).

While both cyclic prodrugs **1** and **2** exhibit evidence of a type I β-turn structure at D-Ala^2-Gly^3-Cha^4-Ala/Leu^5 (Figure 3.6), the spectra also contains a third interaction between Ala^2 and Gly^3 (Figure 3.3). Addition of this third cross-peak illustrates possible distortion away from the type I β-turn geometry. Similar cyclic prodrugs have displayed this connectivity between the second and third amino acid residues and were shown to contain a type II β-turn structure (Figure 3.6; Panel B).[29,30] The cyclic prodrug analogs **1** and **2** show this third cross-peak to be weaker

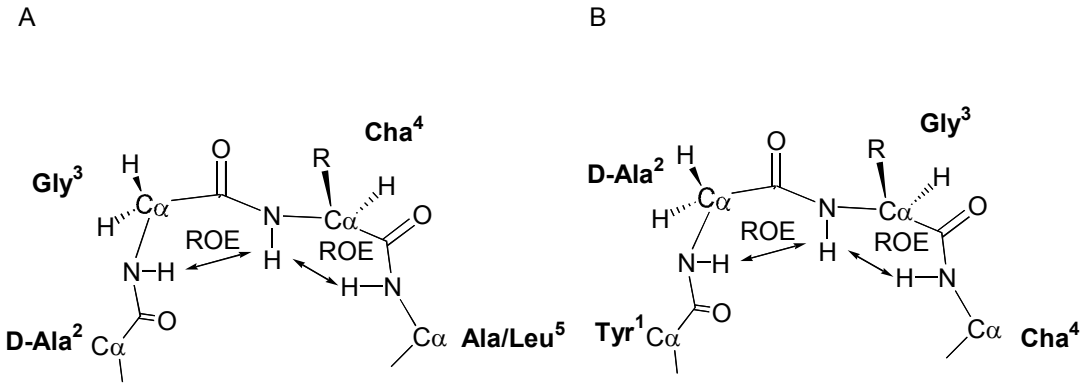

Figure 3.6. Schematic representation of ROE cross-peaks indicative of β-turn structures, type I (Panel A) and type II (Panel B).

than the first two cross-peaks listed (Figure 3.3). This indicates that both β-turn structures, type I and type II, coexist in solution.[32] Since the first group of cross-peaks is more intense, the type I β-turn is most likely the dominant structural feature in cyclic prodrug analogs **1** and **2**. One should also note that the residues of the β-turn in both cyclic prodrugs **1** and **2** exhibit low coupling constants (~3-4 Hz, Table 3.2). This is typically indicative of a well-defined secondary structure and suggests that cyclic prodrugs **1** and **2** are locked into a single conformation.[32] Overall, the data defining the solution conformation of the cyclic prodrugs suggests the following: (i) cyclic prodrugs **1** and **2** exhibit rigid solution structures with a defined type I β-turn, (ii) this β-turn structure is slightly distorted from standard β-turn geometry, (iii) MD simulations show the solution structure of cyclic prodrug analogs **1** and **2** to be comparable, and (iv) the NMR data illustrate a decreased hydrogen-bonding potential compared to DADLE for both cyclic prodrugs **1** and **2**. The solution conformation results and the favorable physicochemical properties indicate the likelihood of enhanced cellular membrane permeation by cyclic prodrugs **1** and **2**.

3.5 CONCLUSION

We have successfully designed, synthesized, and characterized CA-[Cha^4,D-Leu^5]-Enk **(1)** and CA-[Cha^4,D-Ala^5]-Enk **(2),** two new analogs of CA-DADLE. In order to create analogs that potentially have reduced cytrochrome P450 metabolism, the amino acid sequence of the cyclic prodrugs was modified. The synthesis involved

a convergent method where a linker moiety was combined with a peptide and then cyclized in a final step, forming the cyclic prodrugs. The characterization of the cyclic prodrugs illustrates that they are uncharged, lipophilic, and have reduced hydrogen-bonding potential. Given that cytochrome P450 and P-gp substrates have similar structure-activity relationships,[9-12] it stands to reason that these modified prodrugs may also have reduced affinity for efflux transporters and, thereby, enhanced cell membrane permeation compared to CA-DADLE. The data suggest that the CA-DADLE analogs have physicochemical properties favorable to increased cell membrane permeability. Additional studies will be undertaken to test the metabolic stability and permeation of these cyclic prodrugs as well as their affinity toward efflux transporters.

3.6 REFERENCES

1. Bak A, Gudmundsson OS, Gangwar S, Friis GJ, Siahaan TJ, Borchardt RT 1999. Synthesis and evaluation of the physicochemical properties of esterase sensitive cyclic prodrugs of opioid peptides using an (acyloxy)alkoxy linker. J Pept Res 53:393-402.

2. Ouyang H, Borchardt RT, Siahaan TJ, Vander Velde DG 2002. Synthesis and conformational analysis of a coumarinic acid-based cyclic prodrug of an opioid peptide with modified sensitivity to esterase-catalyzed bioconversion. J Pept Res 59:183-195.

3. Ouyang H, Tang F, Siahaan TJ, Borchardt RT 2002. A modified coumarinic acid-based cyclic prodrug of an opioid peptide: Its enzymatic and chemical stability and cell permeation characteristics. Pharm Res 19:794-801.

4. Wang B, Nimkar K, Wang W, Zhang H, Shan D, Gudmundsson O, Gangwar S, Siahaan T, Borchardt RT 1999. Synthesis and evaluation of the physicochemical properties of esterase sensitive cyclic prodrugs of opioid peptides using coumarinic acid and phenylpropionic acid linkers. J Pept Res 53:370-382.

5. Bak A, Gudmundsson OS, Friis GJ, Siahaan TJ, Borchardt RT 1999. Acyloxyalkoxy-based cyclic prodrugs of opioid peptides: Evaluation of the chemical and enzymatic stability as well as their transport properties across Caco-2 cell monolayers. Pharm Res 16:24-29.

6. Ouyang H, Chen W, Anderson TE, Steffansen B, Borchardt RT 2008. Factors that restrict the cell permation of cyclic prodrugs of an opioid peptide (DADLE): (I) The role of efflux transporters in the intestinal mucosa. J Pharm Sci: Submitted.

7. Ouyang H, Weiqing C, Anderson TE, Steffansen B, Borchardt RT 2008. Factors that restrict the cell permeation of cyclic prodrugs of an opioid peptide (DADLE): (II) The role of metabolic enzymes in the intestinal mucosa. J Pharm Sci:Submitted.

8. Tang F, Borchardt RT 2002. Characterization of the efflux transporter(s) responsible for restricting intestinal mucosa permeation of the coumarinic acid-based cyclic prodrug of the opioid peptide DADLE. Pharm Res 19:787-793.

9. Patel J, Mitra AK 2001. Strategies to overcome simultaneous P-glycoprotein-mediated efflux and CYP3A4-mediated metabolism of drugs. Pharmacogenomics 2:401-415.

10. Wacher VJ, Silverman JA, Zhang Y, Benet LZ 1998. Role of P-glycoprotein and cytochrome P450-3A in limiting oral absorption of peptides and peptidomimetics. J Pharm Sci 87:1322-1330.

11. Wang E-j, Lew K, Barecki M, Casciano CN, Clement RP, Johnson WW 2001. Quantitative distrinctions of active molecular recognition by P-glycoprotein and cytochrome P450 3A4. Chem Res Toxicol 14:1596-1603.

12. Zhang Y, Guo Z, Lin ET, Benet LZ 1998. Overlapping substrate specificties of cytochrome P450-3A and P-glycoprotein for a novel cysteine protease inhibitior. Drug Metab Dispos 26:360-366.

13. Ouyang H, Borchardt RT, Siahaan TJ 2002. Steric hindrance is a key factor in the coupling reaction of (acyloxy) alkyl-[alpha]-halides with phenols to make a new promoiety for prodrugs. Tetrahedron Lett 43:577-579.

14. Camenisch G, Alzenz J, van de Waterbeemd H, Folkers G 1998. Estimation of permeability by passive diffusion through Caco-2 cell monolayers using the drug's lipophilicity and molecular weight. Eur J Pharm Sci 6:313-319.

15. Goodwin JT, Mao B, Vidmar TJ, Conradi RA, Burton PS 1999. Strategies toward predicting peptide cellular permeability from computer molecular descriptors. J Pept Res 53:355-369.

16. Yazdanian M, Glynn S, Wright JL, Hawi A 1998. Correlating partitioning and Caco-2 cell permeability of structurally diverse small moleuclar weight compounds. Pharm Res 15:1490-1494.

17. Hruby VJ, Gehring C 1989. Recent developments in the design of receptor specific opioid peptides. Med Res Rev 9:343-401.

18. Lazarus LH, Salvadori S, Balboni G, Tomatis R, Wilson WE 1992. Stereospecificity of amino acid side chains in deltorphin defines binding to opioid receptors. J Med Chem 35:1222-1227.

19. Morgan BA, Smith CFC, Waterfield AA, Hughes J, Kosterlitz HW 1976. Structure-activity relationships of methioine-enkephalin. J Pharm Pharmacol 28:660-661.

20. Schmidt R, Menard D, Mrestani-Klaus C, Chung NN, Lemieux C, Schiller PW 1997. Structural modifications of the N-termial tetrapeptide segment of [D-Ala^2]-

deltorphin I: Effects on opioid receptor affinities and activities *in vitro* and on antinociceptive potency. Peptides 18:1615-1621.

21. Filippi B, Giusti P, Cima L, Borin G, Ricchelli F, Marchiori F 1979. Addicting properties and conformational studies in solution. Int J Pept Protein Res 14:34-40.

22. McFadyen IJ, Sobczyk-Kojiro K, Schaefer MJ, Ho JC, Omnaas JR, Mosberg HI, Traynor JR 2000. Tetrapeptide derivatives of [D-Pen^2, D-Pen^5]-Enkephalin (DPDPE) lacking an N-terminal tyrosine residue are agonists at the opioid receptor. J Pharmacol Exp Ther 295:960-966.

23. Becker JAJ, Wallace A, Garzon A, Ingallinella P, Bianchi E, Cortese R, Simonin F, Kieffer BL, Pessi A 1999. Ligands for K-opioid and ORL1 receptors identified from a conformationally constrained peptide combinatorial library. J Biol Chem 274:27513-27522.

24. Weltrowska G, Lemieux C, Chung NN, Schiller PW 2004. A chimeric opioid peptide with mixed mu agonist/ gamma antagonist properties. J Pept Res 63:63-68.

25. Toth G, Ioja E, Tomboly C, Ballet S, Tourwe D, Peter A, Martinek T, Chung NN, Schiller PW, Benyhe S, Borsodi A 2007. Beta-methyl substitution of cyclohexylalanine in Dmt-Tic-Cha-Phe peptides results in highly potent gamma-opioid Antagonist. J Med Chem 50:328-333.

26. Zaych LA, Yang W, Liao Y, Griffin KR, Wang B 2004. The effect of substitution patterns on the release rates of opioid peptides DADLE and [Leu^5]-enkephalin from coumarin prodrug moieties. Bioorg Chem 32:109-123.

27. Chan ECY, Tan WL, Ho PC, Fang LJ 2005. Modeling Caco-2 permeability of drugs using immobilized artifical membrane chromatography and physicochemical descriptors. J Chromatogr, A 1072:159-168.

28. Refsgaard H, H. F., Jensen BF, Brockhoff PB, Padkjr SB, Guldbrandt M, Christensen MS 2005. In silico prediction of membrane permeability from calculated molecular parameters. J Med Chem 48:805-811.

29. Gudmundsson OS, Jois SDS, Velde DGV, Siahaan TJ, Borchardt RT, Wang B 1999. The effect of conformation on the membrane permeation of coumarinic acid and phenylpropionic acid based cyclic prodrugs of opioid peptides. J Pept Res 53:383-392.

30. Gudmundsson OS, Vander Velde DG, Jois SDS, Bak A, Siahaan TJ, Borchardt RT 1999. The effect of conformation of the acyloxyalkoxy based cyclic prodrugs of opioid peptides on their membrane permeability. J Pept Res 53:403-413.

31. Liederer BM, Fuchs T, VanderVelde D, Siahaan TJ, Borchardt RT 2006. Effects of amino acid chirality and the chemical linker on the cell permeation characteristics of cyclic prodrugs of opioid peptides. J Med Chem 49:1261-1270.

32. Wuthrich K. 1986. NMR of Proteins and Nucleic Acids. ed., New York: John Wiley and Sons.

Chapter 4

Biopharmaceutical Properties of CA-DADLE Analogs

4.1 INTRODUCTION

The biopharmaceutical properties of drugs have recently become a central focus in the drug development pipeline.[1-3] Companies are now looking at these "drugable" properties earlier in the discovery process with the hope of cutting down on the cost and time associated with bringing a drug to market.[2,4] Gone are the days when the discovery scientists knew little to nothing about the development of drug candidates beyond the benchtop. A more complete pharmaceutical profile of a developing drug is now being considered at the discovery stage to cut back on the advancement of drug candidates that are great high affinity ligands in binding assays but are poor drugs.[5] One way to go about this is to preliminarily sort drug candidates into "bins" in relation to their pharmaceutical properties.[4,5] These bins classify the drugs into low, medium, and high range. The more medium-to-high bins a drug candidate fits into, the more likely that molecule is to have favorable drug-like properties and the more successful that candidate is likely to be in preclinical and clinical development stages. It is the investigation into some of these drug-like properties of the cyclic prodrugs of DADLE that is the main focus of this chapter. Many of the physicochemical properties (e.g., charge, size, hydrogen bonding potential) of cyclic prodrugs **2** and **3** have been discussed in the previous chapter. The focus will now be on the biologically based drug-like properties (e.g., metabolism, intestinal mucosal cell permeation, association with cellular transporters) of the cyclic prodrugs.

One way to improve the biopharmaceutical properties of a molecule is the creation of a prodrug. We took this prodrug approach in order to improve the membrane permeability of the opioid peptide DADLE. By making cyclic prodrugs of DADLE, we have been able to design uncharged molecules that were shown to have increased lipophilicity, decreased hydrogen-bonding potential, and unique solution structures.[6-8] While possessing these favorable physiochemical properties would presumably lead to increased transcellular permeability, the cyclic prodrugs have been found instead to exhibit low cell membrane permeability.[9,10] It has been discovered that the cyclic prodrugs exhibit substrate specificity for P-glycoprotein (P-gp), which results in a significant decrease in cellular permeability.[10-12]

Certain biological attributes (i.e. intestinal mucosal cell permeation, metabolism, cellular transporter interactions) are important properties to investigate in order to achieve and optimize the oral bioavailability of a drug. The intestinal mucosa is known to contain a significant amount of cytochrome P450-3A metabolizing enzymes.[11-13] Since the P450-3A4 enzyme is prominent in the intestinal mucosa and many P-gp substrates also show substrate specificity toward cytochrome P450 enzymes,[14-17] the metabolic stability of the cyclic prodrugs becomes suspect. It was shown that with the cyclic prodrug CA-DADLE, this is indeed the case (Chapter 2). Using this information, potentially more metabolically stable cyclic prodrugs of CA-DADLE **(1)** have been designed (Figure 4.1). These CA-DADLE analogs have been shown to possess favorable physicochemical properties (Chapter 3) that would put them in the medium-to-high "bin" for drug-like property characterization. The

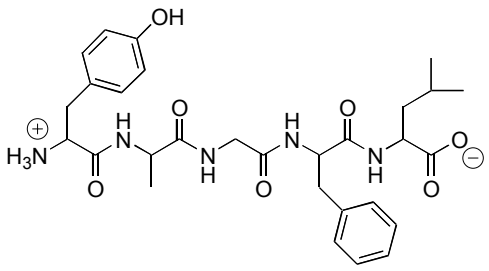

DADLE

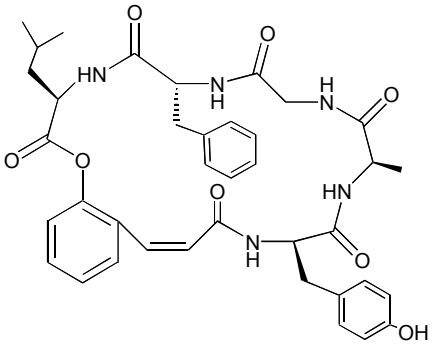

CA-DADLE
(1)

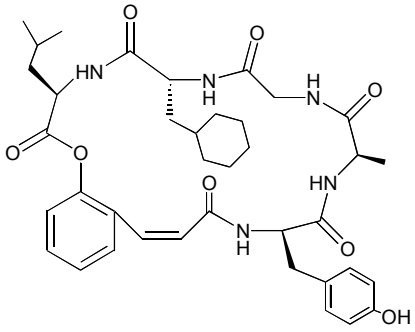

CA-[Cha^4,D-Leu^5]-Enk
(2)

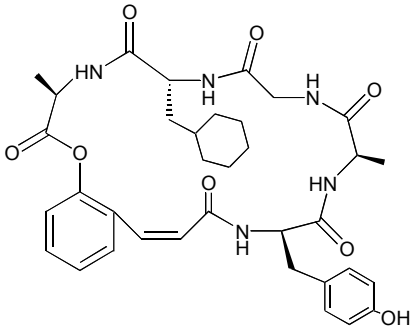

CA-[Cha^4,D-Ala^5]-Enk
(3)

Figure 4.1. Structures of DADLE and cyclic prodrugs of DADLE

biological drug-like properties of CA-[Cha^4,D-Leu^5]-Enk **(2)** and CA-[Cha^4,D-Ala^5]-Enk **(3)**, however, have yet to be tested. To further characterize the "drugable" nature of these analogs, the metabolic stability and cell permeation characteristics of the cyclic prodrugs will be determined *in vitro* and *in vivo*. Studies to identify general sites of oxidative metabolism on cyclic prodrugs **2** and **3** will also be undertaken.

4.2 MATERIAL AND METHODS

4.2.1 Materials

Cyclic prodrugs, CA-DADLE **(1)**, CA-[Cha^4,D-Leu^5]-Enk **(2)** and CA-[Cha^4,D-Ala^5]-Enk **(3)** were synthesized in our laboratory following described procedures.[7] Caco-2 cells were purchased from ATCC (Rockville, MD). Pooled male Sprague-Dawley rat liver microsomes (RLM), pooled male Hartely albino guinea pig liver microsomes (GPLM), pooled mixed gender human liver microsomes (HLM), and recombinant cytochrome P450-3A4 bacrosomes (hCYP3A4) were purchased from Xenotech, LLC (Lenexa, KS). Dulbecco's modified Eagle medium (DMEM) and Hank's balanced salt solution (HBSS) were purchased from SAFC Biosciences (Lenexa, KS). Fetal bovine serum (FBS), L-glutamine [200 mM (100 X)], penicillin-streptomycin solution (10,000 units/mL and 10,000 μg/mL, respectively, in 0.85% saline), MEM non-essential amino acids solution [10 mM (100 X)], and trypsin-EDTA solution (0.25%) were purchased from Invitrogen (Carlsbad, CA). D-[1-^{14}C]-mannitol (specific activity 9.25 GBq/mmol) was purchased from

Amersham Biosciences (Uppsala, Sweden). Polyester Transwells® (0.4 um pore size, 24 mm diameter) were purchased from Fisher Scientific (Pittsburgh, PA). Rat-tail collagen (type I) was purchased from Collaborative Biomedical Products (Bedford, MA). GF120918 was donated by Dr. Kenneth Brower (GlaxoSmithKline, Research Triangle Park, NC). Phosphate buffered saline solution (10 X), trifluoracetic acid, and DADLE were purchased from Sigma-Aldrich (St. Louis, MO). Solvents (HPLC grade) were purchased from Fisher Scientific (Pittsburgh, PA). All chemicals and solvents were used as received.

4.2.2 Metabolite Identification

Phase I oxidative metabolites of cyclic prodrugs **1-3** were determined in 500 µL of phosphate buffer (100 mM, pH 7.4) containing 50 µM cyclic peptide prodrug, 5 mM NADPH, and 300 nM P450 enzyme from RLM, GPLM, HLM, or 20 nM hCYP3A4 bacrosomes (hCYP3A4). The solution was incubated for 60 min at 37°C then quenched with a stop solution (100 µL of methanol and 750 µL of acetonitrile). The mixture was vortexed to mix and centrifuged at 13,000 × g for 15 min. The supernatant (500 µL) was removed and evaporated to dryness (Centrivap concentrator, Labconco, Kansas City, MO). The sample was reconstituted in 100 µL of 25% acetonitrile for analysis.

4.2.3 *In Vitro* Microsomal Stability

Metabolic stability studies of cyclic prodrugs **1-3** were preformed in 500 μL of phosphate buffer solution (100 mM, pH 7.4) containing 2.5 μM of cyclic peptide prodrug, 1 mM NADPH, and 300 nM P450 enzyme from RLM, GPLM, HLM, or 20 nM hCYP3A4. The solution was incubated for 15 min at 37°C then quenched with a stop solution (100 μL of methanol and 750 μL of acetonitrile). The mixture was vortexed to mix and centrifuged at 13,000 × g for 15 min. The supernatant (500 μL) was removed and evaporated to dryness (Centrivap concentrator, Labconco). The sample was reconstituted in 100 μL of 25% acetonitrile and analyzed using LC/MS/MS. Side-by-side control experiments were performed to monitor non-enzyme-mediated degradation. For the control experiments, methanol (100 μL) was added to the buffer/NAPDH/prodrug solution before the addition of hCYP3A4 or microsomes. After the addition of hCYP3A4 or microsomes, the reaction was quickly stopped with 750 μL of acetonitrile and processed as stated above. The amount of substrate remaining was calculated by dividing the average substrate peak area by the average substrate peak area in the control sample. Statistics were performed with Sigma Stat 3.5 using a one-way ANOVA with a Hohn-Sidik multiple comparison.

4.2.4 *In Vitro* Cellular Permeation

4.2.4.1 Cell Culture

Caco-2 cells were purchased from American Type Culture Collection (Rockville MD). The cells were cultured as previously described.[18] Basically, the cells were grown in a controlled atmosphere of 5% CO_2 and 95% relative humidity at 37°C in 150 cm^2 culture flasks. The culture medium consisted of DMEM supplemented with 10% heat-inactivated FBS, 1% nonessential amino acids, 100 μg/mL streptomycin, 100 U/mL penicillin, and 1% L-glutamine. In 3-5 days, 80% confluence was reached, and the cells were detached from the culture flask by partial digestion using a trypsin/EDTA solution. The freshly detached cells were used to subculture a new flask or plated on collagen-coated polycarbonate membranes (Transwell®, 0.4 μm pore size, 24 mm diameter). The cells were seeded at 7.9×10^4 cells/cm^2 on 6-well Transwell® filter inserts. The Caco-2 cells were fed with culture medium the day after seeding, then every other day until transport experiments were preformed [apical (AP) volume 1.5 mL; basolateral (BL) volume 2.6 mL]. The membrane integrity was checked post transport experiment using [^{14}C]-mannitol. The apparent permeability coefficients (P_{app}) of [^{14}C]-mannitol across the cell monolayers were typically in the range of $0.1\text{-}0.8 \times 10^{-6}$ cm/sec. Cells used in these experiments were between passages 26-34.

4.2.4.2 Transport Experiments

Bi-directional transport experiments were conducted in our laboratory[18] with only minor modifications. Briefly, the transport studies were performed at 37°C in a shaking water bath (60 rpm) on 21-28 day-old Caco-2 cell monolayers grown on collegen-coated polyester membranes (Transwells®). Both sides of the cell monolayers were washed 3 times with pre-warmed HBSS, pH 7.4. Drug solutions (20 μM final concentration) were added to the donor side and fresh HBSS was placed in the receiver compartment (1.5 mL for AP chamber and 2.6 mL for BL chamber). During inhibition studies, the cell monolayers were pre-incubated with HBSS containing inhibitors [GF120918 (10 μM) or PSC-833 (10 μM)] for 15 min to inhibit the activity of efflux transports present in the cell monolayers. Drug compounds were then added to the donor side along with their respective inhibitors. Aliquots (200 μL) were withdrawn from the receiver side at various time intervals up to 90 min. Fresh HBSS or HBSS containing inhibitor (200 μL) was replaced in the receiver side after sampling. The samples withdrawn were diluted with 25% acetonitrile in water (v/v) and then frozen at -80°C until analysis by LC/MS/MS. Apparent permeability coefficients (P_{app}) of the cyclic peptides were calculated using the following equation:

$$P_{app} = (\Delta Q/\Delta t)/(A \times C_0)$$

where $\Delta Q/\Delta t$ is the linear appearance rate of mass in the receiver solution, *A* is the cross-sectional area (4.71 cm^2), and C_0 is the initial peptide concentration in the donor compartment at t = 0.

4.2.5 *In Situ* Rat Intestinal Perfusion

4.2.5.1 Surgical Procedures and Sample Preparation

The surgical procedures used in the rat intestinal perfusion experiments have been previously described.[19] Both perfusate and blood samples were collected simultaneously during the study. The isolated ileum segment was perfused at a flow rate of 0.2 mL/min with the perfusate being collected at the outlet. The perfusate consisted of perfusion buffer (57.9 mM NaH_2PO_4, 79.5 mM Na_2SO_4, pH 6.5) containing cyclic prodrug (20 μM) with or without a P-gp inhibitor (PSC-833, 10 μM). Blood samples were collected via a direct cannulation of the mesenteric vein that was fed from isolated perfused tissue only. The perfusate and blood samples were collected over 5 min intervals from 30-60 min. The perfusate samples were mixed with acetonitrile (1:3, v/v) containing internal standards. The internal standard used to quantify the linear peptide was [Leu^5]-Enk, and quantification of the cyclic DADLE prodrugs was performed with cyclic [Leu^5]-Enk containing a coumarinic acid linker. The blood samples were collected over an esterase inhibitor (paraoxon, 0.5 mM) to retard the degradation of the cyclic prodrugs by intestinal esterases.

Immediately upon collection of each blood sample, the plasma fraction was isolated via centrifugation at 1800 × g for 5 min. The plasma fraction was then mixed with acetonitrile (1:3, v/v) containing internal standards. After all the plasma samples were collected, they were centrifuged at 21,000 × g for 15 min to pellet precipitate proteins. Finally, the supernatants from the plasma samples and the perfusate samples were dried using a Centrivap Concentrator (Labconco) and stored at -80°C until analysis. For analysis, the samples were reconstituted in 100 μL of 25 % acetonitrile, centrifuged to remove particulates, and analyzed by LC/MS/MS (see analytical methods). Each sample was evaluated for the presence of cyclic prodrug, linear drug, and oxidative metabolites.

4.2.5.2 Calculations of P_B Values From *In Situ* Rat Intestinal Perfusion Experiments

The apparent mesenteric permeability coefficients (P_B) were determined using the following equation:

$$P_B = (\Delta M_B/\Delta t)/(2\pi rl \times \langle C \rangle)$$

where M_B is the cumulative amount of drugs (both cyclic and linear) in the blood over time (t), r is the luminal radius of the intestine, l is the length of the perfused ileum segment and <C> is the logarithmic mean concentration of the drugs within the segment. <C> was calculated using the following equation:

$$<C> = C_0[1-(C_1/C_0)]/\ln(C_0/C_1)$$

where C_0 is the initial concentration of the drugs being perfused and C_1 is the concentration of drugs being collected at the outlet of the perfused ileum segment.

4.2.6 Analytical Methods

High-performance liquid chromatography with tandem mass spectrometry detection (LC/MS/MS) was employed using a Quattro Micro triple quadrupole mass spectrometer. Liquid chromatography was conducted using a Waters 2690 HPLC system. The separation was preformed on a Vydac C18 column (50 × 1.0 mm i.d., 300Å). The cyclic peptide prodrugs were isolated using a gradient from 5% to 95% B [solvent A: water with 0.1% formic acid (v/v) and solvent B: acetronitrile with 0.1% formic acid (v/v)]. The total run time was 20 min with a flow rate of 0.2 mL/min (3 min gradient from 5% to 40% B; 3 min gradient from 40% to 95% B; 2 min at 95%; 2 min return to 5% B; 10 min equilibration at 5% B). The eluate was analyzed by electrospray ionization (ESI) in positive mode. Multiple reaction monitoring (MRM) scans were used to determine the presence of the cyclic prodrug parent and the linear peptide using the following *m/z* transitions: parent > 136.0 with parent *m/z* set at: 698.4 {CA-DADLE **(1)**}, 704.2 {CA-[Cha^4,D-Leu^5]-Enk **(2)**}, and 662.6 {CA-[Cha^4,D-Ala^5]-Enk **(3)** }. The oxidative metabolites were identified with the following *m/z* transitions: parent > 102.0, 136.0, 152.0, and 223.0 with parent *m/z* set

at: 714.4 (CA-DADLE + OH), 720.3 (CA-[Cha^4,D-Leu^5]-Enk +OH), and 678.6 (CA-[Cha^4,D-Ala^5]-Enk +OH).

4.3 RESULTS

4.3.1 Metabolite Identification

Metabolites arising from phase I oxidation of CA-DADLE **(1)**, CA-[Cha^4,D-Leu^5]-Enk **(2)** and CA-[Cha^4,D-Ala^5]-Enk **(3)** are seen in Table 4.1. The data show CA-DADLE **(1)** to be hydroxylated at the Tyr^1 and Phe^4 positions in the presence RLM, but CA-DADLE analogs **(2** and **3)** show oxidation at only the Tyr^1 position. GPLM give similar results for CA-DADLE **(1),** showing hydroxylation at Tyr^1 and Phe^4. CA-[Cha^4,D-Leu^5]-Enk **(2)** mirrors this pattern showing hydroxylation on Tyr^1 and Cha^4. But hydroxylated Tyr^1 is the only metabolite formed from CA-[Cha^4,D-Ala^5]-Enk **(3)** in the presence of GPLM. HLM exhibited the same metabolite formation as with GPLM for cyclic prodrug analogs **2** and **3** showing hydroxylation at Tyr^1 and Cha^4 for CA-[Cha^4,D-Leu^5]-Enk **(2),** and Tyr^1 for CA-[Cha^4,D-Ala^5]-Enk **(3)**. CA-DADLE **(1)**, however, only shows hydroxylation at Tyr^1 in the presence of HLM. Interestingly, in the presence of hCYP3A4, CA-DADLE **(1)** shows oxidation at the Phe^4 position while cyclic prodrug analogs **2** and **3** show no significant metabolite formation under the same conditions (Table 4.1).

Table 4.1. Metabolites arising from phase I oxidation of CA-DADLE, CA-[Cha^4,D-Leu^5]-Enk and CA-[Cha^4,D-Ala^5]-Enk.

Compound	RLM oxidation	GPLM oxidation	HLM oxidation	hCYP3A4 oxidation
CA-DADLE	Tyr^1, Phe^4	Tyr^1,Phe^4	Tyr^1	Phe^4
CA-[Cha^4,D-Leu^5]-Enk	Tyr^1	Tyr^1, Cha^4	Tyr^1, Cha^4	No significant metabolites
CA-[Cha^4,D-Ala^5]-Enk	Tyr^1	Tyr^1	Tyr^1	No significant metabolites

4.3.2 *In Vitro* Microsomal Stability

The metabolic stability of DADLE and cyclic prodrugs of DADLE was investigated in the presence of RLM, GPLM, HLM, and hCYP3A4 with and without inhibitors. Paraoxon, an esterase B inhibitor, and ketoconazole, a cytochrome P 450 inhibitor, were the two inhibitors used in the liver microsomal assays. In the presence of hCYP3A, only ketoconazole was used since this metabolic stability assay contains only P450 enzymes. As seen in Figure 4.2, DADLE shows 100% parent compound remaining in the presence of RLM with and without inhibitors. The cyclic DADLE prodrugs **1-3**, however, show a significant decrease in metabolic stability. In the presence of RLM in the absence of inhibitors, CA-DADLE **(1)**, CA-[Cha^4,D-Leu^5]-Enk **(2),** and CA-[Cha^4,D- Ala^5]-Enk **(3)** show only 20%, 48%, and 17% of cyclic parent remaining, respectively (Figure 2). Paraoxon did little to improve the metabolic stability of the compounds with only 27% of the cyclic parent remaining for CA-DADLE **(1)**, 60% for CA-[Cha^4,D-Leu^5]-Enk **(2)** and 27% for CA-[Cha^4,D-Ala^5]-Enk **(3)** (Figure 2). The addition of ketoconazole brought about a significant increase in metabolic stability. The data showed 89% of the cyclic parent remaining for cyclic prodrugs **1-2** and 100% remaining for cyclic prodrug **3** (Figure 4.2). The combination of inhibitors produced greater than 90% of the cyclic prodrugs being detected after a 15-min incubation.

In the presence of GPLM, the studies indicate that DADLE has 90% of the parent compound remaining at 15 min with and without inhibitors (Figure 4.3). Cyclic prodrugs **1-3**, however, show a significantly decreased amount of cyclic parent

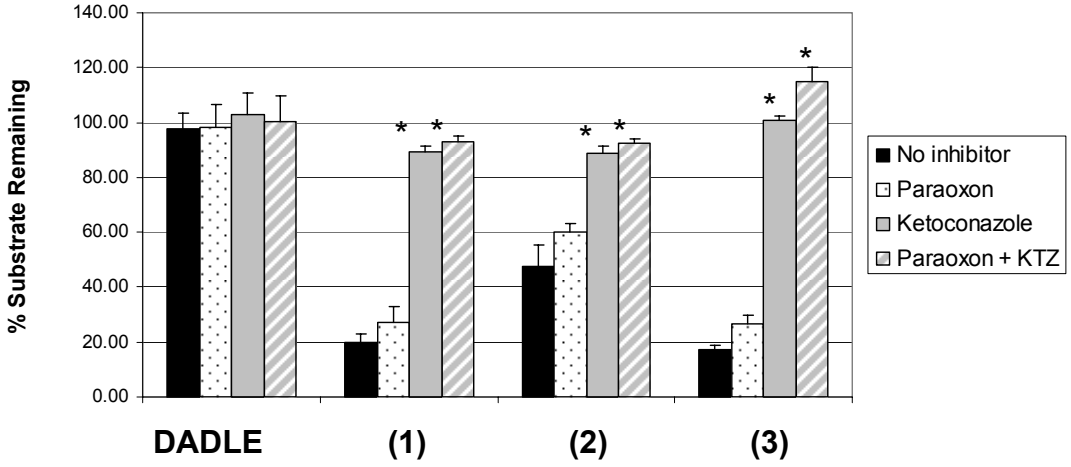

Figure 4.2. Stability of DADLE and the cyclic prodrugs CA-DADLE **(1)**, CA-[Cha^4,D-Leu^5]-Enk **(2)**, and CA-[Cha^4,D-Ala^5]-Enk **(3)** in the presence of rat liver microsomes with and without inhibitors after 15 min incubation. (*P<0.001)

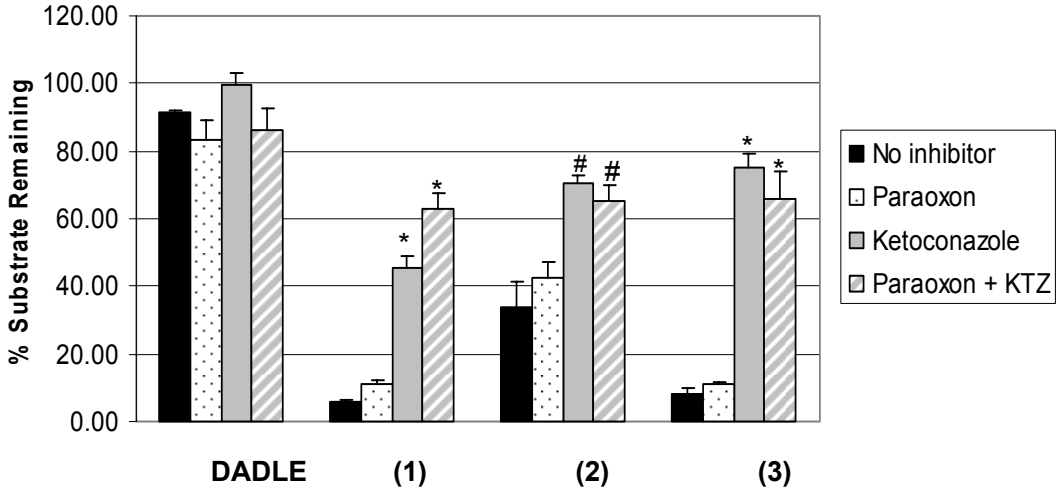

Figure 4.3. Stability of DADLE and the cyclic prodrugs CA-DADLE **(1)**, CA-[Cha^4,D-Leu^5]-Enk **(2)**, and CA-[Cha^4,D-Ala^5]-Enk **(3)** in the presence of guinea pig liver microsomes with and without inhibitors after 15 min incubation. (*P<0.001 and #P<0.003)

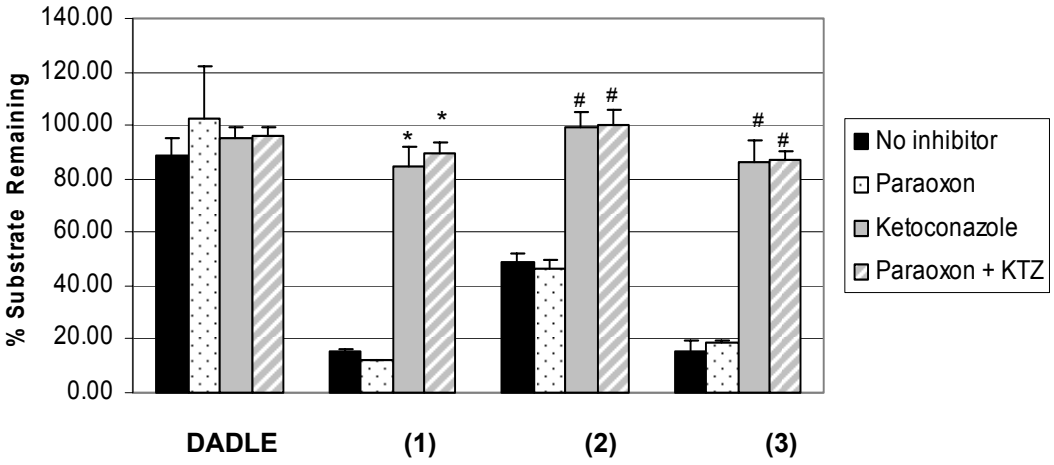

Figure 4.4. Stability of DADLE and the cyclic prodrugs CA-DADLE **(1)**, CA-[Cha^4,D-Leu^5]-Enk **(2)**, and CA-[Cha^4,D-Ala^5]-Enk **(3)** in the presence of human liver microsomes with and without inhibitors after 15 min incubation. (*P=0.022 and #P<0.001)

remaining in the absence of inhibitors. This is illustrated in Figure 4.3 where CA-DADLE **(1)** shows 6% of cyclic parent remaining, CA-[Cha^4,D-Leu^5]-Enk **(2)** has 34% remaining and CA-[Cha^4,D-Ala^5]-Enk **(3)** shows only 8% remaining. The presence of paraoxon did little to enhance the metabolic stability of cyclic prodrugs CA-DADLE **(1)**, CA-[Cha^4,D-Leu^5]-Enk **(2),** and CA-[Cha^4,D-Ala^5]-Enk **(3)**, with only 11%, 42%, and 11% of cyclic parent remaining, respectively. The metabolic stability of cyclic prodrugs **1-3** dramatically increases with the addition of ketoconazole to over 70% cyclic parent remaining for the CA-DADLE analogs **(2** and **3)** to 44% for CA-DADLE **(1)**. The results from the ketoconazole/paraoxon cocktail again mirror the results from ketoconazole alone, showing about 65% cyclic parent remaining for all three cyclic prodrugs **(1-3)**.

In the HLM assays, DADLE again shows a significant amount (94%) of parent drug remaining under all conditions (Figure 4.4). With no inhibitors present, 15%, 50%, and 20% of CA-DADLE **(1)**, CA-[Cha^4,D-Leu^5]-Enk **(2)**, and CA-[Cha^4,D-Ala^5]-Enk **(3)** remain (Figure 4.4). The low recovery of cyclic prodrugs **1-3** is reversed with the addition of ketoconazole to above 80% in all cases, but remains low with the addition of paraoxon alone, showing under 20% of parent drug remaining for CA-DADLE **(1)** and CA-[Cha^4,D-Ala^5]-Enk **(3)** and 44% for CA-[Cha^4,D-Leu^5]-Enk **(2)**. A combination of both inhibitors resulted in over 90% of cyclic prodrugs **1-3** being detected.

Cyclic prodrugs **1-3** show significantly different metabolic stability profiles in the recombinant hCYP3A4 assays (Figure 4.5). DADLE shows high stability in the

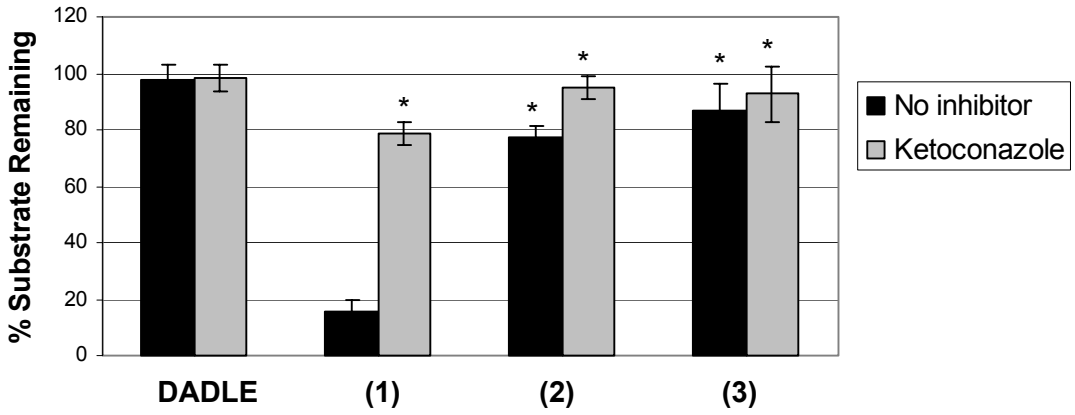

Figure 4.5. Stability of DADLE and the cyclic prodrugs CA-DADLE **(1)**, CA-[Cha^4,D-Leu^5]-Enk **(2)**, and CA-[Cha^4,D-Ala^5]-Enk **(3)** in the presence of hCYP3A4 with and without ketoconazole after 15 min incubation. (*P<0.001)

presence of hCYP3A4 with 98% of parent remaining with and without inhibitors. CA-DADLE **(1)** did not show high stability in the presence of hCYP3A4 in the absence of inhibitors, with only 9% of the parent drug remaining under this condition. CA-DADLE analogs **2** and **3**, however, did display relatively high metabolic stability in the presence of hCYP3A4. The data show 78% of the cyclic parent remaining for CA-[Cha^4,D-Leu^5]-Enk **(2)** and 87% remaining for CA-[Cha^4,D-Ala^5]-Enk **(3)**. The addition of ketoconazole did improve the metabolic stability of CA-DADLE **(1)** five-fold, but had relatively little effect on CA-DADLE analogs **2** and **3**.

4.3.3 *In Vitro* Cellular Permeation

The *in vitro* cell permeability of the cyclic DADLE prodrugs was investigated in a Caco-2 cell culture model in the presence and absence of inhibitors (Table 4.2-4.4). CA-DADLE **(1)** shows an apparent permeability coefficient (P_{app}) ratio of 20.8 without inhibitors present. This is significantly reduced in the presence of P-gp inhibitors where a P_{app} ratio of 4.8 is seen in the presence of GF120918 and 3.2 with PSC-833. In the absence of inhibitors, the P_{app} ratios for cyclic analogs **2** and **3** are significantly higher than that for CA-DADLE **(1)**. CA-[Cha^4,D-Leu^5]-Enk **(2)** shows a P_{app} ratio of 131 and CA-[Cha^4,D-Ala^5]-Enk **(3)** shows a P_{app} ratio of greater than 500 (Table 4.3, 4.4). As with CA-DADLE **(1)**, the cyclic prodrugs **2** and **3** exhibit lower P_{app} values in the presence of inhibitors. CA-[Cha^4,D-Leu^5]-Enk **(2)** has a P_{app} ratio of 10.7 in the presence of GF120918 and only 2.2 with PSC-833 (Table 4.3).

Table 4.2. P_{app} values of CA-DADLE **(1)** across a Caco-2 cell monolayer in the presence and absence of known P-gp inhibitors (10 μM).

Treatment	$P_{app} \times 10^7$ (cm/s)		Ratio ($P_{app\ BL\text{-}to\text{-}AP}$/ $P_{app\ AP\text{-}to\text{-}BL}$)
	AP-to-BL	BL-to-AP	
-	13.3 ± 2.3	276 ± 89.6	20.80
GF120918	49.0 ± 5.7	237 ± 22.8	4.84
PSC-833	23.0 ± 1.0	74.1± 7.2	3.22

Table 4.3. P_{app} values of CA-[Cha^4,D-Leu^5]-Enk **(2)** across a Caco-2 cell monolayer in the presence and absence of known P-gp inhibitors (10 μM).

Compound	$P_{app} \times 10^7$ (cm/s)		Ratio ($P_{app\ BL\text{-}to\text{-}AP}$/ $P_{app\ AP\text{-}to\text{-}BL}$)
	AP-to-BL	BL-to-AP	
-	3.4 ± 0.8	442 ± 4.2	131.01
GF120918	42.6 ± 2.2	457 ± 29.1	10.74
PSC-833	74.3 ± 8.4	161 ± 11.9	2.17

Table 4.4. P_{app} values of CA-[Cha^4,D-Ala^5]-Enk **(3)** across a Caco-2 cell monolayer in the presence and absence of known P-gp inhibitors (10 μM).

Compound	$P_{app} \times 10^7$ (cm/s)		Ratio ($P_{app\ BL\text{-}to\text{-}AP}$/ $P_{app\ AP\text{-}to\text{-}BL}$)
	AP-to-BL	BL-to-AP	
-	<0.03*	62.2 ± 1.8	>500
GF120918	21.1 ± 3.5	65.7 ± 10.9	3.12
PSC-833	31.5 ± 11.5	50.3 ± 11.9	1.60

*$P_{app\ AP\text{-}to\text{-}BL}$ calculated using lowest detectable limits

CA-[Cha^4,D-Ala^5]-Enk **(3)** shows P_{app} ratios of 3.1 and 1.6 in the presence of GF120918 and PSC-833, respectively (Table 4.4). The data demonstrate that without inhibitors cyclic prodrugs **1-3** have low P_{app} ratios, but with the addition of P-gp inhibitors, a dramatic increase in P_{app} ratios is seen. This indicates that the cyclic prodrugs **1-3** are substrates for P-gp.

4.3.4 In Situ Rat Intestinal Perfusion

The *in vivo* permeation of CA-DADLE **(1)** and CA-[Cha^4,D-Leu^5]-Enk **(2)** has been tested via an *in situ* rat intestinal perfusion model. Using the *in vitro* permeability data as a guide, the CA-DADLE analog showing the best *in vitro* permeation {CA-[Cha^4,D-Leu^5]-Enk **(2)**} and the P-gp inhibitor showing the highest inhibition (PSC-833) were used in the *in vivo* studies. The permeability is reported as apparent permeability coefficients (P_B) in Table 4.5. The data show that, in the absence of inhibitors, very little of the cyclic prodrug is detected in the blood. This is seen by P_B values less than 7 (Table 4.5). However, in the presence of PSC-833, the P_B values significantly increase. CA-DADLE **(1)** has a P_B value of 71.6 $\times 10^7$ cm/s and CA-[Cha^4,D-Leu^5]-Enk **(2)** is found to have a P_B value of 65.2 $\times$ 10^7 cm/s. Oxidative metabolites are not detected in any of the blood samples. It should be noted that the control P_B value for CA-[Cha^4,D-Leu^5]-Enk **(2)** was obtained from lowest detectable limit (LDL) calculations. These calculations were performed since detection was not possible because so little of the cyclic prodrug crossed the intestinal barrier.

Table 4.5. Apparent permeability coefficients of CA-DADLE **(1)** and CA-[Cha^4,D-Leu^5]-Enk **(2)** on the mesenteric blood (P_B) side in the presence and absence of PSC-833.[a]

	$P_B \times 10^7$ (cm/s)	
Compound	Control	PSC-833[c]
CA-DADLE	2.5 ± 0.92	71.6 ± 32.2
CA-[Cha^4,D-Leu^5]-Enk	6.5 ± 4.5[b]	65.2 ± 35.7

a. The rat ileum was perfused with 20 μM of each compound in the presence of 10 μM PSC-833. The mesenteric blood was sampled after steady-state at 5-min intervals for 30 min. The blood samples were extracted and analyzed using LC/MS/MS as described in Methods. Results presented as mean (± SEM) with n = 3-5.
b. The P_B values were estimated from the lowest detectable limits of the compound.
c. P_B values for the cyclic prodrugs were based on a sum of prodrug and linear compound present in the blood.

4.4 DISCUSSION

The biopharmaceutical properties of CA-DADLE **(1)**, CA-[Cha^4,D-Leu^5]-Enk **(2),** and CA-[Cha^4,D-Ala^5]-Enk **(3)** have been investigated to characterize the drug-like properties of these molecules. Metabolic stability, oxidative metabolite identification, and cellular permeation were determined for the cyclic prodrugs **1-3**. Metabolic stability assays and metabolite identification have been performed in the presence of liver microsomes (RLM, GPLM and HLM) and human recombinant 3A4 bacrosomes (hCYP3A4). Under all conditions studied, DADLE was found to be metabolically stable (Figures 4.2-4.5). Cyclic prodrugs **1-3**, however, were found to be metabolically instable under many of the same conditions. In the presence of liver microsomes, less then 20% of CA-DADLE **(1)** and CA-[Cha^4,D-Ala^5]-Enk **(3)** remain in the absence of inhibitors (Figures 2-4). For CA-[Cha^4,D-Leu^5]-Enk **(2)**, the amount of cyclic prodrug remaining after 15-min incubation was slightly higher at 48%. This shows a slight increase in stability for CA-[Cha^4,D-Leu^5]-Enk **(2)** compared to the other prodrugs in the presence of liver microsomes (Figure 4.2-4.4). The instability of cyclic prodrugs **1-3** in the tested biological media was found to be related to cytochrome P450 metabolism. The data show a significant increase in the amount of cyclic parent recovered with the addition of ketoconazole, a cytochrome P450 inhibitor. For CA-DADLE **(1)** and CA-[Cha^4,D-Ala^5]-Enk **(3)**, the addition of ketoconazole leads to a four-fold increase in stability. For CA-[Cha^4,D-Leu^5]-Enk **(2)**, the results are less dramatic showing only a two-fold increase. This suggests that CA-[Cha^4,D-Leu^5]-Enk **(2)** is slightly more stable toward cytochrome P450 oxidative

metabolism than the other prodrugs. While addition of ketoconazole results in a significant increase in the amount of cyclic prodrugs recovered, the addition of paraoxon, an esterase B inhibitor, only marginally increases the amount of cyclic parent recovered in the stability assays (Figures 4.2-4.4). This suggests that the metabolic instability of cyclic prodrugs **1-3** is not likely due to a premature bioconversion of the ester prodrugs.

The metabolic stability assays in the presence of hCYP3A4 show entirely different results than those from the metabolic stability studies with liver microsomes. CA-DADLE **(1)** is found to be metabolically unstable in the presence of hCYP3A4, but the CA-DADLE analogs **2** and **3** are found to be stable under the same conditions (Figure 4.5). CA-[Cha^4,D-Leu^5]-Enk **(2)** and CA-[Cha^4,D-Ala^5]-Enk **(3)** both show greater then 75% cyclic parent recovered in the presence of hCYP3A4 without inhibitors compared to 9% for CA-DADLE **(1)** (Figure 4.5). With the addition of ketoconazole, this number climbs to 95% for cyclic prodrugs **2** and **3**. This indicates that, while CA-[Cha^4,D-Leu^5]-Enk **(2)** and CA-[Cha^4,D-Ala^5]-Enk **(3)** are metabolized to a small extent by CYP3A4, there are probably other isozymes of cytochrome P450 that are involved in the metabolism of these prodrugs.

Metabolite identification studies have been performed to identify the areas of metabolic instability in the cyclic prodrugs. Since opioid activity of the cyclic prodrugs has been shown to rely highly on an unmodified tyrosine remaining in the first position of the opioid peptide,[20-23] this position was chosen to remain unaltered in the CA-DADLE analog design. Unfortunately, oxidation at the Tyr^1 position forms a

majority of the metabolites for all three cyclic prodrugs (Table 4.1). Cyclic prodrug **3** does show less metabolite formation than CA-DADLE **(1)** in the presence of liver microsomes, but it does not show increased metabolic stability in the liver microsomal assays compared to CA-DADLE **(1)** (Figure 4.2-4.4). The reason for this could be that enhancing the metabolic stability of position four in CA-[Cha^4,D-Ala^5]-Enk **(3)** makes Tyr^1 more susceptible to hydroxylation in the presence of liver microsomes.

The metabolite identification results are again very different in the presence of hCYP3A4 than in the liver microsomal assays. After a 60-min incubation with hCYP3A4, CA-DADLE **(1)** shows hydroxylation at Tyr^1 while the cyclic prodrugs **2** and **3** show no significant metabolite formation (Table 4.1). This is consistent with the metabolic stability results, which show cyclic prodrugs **2** and **3** to have greatly enhanced metabolic stability in the presence of hCYP3A4 (Figure 4.5). Since CYP3A4 is an important barrier to intestinal absorption, proving that CA-[Cha^4,D-Leu^5]-Enk **(2)** and CA-[Cha^4,D-Ala^5]-Enk **(3)** are metabolically stable and show no metabolite formation in the presence of hCYP3A4 is a significant result. The increased metabolic stability of the chemically modified prodrugs **2** and **3** in the presence of hCYP3A4 makes them good candidates for evaluation of their absorption after oral administration.

The *in vitro* cell membrane permeation of the cyclic prodrugs was tested using Caco-2 cell monolayers, a model for the human intestinal mucosa barrier. These results are reported in Tables 4.2-4.4. The apparent permeability coefficient (P_{app})

ratios cyclic prodrugs **1-3** in the absence of inhibitors are relatively high. In each case, the intrinsic permeability (AP-to-BL) is quite low compared to the BL-to AP values. This indicates that the cyclic prodrugs are not penetrating the cell membrane, and their low permeation is most likely due to apically localized efflux transporters. Confirmation of this is seen with the addition of P-gp inhibitors GF120918 and PSC-833. In the presence of P-gp inhibitors, the intrinsic permeability dramatically increases for all the cyclic prodrugs (Tables 4.2-4.4). The data show that the cyclic CA-DADLE analogs created to solve the metabolism issue are still substrates for P-gp. They are, in fact, even better P-gp substrates than the parent CA-DADLE **(1)**. Due to the remarkably low intrinsic permeability of cyclic prodrug **3**, cyclic prodrug **2** has been chosen for *in vivo* permeability experiments. Since PSC-833 is the best P-gp inhibitor for cyclic prodrug **2**, it has also been chosen for the *in vivo* permeability experiments.

Cyclic analog CA-[Cha^4,D-Leu^5]-Enk **(2)** and parent CA-DADLE **(1)** have been used in *in situ* rat intestinal perfusion studies with the aim of testing the *in vivo* membrane permeability. The *in situ* rat intestinal perfusion model allows the membrane permeability of the cyclic prodrugs to be tested while simultaneously looking for oxidative metabolites. Since the cyclic prodrugs are known substrates for P-gp, inhibitor studies using PSC-833 were performed. The control experiments (cyclic prodrug alone) showed very little membrane permeation by cyclic prodrugs **1** and **2** (Table 4.5). However, with the addition of a P-gp inhibitor, the apparent permeability coefficient values (P_B) showed a 28-fold increase for CA-DADLE **(1)**

and a 10-fold increase in permeation for CA-[Cha^4,D-Leu^5]-Enk **(2)** (Table 4.5). The large increase in permeation for both cyclic prodrugs **1-2** in the presence of a P-gp inhibitor illustrates that these compounds are substrates for efflux transporters *in vivo*. No metabolites of the cyclic prodrugs were found to permeate the rat intestine even in the presence of a P-gp inhibitor.

4.5 CONCLUSION

The biopharmaceutical characteristics of cyclic prodrug analogs **2** and **3** were evaluated to test the "drugability" of these molecules. In the presence of liver microsomes, cyclic prodrug analogs **2** and **3** did not show significant increases in metabolic stability compared to CA-DADLE **(1).** It was found that these compounds are metabolized by cytochrome P450 enzymes. In the presence of hCYP3A4, however, cyclic prodrug analogs **2** and **3** were found to have increased oxidative metabolic stability compared to CA-DADLE **(1)**. The improved metabolic stability towards hCYP3A4 is important for oral drug delivery since CYP3A4 is the main metabolic barrier to intestinal absorption. Unfortunately, cyclic prodrug analogs **2** and **3** were found to exhibit poor *in vitro* permeation. This is contrary to what was anticipated. Based on the structural and physiochemical properties (i.e., unique solution structure, reduced intramolecular hydrogen bonding, increased lipophilicity, and decreased charge), the cyclic prodrugs were expected to have good permeation. However, the permeation data showed both CA-[Cha^4,D-Leu^5]-Enk **(2)** and CA-

[Cha^4,D-Ala^5]-Enk **(3)** to be substrates of P-gp. In fact, cyclic prodrugs **2** and **3** were found to be even better substrates for P-gp than the parent CA-DADLE **(1)**. The *in vivo* results support the *in vitro* results showing that P-gp is a major barrier to intestinal absorption *in vivo*. Increasing the CYP3A4 metabolic stability of cyclic prodrug analogs **2** and **3** by amino acid modification did not translate into decreased P-gp substrate specificity as hoped. The overlap in structure-activity relationships between cytochrome P450 substrates and P-gp substrates does not hold true in this case. Regrettably, these studies indicated that, in order to improve the oral bioavailablity of the cyclic prodrugs, their affinity for P-gp and oxidative metabolic stability in the liver would need to be addressed.

4.6 REFERENCES

1. Caldwell GW, Ritchie DM, Masucci JA, Hageman W, Yan Z 2001. The new pre-preclinical paradigm: Compound optimization in early and late phase drug discovery. Curr Top Med Chem 1:353-366.

2. Lesko LJ, Rowland M, Peck CC, Blaschke TF 2000. Optimizing the science of drug development: Opportunities for better candidate selection and accelerated evaluation in humans. Pharm Res 17:1335-1344.

3. Varma MVS, Khandavilli S, Ashokraj Y, Jain A, Dhanikula A, Sood A, Thomas NS, Pillai O, Sharma P, Gandhi R, Agrawal S, Nair V, Panchagnula R 2004. Biopharmacetuic classification system: A scientific framework for pharmacokinetic optimization in drug research. Curr Drug Metab 5:375-388.

4. Panchagnula R, Thomas NS 2000. Biopharmaceutics and pharmacokinetics in drug research. Int J Pharm 201:131-150.

5. Borchardt RT. 217th ACS National Meeting, Anaheim, CA, 1999.

6. Bak A, Gudmundsson OS, Gangwar S, Friis GJ, Siahaan TJ, Borchardt RT 1999. Synthesis and evaluation of the physicochemical properties of esterase sensitive cyclic prodrugs of opioid peptides using an (acyloxy)alkoxy linker. J Pept Res 53:393-402.

7. Ouyang H, Borchardt RT, Siahaan TJ, Vander Velde DG 2002. Synthesis and conformational analysis of a coumarinic acid-based cyclic prodrug of an opioid peptide with modified sensitivity to esterase-catalyzed bioconversion. J Pept Res 59:183-195.

8. Wang B, Nimkar K, Wang W, Zhang H, Shan D, Gudmundsson O, Gangwar S, Siahaan T, Borchardt RT 1999. Synthesis and evaluation of the physicochemical properties of esterase sensitive cyclic prodrugs of opioid peptides using coumarinic acid and phenylpropionic acid linkers. J Pept Res 53:370-382.

9. Bak A, Gudmundsson OS, Friis GJ, Siahaan TJ, Borchardt RT 1999. Acyloxyalkoxy-based cyclic prodrugs of opioid peptides: Evaluation of the chemical and enzymatic stability as well as their transport properties across Caco-2 cell monolayers. Pharm Res 16:24-29.

10. Ouyang H, Tang F, Siahaan TJ, Borchardt RT 2002. A modified coumarinic acid-based cyclic prodrug of an opioid peptide: Its enzymatic and chemical stability and cell permeation characteristics. Pharm Res 19:794-801.

11. Ding X, Kaminsky LS 2003. Human extrahepatic cytochromes P450: Function in xenobiotic metabolism and tissue-selective chemical toxicity in the respiratory and gastrointestinal tracts. Annu Rev Pharmacol Toxicol 43:149-173.

12. Paine MF, Hart HL, Ludington SS, Haining RL, Rettie AE, Zeldin DC 2006. The human intestinal cytochrome P450 "PIE". Drug Metab Dispos 34:880-886.

13. Suzuki H, Sugiyama Y 2000. Role of metabolic enzymes and efflux transporters in the absorption of drugs from the small intestine. Eur J Pharm Sci 12:3-12.

14. Patel J, Mitra AK 2001. Strategies to overcome simultaneous P-glycoprotein-mediated efflux and CYP3A4-mediated metabolism of drugs. Pharmacogenomics 2:401-415.

15. Wacher VJ, Silverman JA, Zhang Y, Benet LZ 1998. Role of P-glycoprotein and cytochrome P450-3A in limiting oral absorption of peptides and peptidomimetics. J Pharm Sci 87:1322-1330.

16. Wang E-j, Lew K, Barecki M, Casciano CN, Clement RP, Johnson WW 2001. Quantitative distrinctions of active molecular recognition by P-glycoprotein and cytochrome P450 3A4. Chem Res Toxicol 14:1596-1603.

17. Zhang Y, Guo Z, Lin ET, Benet LZ 1998. Overlapping substrate specificties of cytochrome P450-3A and P-glycoprotein for a novel cysteine protease inhibitior. Drug Metab Dispos 26:360-366.

18. Gao J, Hugger ED, Beck-Westermeyer MS, Borchardt RT. 2000. Protocols in the application of Caco-2 cells in measuring permeability coefficient of drugs. Current Protocols in Pharmacology, ed., New York: John Wiley and Sons. p 1-23.

19. Ouyang H, Chen W, Anderson TE, Steffansen B, Borchardt RT 2008. Factors that restrict the cell permation of cyclic prodrugs of an opioid peptide (DADLE): (I) The role of efflux transporters in the intestinal mucosa. J Pharm Sci: Submitted

20. Hruby VJ, Gehring C 1989. Recent developments in the design of receptor specific opioid peptides. Med Res Rev 9:343-401.

21. Lazarus LH, Salvadori S, Balboni G, Tomatis R, Wilson WE 1992. Stereospecificity of amino acid side chains in deltorphin defines binding to opioid receptors. J Med Chem 35:1222-1227.

22. Morgan BA, Smith CFC, Waterfield AA, Hughes J, Kosterlitz HW 1976. Structure-activity relationships of methioine-enkephalin. J Pharm Pharmacol 28:660-661.

23. Schmidt R, Menard D, Mrestani-Klaus C, Chung NN, Lemieux C, Schiller PW 1997. Structural modifications of the N-termial tetrapeptide segment of [D-Ala^2]-deltorphin I: Effects on opioid receptor affinities and activities *in vitro* and on antinociceptive potency. Peptides 18:1615-1621.

Chapter 5

Conclusions

The main goal of this dissertation research was to investigate and potentially to improve the biopharmaceutical properties of cyclic prodrugs of the opioid peptide DADLE. The cyclic peptide prodrug CA-DADLE (DADLE cyclized with a coumarinic acid linker) was used as a model for the development of new cyclic prodrugs. Initially, it was found that incorporation of the peptide into a cyclic prodrug caused the peptide to become metabolically unstable. Investigations into the metabolism and metabolite formation led to the discovery that the metabolic instability resulted from cytochrome P450 metabolism. The major metabolites formed from CA-DADLE were found to be hydroxylated on the Tyr^1 and Phe^4 residues of the peptide. Using this information, an attempt was made to design cyclic prodrugs that would be more metabolically stable. The amino acid sequence of the peptide was modified, creating two new CA-DADLE cyclic prodrug analogs, CA-[Cha^4, D-Leu^5]-Enk and CA-[Cha^4, D-Ala^5]-Enk.

Metabolite identification and metabolic stability studies of the new cyclic prodrugs were explored using liver microsomes and hCYP3A4. In the presence of liver microsomes, the cyclic prodrug analogs were found to form oxidative metabolites similar to the metabolites of CA-DADLE, and were found to be metabolically unstable in the absence of cytochrome P450 inhibitors. The recombinant human cytochrome P450-3A4 (hCYP3A4) results, however, showed that the cyclic prodrug analogs have high metabolic stability and no metabolite formation in the presence of hCYP3A4. This was a vast improvement over CA-DADLE, which exhibited metabolic instability and metabolite formation under the same conditions.

Physicochemical properties and solution conformations were determined to further characterize the two new cyclic prodrugs. 2D-NMR studies and MD simulations showed that these cyclic prodrugs posed a unique solution conformation containing a type I β-turn. This defined secondary structure provided evidence of a decreased hydrogen-bonding potential for the cyclic prodrugs in comparison to DADLE. Determination of the molecular surface area and cLogP calculations demonstrated that the two CA-DADLE analogs were uncharged and more lipophilic than linear DADLE. Overall, these studies illustrated that the cyclic CA-DADLE analogs have favorable physicochemical properties, making them good drug candidates.

The favorable physicochemical properties and enhanced cytochrome P450-3A4 metabolic stability, however, did not lead to increased cell membrane permeation. *In vitro* cell culture studies showed that the cyclic prodrugs were substrates for apically polarized efflux transporters. Specifically, P-glycoprotein (P-gP) was found to significantly limit the cell membrane permeation of the cyclic prodrugs. Analysis of the *in vivo* cell membrane permeability was performed using an *in situ* rat intestinal perfusion model. This model was utilized to further characterize the cell membrane permeability *in vivo* as well as to identify permeable metabolites. As expected, the *in vivo* experimental results reinforced the *in vitro* results, confirming poor intestinal permeability *in vivo*. There were no oxidative metabolites detected in these studies. The overall results suggest that in order for the

cyclic prodrugs to be viable oral drugs, they must have increased oxidative metabolic stability, especially in the liver, and greatly enhanced membrane permeation.

The poor metabolic stability of the cyclic prodrugs could be addressed in two ways: (i) identification of the specific cytochrome P450 enzyme responsible for the oxidative metabolism and/or (ii) modification of the peptide to give greater metabolic stability. A further understanding of the cytochrome P450 metabolism in the cyclic prodrugs would be valuable. It was discovered that the cyclic prodrugs were metabolically unstable in the presence of rat liver microsomes and guinea pig liver microsomes but showed no metabolite formation and high metabolic stability in the presence of hCYP3A4. Interestingly, they did not show increased metabolic stability in the presence of human liver microsomes. This led to the conclusion that other P450 isozymes rather than P450-3A4 are responsible for the majority of the metabolism of the cyclic prodrug analogs. It would be of interest to use other recombinant cytochrome P450 isolates to identify the particular isozyme that leads to this metabolic instability.

Additional changes to the amino acid sequence of the peptide could also be considered to increase metabolic stability. In designing the cyclic prodrug analogs, the tyrosine residue was not modified since it is thought to be necessary for opioid receptor recognition. Unfortunately, it was found that a majority of the metabolites identified were related to the Tyr^1 residue. To truly eliminate the cytochrome P450 metabolism, further modification of the peptide sequence would be needed. Discounting the synthetic rigor, future studies could include modification of the Tyr^1

residue with an amino acid mimic. Recent opioid peptide research suggests that replacing the tyrosine residue with certain tyrosine-like molecules can lead to active opioid peptides.[1-3] When modifying the tyrosine residue, however, care must be taken to maintain opioid receptor affinity.

Besides the cytochrome P450 metabolism, enhancing the membrane permeability of the cyclic prodrugs was a concern with the new cyclic prodrug analogs. The issues of P-gp substrate specificity and membrane permeability, however, are complex. One solution might be to pre-administer and/or co-administer a P-gp inhibitor with the cyclic prodrugs. While not ideal from a clinical perspective, we have found that this strategy does significantly increase the bioavailability of the cyclic prodrugs in rats.[4] Another possible change would be to alter the solution conformation of the compounds by increase the ring size of the cyclic prodrugs. Addition of amino acids to the peptide backbone or "filler atoms" to the linker would form a larger, more mobile structure. These molecules could possibly have the ability to be flexible enough to reach a conformation that would not be recognized as a substrate for P-gp and, as cyclic molecules, they would still be lipophilic enough to permeate the cell membrane. In taking this approach, however, size might become an issue with cell membrane permeability. Naturally, when taking this course of action, one would need to consider changes in the physiochemical properties caused by the addition as well as the bioconversion of the cyclic prodrug.

REFERENCES

1. Dolle RE, Machaut M, Martinez-Teipel B, Belanger S, Cassel JA, Stabley GJ, Graczyk TM, DeHaven RN 2004. (4-Carboxamido) phenylalanine is a surrogate for tyrosine in opioid receptor peptide ligands. Bioorg Med Chem Lett 14:3545-3548.

2. Lu Y, Lum TK, Augustine YWL, Weltrowska G, Nguyen TM-D, Lemieux C, Chung NN, Schiller PW 2006. Replacement of the N-terminal tyrosine residue in opioid peptides with 3-(2,6-Dimethyl-4-carbamoylphenyl)propanoic acid (Dcp) results in novel opioid antagonists. J Med Chem 49:5382-5385.

3. Weltrowska G, Lu Y, Lemieux C, Chung NN, Schiller PW 2004. A novel cyclic enkephalin analogue with potent opioid antagonist activity. Bioorg Med Chem Lett 14:4731-4733.

4. Ouyang H, Weiqing C, Anderson TE, Steffansen B, Borchardt RT 2008. Factors that restrict the cell permeation of cyclic prodrugs of an opioid peptide (DADLE): (II) The role of metabolic enzymes in the intestinal mucosa. J Pharm Sci:Submitted.